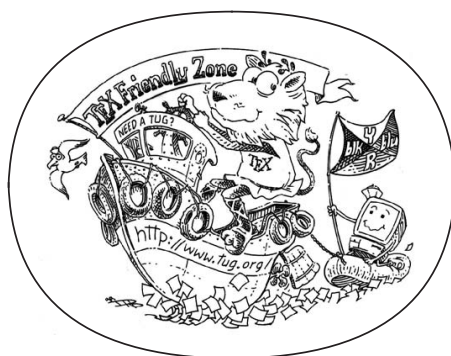MICHAEL JOHN DEVINE

PATIENT-DERIVED CELL MODELS OF
PARKINSON'S DISEASE

PATIENT-DERIVED CELL MODELS OF PARKINSON'S DISEASE

MICHAEL JOHN DEVINE

Department of Molecular Neuroscience

Institute of Neurology

University College London

July 2012

omnia vincit amor.

— Virgil

For Laura.

DECLARATION

I, Michael Devine, confirm that the work presented in this thesis is my own. Where information has been derived from other sources, I confirm that this has been indicated in the thesis.

London, July 2012

<div style="text-align: right;">

_____

Michael John Devine

</div>

ABSTRACT

Parkinson's disease is the commonest neurodegenerative movement disorder. Although the pathological loss of dopaminergic neurons in the substantia nigra has long been recognised, the disease remains incurable because the mechanisms underlying this loss are not understood. Finding genes that cause inherited forms of the disease can help by pinpointing pathways that lead to neuronal death when faulty. However, analysis of these genes is complicated by the inaccessibility of diseased tissue during life.

One possible solution is to use fibroblasts from patients, which retain pathogenic mutations and might act as a surrogate for diseased cells. But a major advance might be provided by reprogramming fibroblasts into induced pluripotent stem cells. These can be differentiated into multiple cell lineages, including those specific cells affected by disease.

Here, two studies are described using fibroblasts from Parkinson's disease patients with *LRRK2* mutations. The first suggests that 4E-BP, a component of the mTOR pathway, is hyperphosphorylated in patient fibroblasts. In contrast, the second study suggests that gene transcription is not significantly altered in these cells.

To improve on this non-neuronal model, induced pluripotent stem cells were generated using fibroblasts from a Parkinson's disease patient with triplication of the α-synuclein locus, alongside healthy controls. When these cells are differentiated into dopaminergic neurons, those from the patient have double dosage of α-synuclein protein, but only when clonal variation and efficiency of neuralisation are addressed. Nevertheless, these cells precisely recapitulate the cause of Parkinson's disease in this kindred.

These studies demonstrate the feasibility of generating cells of interest from a patient with a neurodegenerative disorder, but also

highlight the inherent variability in induced pluripotent stem cell systems. These data emphasise the need for robust methods of neuronal differentiation, and the need to generate multiple induced pluripotent stem cell clones from each subject when developing such disease models.

PUBLICATIONS

Some ideas and figures have appeared previously in the following publications:

1. **Devine MJ**, Plun-Favreau H, Wood NW (2011) Parkinson's disease and cancer: two wars, one front. Nature Reviews Cancer 11:812-23

2. **Devine MJ**, Ryten M, Vodicka P, Thomson AJ, Burdon T, Houlden H et al. (2011) Parkinson's disease induced pluripotent stem cells with triplication of the α-synuclein locus. Nature Communications 2:440

3. **Devine MJ**, Gwinn K, Singleton A and Hardy J (2011) Parkinson's disease and α-synuclein expression. Movement Disorders 26:2160-8

4. **Devine MJ**, Kaganovich A, Ryten M, Mamais A, Trabzuni D, Manzoni C, et al. (2011) Pathogenic LRRK2 mutations do not alter gene expression in cell model systems or human brain tissue. PLoS One 6:e22489

5. Gwinn K, **Devine MJ**, Jin LW, Johnson J, Bird T, Muenter M, et al. (2011) Clinical features, with video documentation, of the original familial Lewy body Parkinsonism caused by α-synuclein triplication (Iowa kindred). Movement Disorders 26:2134-6

6. **Devine MJ** and Lewis PA (2008) Emerging pathways in genetic Parkinson's disease: tangles, Lewy bodies and LRRK2. FEBS Journal 275:5748-57

To achieve the impossible,
one must attempt the absurd.

— Cervantes Saavedra (1605)

ACKNOWLEDGMENTS

I have many people that I must thank, without whom this thesis could not have been written.

Above all I would like to thank the patients, carers, relatives and other individuals who donated samples and their time, freely and without benefit to themselves. I am very grateful to the organisations that funded this work: the Medical Research Council for their ongoing personal support, Parkinson's UK, the Wellcome Trust and the Michael J Fox Foundation.

I am indebted to my supervisors: John Hardy for continual support despite less than continual presence in his lab, a very refreshing angle on bureaucracy, and his wisdom with the strange ways of science. I am very grateful to have had the opportunity to work in his lab. Patrick Lewis I must thank for support during the early stages of this project, introducing me to the complexities of biochemistry, and for letting me in on the secret that a scientific conference can be combined with a skiing holiday. I owe a great deal to Tilo Kunath for taking me in to his lab in Edinburgh, undiminished enthusiasm in the face of seemingly perpetual obstacles, and his excellent hospitality, all whilst juggling a very busy family life.

I also thank all members of the Department of Molecular Neuroscience for creating such a friendly and open working environment, for help with answering lots of daft questions from a medic with limited pipetting experience, and especially sharing the inevitable tales of woe! Many, many thanks to Kat Wanek and Parmjit Jat for a great deal of help and expertise during what turned out to be the toughest

CONTENTS

LIST OF FIGURES

LIST OF TABLES

ABBREVIATIONS

AD   Alzheimer's disease

ALS   Amyotrophic lateral sclerosis

ANOVA   Analysis of variance

AST   Alpha-synuclein triplication (cell line)

ATP   Adenosine triphosphate

BDNF   Brain-derived neurotrophic factor

bpm   Beats per minute

CBD   Cortico-basal degeneration

COR   C-terminal of ROC

DAPI	4′,6-Diamidino-2-phenylindole
DAT	Dopamine transporter
DLB	Dementia with Lewy bodies
DMEM	Dulbecco's modified Eagle's medium
DTT	Dithiothreitol
EC	Embryonic carcinoma (cell)
EDTA	Ethylenediaminetetraacetic acid
ELISA	Enzyme-linked immunosorbent assay
ERK	Extracellular signal-regulated kinase
ES	Embryonic stem (cell)
FACS	Fluorescence-activated cell sorting
FBS	Foetal bovine serum
FGF2	Fibroblast growth factor 2
FGF8	Fibroblast growth factor 8
FTD	Frontotemporal dementia
FTDP-17	Frontotemporal dementia with parkinsonism linked to chromosome 17
GDNF	Glial cell-derived neurotrophic factor
GEO	Gene expression omnibus
GFP	Green fluorescent protein
GTP	Guanosine triphosphate
GSEA	Gene set enrichment analysis
HBSS	Hank's buffered saline solution

hES	Human embryonic stem (cell)
hESC	Human embryonic stem cell
HPLC	High pressure liquid chromatography
HRP	Horseradish peroxidase
ICM	Inner cell mass
IPD	Idiopathic Parkinson's disease
iPS	Induced pluripotent stem (cell)
iPSC	Induced pluripotent stem cell
IRES	Internal ribosome entry site
KEGG	Kyoto encyclopaedia of genes and genomes
KSR	Knockout serum replacement media
LRRK2	Leucine-rich repeat kinase 2
MAPT	Microtubule-associated protein tau
MEF	Mouse embryonic fibroblast
MEF-CM	MEF conditioned media
MIAME	Minimum information about a microarray experiment
MMSE	Mini-mental state examination
MOI	Multiplicity of infection
MPTP	1-methyl-4-phenyl-1,2,3,6-tetrahydropyridine
MSA	Multiple systems atrophy
mTOR	Mammalian target of rapamycin
NAS	Normal alpha-synuclein (cell line)
NFT	Neurofibrillary tangle

NIH	National institutes of health
NSBDM	Noggin-SB431542-dorsomorphin media
NSF	N-ethylmaleimide sensitive fusion protein
PCA	Principal component analysis
PBS	Phosphate buffered saline
PCR	Polymerase chain reaction
PD	Parkinson's disease
PH	Postural hypotension
PVDF	Polyvinylidene fluoride
qRT-PCR	Quantitative reverse transcriptase PCR
RBD	REM sleep behaviour disorder
REM	Rapid eye movement
ROC	Ras of complex proteins
ROCK	Rho-associated protein kinase
RT-PCR	Reverse transcriptase PCR
RTP	Room temperature and pressure
SD	Standard deviation
SDS	Sodium dodecyl sulfate
SHH	Sonic hedgehog
SNARE	Soluble NSF attachment protein receptor
SNP	Single nucleotide polymorphism
SSEA	Stage specific embryonic antigen
TALEN	Transcription activator-like effector nuclease

TDP-43   TAR DNA binding protein 43

TH   Tyrosine hydroxylase

TU   Transforming unit

UNF   Unrelated female (cell line)

UNM   Unrelated male (cell line)

UPL   Universal probe library

UPS   Ubiquitin proteasome system

UPSIT   University of Pennsylvania smell identification test

VPA   Valproic acid

VSV   Vesicular stomatitis virus

ZFN   Zinc finger nuclease

TDP-43   TAR DNA binding protein 43

Part I

BACKGROUND

INTRODUCTION

> *Involuntary tremulous motion . . .*
> *with a propensity to bend the trunk forward,*
> *and to pass from a walking to a running pace:*
> *the senses and intellects being uninjured.*
>
> — Parkinson (1817)

Parkinson's disease (PD) is the most common neurodegenerative movement disorder, estimated to affect one person in every 500. Prevalence increases with age, thus PD is set to become even more common with our ageing population. The economic burden in the UK alone is already upwards of £6 billion per annum (Findley et al., 2003). No curative or disease modifying treatments exist for this condition, owing to the fact that we understand relatively little about why certain neurons progressively die off in the disease.

1.1 HISTORICAL PERSPECTIVE

Possibly the earliest recorded descriptions of PD are housed in the ancient library of the Hindu University of the Holy City of Benares (Varanasi), in which can be found the Charakasamhita, a Sanskrit treatise on Ayurvedic medicine compiled by Agnivesha (c2500 BC). Chapter 20 of this volume (entitled Vepathy) contains descriptions of different patterns of tremor, some of which are associated with certain Vatas or palsies (Stern, 1989).

An Egyptian papyrus of the nineteenth dynasty (c1350–1200 BC) describes a king with what resembles Parkinsonian dribbling:

> "A divine old age had slackened his mouth. He cast his
> spittle upon the ground and spat it out." (Stern, 1989).

Later, Galen (129–199), born in Pergamon, studied in Alexandria and exposed to the Platonic, Stoic and Epicurean schools, became the most influential physician since Hippocrates. There are many references to tremor in his writings:

> "It is the impairment of the free exercise of one's faculties
> ... it is an unfortunate condition in which movement is
> unstable and not under one's own control ..." (Galen,
> 1539).

He also recognises gait disorders including *scelotybre* (troubled limbs):

> "a kind of paralysis which prevents people walking straight
> by mixing up the sides ... failing to lift the foot and putting
> it back instead, like those walking up a steep incline."
> (Galen, 1539).

Following these historical glimpses, in 1817 James Parkinson published a monograph entitled *An Essay on the Shaking Palsy*, the first detailed description of the disease which would later bear his name (Parkinson, 1817). He personally examined three of the cases, and observed the other three on the streets of London, near his Hoxton home. He described the three hallmark characteristics of the disorder which he referred to as 'paralysis agitans': tremor, rigidity and slowness of movement (bradykinesia) (Jankovic, 2008). By the late 1800s, Jean-Martin Charcot credited him with these original reports by renaming the condition 'maladie de Parkinson' or Parkinson's disease.

Nearly a century after Parkinson's published observations, Friedrich Lewy reported the presence of abnormal intraneuronal inclusions (subsequently called Lewy bodies, in his honour) in the brains of PD patients at autopsy (Lewy, 1912) and a few years later, Constantin Tretiakoff established that the substantia nigra is the main structure affected by the disease (Tretiakoff, 1919).

Once the anatomy of the disease had been clarified, the next step was to confirm the pharmacology. In 1957, Arvid Carlsson reported dopamine as a putative neurotransmitter (Carlsson et al., 1957). Shortly thereafter, Ehringer and Hornykiewicz found that dopamine concentrations are markedly reduced in the striatum of PD patients (Ehringer and Hornykiewicz, 1960). They later found that this deficiency is specifically due to loss of midbrain dopaminergic neurons. Confirmation of the critical role of dopamine was established in 1961, when intravenous L-dopa, a metabolic precursor of dopamine, was first shown to relieve the symptoms of PD (Birkmayer and Hornykiewicz, 1961). By the late 1960s, oral L-dopa had been established as a viable symptomatic treatment for PD (Cotzias et al., 1969).

The next phase of PD research was triggered by the accidental exposure of a group of Californian drug users to the toxin 1-methyl-4-phenyl-1,2,3,6-tetrahydropyridine (MPTP) in the early 1980s (Langston et al., 1983). This toxin caused an acute, irreversible Parkinsonian syndrome via inhibition of complex I of the mitochondrial electron transport chain, which rapidly caused the death of midbrain dopaminergic neurons with remarkable specificity. Reduced complex I activity was subsequently found in sporadic PD brain at postmortem (Schapira et al., 1989). By this point it was clear that mitochondria must surely play a central role in maintaining the viability of midbrain dopaminergic neurons.

The most recent era of PD research, which continues to this day, began with the discovery of the first genetic cause of PD – a condition that historically had been regarded as a sporadic disorder. In 1997, mutations in the *SNCA* gene (which encodes α-synuclein) were discovered in a large Greek-Italian kindred, many members of which had PD inherited in an autosomal dominant fashion (Polymeropoulos et al., 1997). Whilst *SNCA* mutations remain a particularly rare cause of PD, more recently a much more commonly mutated gene, called *LRRK2*, was codiscovered by two independent research groups as a cause of autosomal dominant PD, and simultaneously reported (Paisan-Ruiz

et al., 2004; Zimprich et al., 2004)). These two genes form the focus of investigation for this thesis.

To date, over a dozen loci have been linked to familial PD, and several further responsible genes have been cloned. A summary of Mendelian genes linked to PD is shown in Table 1.1.

1.2 α-SYNUCLEIN, LEWY BODIES AND SYNUCLEINOPATHIES

Depigmentation of the substantia nigra (a marker of loss of dopaminergic neurons from this area) is a pathological hallmark of PD. Lewy bodies are seen in surviving nigrostriatal neurons at autopsy and are required to make a pathologically-defined diagnosis of this disorder (Braak and Braak, 2000). A53T was the first point mutation described in *SNCA,* in a Greek/Italian kindred (Polymeropoulos et al., 1997). Two other missense mutations, A30P (Krüger et al., 1998) and E46K (Zarranz et al., 2004), have since been reported in German and Spanish kindreds respectively (see Figure 1.1 for a summary of *SNCA* mutations). The protein encoded by *SNCA*, α-synuclein, was subsequently discovered to be the predominant constituent of Lewy bodies, suggesting that it plays a central role in the pathogenesis of PD (Spillantini et al., 1997).

Triplication of the *SNCA* locus has also been reported in a separate kindred with familial PD (Singleton et al., 2003); branches of this family had been previously reported, but found via genealogical methods to be the same (Iowa, Spellman-Muenter, Waters-Miller kindred) (Spellman, 1962; Waters and Miller, 1994; Muenter et al., 1998; Farrer et al., 1999). Affected individuals from this kindred, with four copies of *SNCA* rather than the normal two, were found to have a corresponding doubling of *SNCA* mRNA and α-synuclein protein in post-mortem brain tissue (Miller et al., 2004). The observation that *SNCA* multiplication as well as point mutation can cause disease parallels a similar mechanism in Alzheimer's disease (AD) pathogenesis where either in-

GENE	YEAR	POSSIBLE ROLE	REFERENCE
SNCA (PARK1/4)	1997	synaptic or mitochondrial regulation	Polymeropoulos et al. (1997)
parkin (PARK2)	1998	E3 ubiquitin ligase specificity	Kitada et al. (1998)
UCH-L1 (PARK5)	1998	unknown	Leroy et al. (1998)
DJ-1 (PARK7)	2003	oxidative stress response	Bonifati et al. (2003)
PINK1 (PARK6)	2004	mitophagy or PI3K/Akt/mTOR pathway	Valente et al. (2004)
LRRK2 (PARK8)	2004	PI3K/Akt/mTOR pathway or miRNA regulation	Paisan-Ruiz et al. (2004); Zimprich et al. (2004)
GBA	2004	lysosomal or ubiquitin-proteasome regulation	Lwin et al. (2004)
ATP13A2 (PARK9)	2006	lysosomal function	Ramirez et al. (2006)
FBXO7	2009	E3 ubiquitin ligase specificity or cyclin D/CDK6 complex stability	Di Fonzo et al. (2009)
VPS35	2011	unknown	Zimprich et al. (2011); Vilariño-Güell et al. (2011)

Table 1.1: Mendelian genes linked to Parkinson's disease.
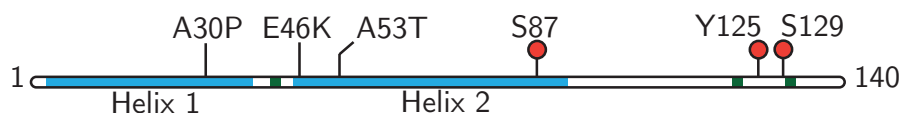
Figure 1.1: α-Synuclein ideogram showing the positions of the three pathological mutations (A30P, E43K and A53T). Phosphosites on α-synuclein are indicated by red circles. α-Helices are represented by blue and β-sheets/turns indicated by areas of green. Adapted from Hardy et al. (2009).

creased dosage or missense mutations of the *APP* (amyloid precursor protein) gene causes early-onset disease (Hardy, 2006).

Two large genome wide association studies have established *SNCA* variation as the most important genetic risk factor for sporadic PD (Satake et al., 2009; Simon-Sanchez et al., 2009). Considering all of the above findings, understanding α-synuclein biology is clearly pivotal to our understanding of PD and much of the basic research into the disease over the last decade has centred on this protein. In the following section I will review the phenotypic spectrum of *SNCA* gene dosage alterations, and discuss how this informs our understanding of PD pathogenesis.

1.3   SNCA MULTIPLICATION KINDREDS

1.3.1   *Iowa kindred*

The Iowa kindred is striking because of the wide range of disease seen in family members, probably the consequence of the large size of the kindred, described since the early 1900s (Spellman, 1962; Waters and Miller, 1994; Muenter et al., 1998; Farrer et al., 1999). Video documentation of several members of this kindred is available in Gwinn et al. (2011). Muenter et al. (1998) gave a detailed account of 13 affected individuals from this family over four generations with 'hereditary parkinsonism with dementia'. Clinical and pathological features of most affected members were typical for PD except for earlier age of

onset (mean age 33) and more fulminant course (mean life expectancy 8.1 years after disease onset, in contrast to 18.4 years in sporadic PD with onset before age 50 (Hoehn and Yahr, 1967)).

Many affected individuals in the family have carried the diagnosis of PD, and met published clinical criteria (except for a positive family history) (Hughes et al., 2001). Positron Emission Tomography scanning with 6-[18F]fluorodopa has revealed severe depletion of striatal dopamine in those family members with typical PD clinically (Muenter et al., 1998), and the presence of Lewy bodies and neuronal loss in the substantia nigra has been well described (Gwinn-Hardy et al., 2000). However, others have more prominent and early dementia, with parkinsonism, hallucinations, and fluctuations in cognition, consistent with dementia with Lewy bodies (DLB), which has been correlated pathologically with cortical Lewy bodies and Lewy neurites (McKeith et al., 2003). Another individual in this family had clinical features of parkinsonism, dementia, and dysautonomia, and dramatic α-synuclein immunoreactive glial inclusions were seen at autopsy – neuropathologically consistent with multiple system atrophy (MSA) (Gwinn-Hardy et al., 2000).

PD, DLB and MSA are collectively known as synucleinopathies, because they feature intracellular α-synuclein deposition neuropathologically, and α-synuclein is believed to be integral to their pathogenesis (Spillantini and Goedert, 2000). Therefore, the clinical phenomenology within this one kindred demonstrates that increased dosage of α-synuclein can generate the full spectrum of synucleinopathies.

1.3.2 *Additional SNCA triplication kindreds*

Farrer et al. (2004) documented a separate *SNCA* triplication kindred, called the Swedish-American kindred, after screening 42 probands with early-onset autosomal dominant PD. The proband had a similar phenotype to some Iowa kindred affecteds, with a rapidly progres-

sive dopa-responsive parkinsonism starting age 31 years. Postural hypotension, visual and auditory hallucinations arose 14 years later with worsening dementia, severe generalised rigidity and death aged 52. Elevated *SNCA* mRNA was found in postmortem brain tissue of affecteds, with doubling of α-synuclein protein, corroborating equivalent findings in the Iowa kindred (Miller et al., 2004). Severe neuronal degeneration in the substantia nigra and locus coeruleus, with widespread Lewy body pathology, was seen at autopsy. There was also severe neuronal loss in the CA2/3 area of the hypothalamus – unusual for PD or DLB but similar to that seen in six of seven autopsied cases from the Iowa kindred (Waters and Miller, 1994; Muenter et al., 1998; Gwinn-Hardy et al., 2000).

Ibanez et al. (2009) described a French kindred with *SNCA* triplication after screening 22 families with atypical autosomal dominant parkinsonism. The three affecteds had rapidly evolving symptoms with severe cognitive impairment and short disease duration until death (mean 7 years).

The fourth triplication kindred reported to date is a Japanese family comprising three individuals of consecutive generations afflicted with early-onset parkinsonism with dementia and orthostatic hypotension (Sekine et al., 2010). Triplication was confirmed in the grandson, with disease onset of 31. His father had disease onset aged 31 (and died aged 40). The proband's grandfather's age of onset was 49; he subsequently died aged 57.

Clinical features of members of these triplication kindreds are summarised in Table 1.2 (rigidity and bradykinesia were present in all cases).

1.3.3 *SNCA duplication kindreds*

SNCA duplication is now also recognised as a rare cause of familial parkinsonism, including cases which are phenotypically similar to

REFERENCE	KINDREDS	ONSET	DURATION	L-DOPA	TREMOR	AUTONOMIC	SLEEP	HALL.	DEMENT.	DEPRES.
Muenter et al. (1998)	1 (10 cases)	36 (SD 8.2)	8.4 (SD 3.7)	7/7	7/7	6/7 PH; 3/5 UI; 1/5 imp.	2/7 ins.; 3/7 RBD	NA	7/8	9/9
Farrer et al. (2004)	1 (1 case)	31	Rapid	Dramatic	7/7	Early PH	NA	Yes	Yes age 47	Yes
Ikeuchi et al. (2008)	1 (1 case)	Mc	20	NA	7/7	PH	NA	Yes	Yes age 35	NA
Ibanez et al. (2009)	1 (3 cases)	48.3 (SD 12.5)	7 (SD 2.6)	Limited	2/2	3/3 UI	NA	NA	NA	3/3
Sekine et al. (2010)	1 (3 cases)	1: 49; 2: 33; 3: 28	1: 8; 2: 7; 3: NA	3/3	3/3	3/3 PH; 1/3 imp.	1, 2: NA; 3: nil	1, 2: NA; 3: nil	1: Yes; 2: NA	1, 2: Yes

Table 1.2: Summary of clinical features of *SNCA* triplication cases. SD, standard deviation; sp., sporadic; RBD, REM sleep behavior disorder; PH, postural hypotension; UI, urinary incontinence; imp., impotence; ins., insomnia; Hall., hallucinations; Dement., dementia; Depres., depression.

idiopathic PD, with no atypical features (Chartier-Harlin et al., 2004; Ibanez et al., 2004). Duplication has also been documented in sporadic PD and these cases are clinically indistinguishable from idiopathic PD (Ahn et al., 2008; Ibanez et al., 2009).

However, more recent reports have described atypical features in duplication cases, with variability within the same family (Nishioka et al., 2006; Ahn et al., 2008). In a report of four duplication kindreds, 11 members presented with parkinsonism, six of whom developed hallucinations or delusions and three developed dementia (Nishioka et al., 2009). All kindreds had asymptomatic carriers, the oldest aged 79; the lifetime penetrance was estimated at 43.8%. A recent screen found two patients with *SNCA* duplication who developed parkinsonism around the 5th decade, followed by rapid cognitive decline, hallucinations and orthostatic hypotension (Shin et al., 2010). Neither had any family history. The authors retrospectively reviewed 32 duplication patients and found cognitive dysfunction in one third. This is comparable to the prevalence of dementia in sporadic PD, which has been estimated to be between 24 and 31% of cases(Aarsland et al., 2005). Autonomic involvement was seen in half – a similar prevalence to that seen in triplication cases. The overall time course of disease progression was also comparable to triplication cases, but with an onset over two decades later.

The Swedish-American kindred also includes an individual with *SNCA* duplication, presenting with orthostatic hypotension aged 71 and parkinsonism a year later, with frequent falls and urinary incontinence, although tremor was very mild (Fuchs et al., 2007). Imaging revealed significant reduction of dopamine transporter (DAT) in both striata. The clinical diagnosis was MSA.

Four members of a Japanese *SNCA* duplication kindred developed dopa-responsive parkinsonism, accompanied by dementia and visual hallucinations during the late stages of the disease (Ikeuchi et al., 2008). A further member developed parkinsonism aged 28, dementia aged 35 and died aged 48: a disease trajectory similar to many trip-

lication cases, including the premature onset. He was in fact found to have homozygous duplication of *SNCA*, due to consanguinuity in the family, and therefore had four copies of the gene, rather than the three expected from a single duplication.

Clinical features of duplication cases are summarised in Table 1.3 (rigidity and bradykinesia were present in all cases). Overall, the data from all of the multiplication kindreds demonstrate that gene dosage of *SNCA* determines disease onset and the severity of progression, rather than extent of the replicated region, which varies from kindred to kindred (Ross et al., 2008a; Ibanez et al., 2009).

1.4 α-SYNUCLEIN EXPRESSION IN SPORADIC PD

How might increased *SNCA* dosage be relevant to sporadic disease? Postmortem sporadic PD brain tissue has a higher expression of α-synuclein mRNA compared to controls (Chiba-Falek et al., 2006), suggesting that a similar pathogenic mechanism might be responsible. Polymorphisms in the Rep1 complex repeat site (located in the promoter region of *SNCA* approximately 10 kb upstream of the translational start of the gene) have been linked to sporadic PD (Kruger et al., 1999; Tan et al., 2000; Farrer et al., 2001b; Maraganore et al., 2006). A luciferase-based assay found a marked three-fold difference in α-synuclein expression with different Rep1 alleles in SH-SY5Y cells (Chiba-Falek and Nussbaum, 2001).

Moreover, associations have been found between Rep1 and levels of α-synuclein protein in blood samples from PD patients (Fuchs et al., 2008) and *SNCA* mRNA in control brain (Linnertz et al., 2009) whilst *SNCA* mRNA varied 1.7-fold in transgenic mice carrying the different Rep1 alleles (Cronin et al., 2009).

It is not yet known whether the higher expressing mice also have a higher incidence of PD-type pathology, but nevertheless these data

REFERENCE	KINDREDS	ONSET	DURATION	L-DOPA	TREMOR	AUTONOMIC	SLEEP	HALL.	DEMENT.	DEPRES.
Chartier-Harlin et al. (2004)	1 (5 cases)	48 (SD 10)	17 (SD 7.2)	Yes	4/5	3/5 PH	-	-	-	2/5
Ibanez et al. (2004)	2 (2 cases)	46, 50	NA	Yes	+; -	-	-	-	-	-
Nishioka et al. (2006)	2 (3 cases)	44 (SD 5.5)	NA	Yes	-	1/3 PH	NA	1/3	++ 1/3	NA
Fuchs et al. (2007)	1	71	NA	Slight	Mild	Early PH, UI	NA	Yes	Late	Brief
Ahn et al. (2008)	1 + 2 sp.	1: 40; 2: 65; 3: 50	1: short; 2,3: IPD	Yes	1: mod.; 2,3: NA	1: PH	NA	NA	1: mod; 2,3: -	NA
Uchiyama et al. (2008)	1 (2 cases)	1: 47; 2: 73	1: rapid	Yes	1: mod.; 2: mild	-	NA	2/2	1: 50; 2: 72	NA
Ikeuchi et al. (2008)	1 (3 cases)	57 (SD 16.4)	10.3 (SD 4.2)	NA	3/3	NA	NA	NA	3/3	NA
Nishioka et al. (2009)	4 (10 cases) + 1 sp.	48.5 (SD 11.2)	NA	8/11	Mild	NA	1/6 RBD	6/11	3/11	3/3
Ibanez et al. (2009)	4 (9 cases)	46 (SD 8.7)	10.5 (SD 7.2)	Yes	6/9	-	NA	NA	-	NA
Shin et al. (2010)	2 sp.	1: 48; 2:55	Rapid	Yes	Yes	Plain	NA	2/2	1: 52; 2: 59	NA
Sironi et al. (2010)	1 (1 case)	41	Rapid	Yes	-	PH	PLMD	-	-	Yes

Table 1.3: Summary of clinical features of *SNCA* duplication cases. SD, standard deviation; sp., sporadic; RBD, REM sleep behavior disorder; PH, postural hypotension; UI, urinary incontinence; imp., impotence; ins., insomnia; Hall., hallucinations; Dement., dementia; Depres., depression.

point to the possibility that sporadic disease is also caused by higher expression of α-synuclein.

Indeed, genome wide association studies reveal that variation at the *SNCA* locus is associated with sporadic PD (Satake et al., 2009; Simon-Sanchez et al., 2009) and variation at this locus has also been demonstrated in MSA (Scholz et al., 2009). In both of these studies, the association signal localises to the 3' end of *SNCA* and shows partial linkage disequilibrium with Rep1, suggesting that these variants may be different markers of a single causal variant, which likely affects gene expression levels.

1.5 IMPLICATIONS FOR α-SYNUCLEIN PATHOGENESIS

These clinical studies point to a striking dosage relationship between α-synuclein and disease. Genetic variation in *SNCA* may well increase risk of sporadic PD through increasing expression, whilst three copies of the locus rather than the normal two can, in around half of individuals, lead to parkinsonism resembling idiopathic PD (albeit with atypical features being more common). However, one additional copy confers full penetrance of what is in most cases an early-onset condition, with clinical features that can encompass PD, DLB and MSA. Therefore, modest alterations in expression level are sufficient to cause a wide spectrum of disease. Degeneration may be initially confined to the nigrostriatal pathway, but as α-synuclein dosage increases, the likelihood of more widespread pathology (e.g. cortical involvement in DLB or glial and cerebellar involvement in MSA) increases in tandem.

Increased accumulation of α-synuclein is also seen with dysfunction of several other PD genes. including *LRRK2* and *GBA*, mutations in which comprise the two commonest genetic causes of PD (Cookson, 2010; Velayati et al., 2010). Most cases of PD caused by mutations in *LRRK2* have α-synuclein pathology (discussed below in Section 1.7.1). Previously, overexpression of mutant *LRRK2* was seen to increase α-

synuclein deposition and neurodegeneration in A53T transgenic mice, perhaps explained by the observed impaired microtubule dynamics and Golgi fragmentation increasing local concentrations of α-synuclein in the soma, whilst knockout of *LRRK2* was found to be protective (Lin et al., 2009). However, recent contradictory data suggest that neuropathology in the A53T mouse proceeds irrespective of deletion of *LRRK2* or overexpression of wildtype or G2019S mutant *LRRK2* (Daher et al., 2012; Herzig et al., 2012), implying that the interaction is more complex than previously thought, if it exists at all.

GBA encodes glucocerebrosidase, and mutations lead to a deficiency of this protein. This in turn precipitates accumulation of its substrate glucocerebroside, which has recently been shown to stabilise oligomeric α-synuclein intermediates – permitting their conversion into fibrils – whilst α-synuclein itself inhibits the normal lysosomal activity of glucocerebrosidase, leading to further accumulation of glucocerebroside, thus forming a pathogenic positive feedback loop (Mazzulli et al., 2011).

Recessive mutations in *parkin* cause young-onset disease (Kitada et al., 1998). Here too a mechanism increasing local concentrations of α-synuclein may be responsible. *Parkin* encodes an E3 ubiquitin ligase which provides specificity for the process of tagging proteins for degradation in the proteasome (Shimura et al., 2000) and PD-associated mutations disrupt this ligase activity (Tanaka et al., 2004). A glycosylated form of α-synuclein has been shown to be a potential target of this ligase activity (Shimura et al., 2001) although it remains unclear whether this form is pathologically relevant. Furthermore, PD caused by mutations in *parkin* generally cause nigral degeneration without Lewy body pathology (Hardy et al., 2009), although Lewy bodies have been reported in individuals with heterozygous mutations in this gene (Farrer et al., 2001a; Pramstaller et al., 2005). Therefore perhaps *parkin* mutations can also augment accumulation of α-synuclein via impairing its degradation in the proteasome.

Taking this clinical and genetic evidence together (summarised in Figure 1.2), what can be inferred about the possible mechanisms of α-synuclein-mediated pathogenesis?

1.5.1 *Disruption of the normal role of α-synuclein*

Synucleins are abundant neuronal proteins, enriched in presynaptic termini (Maroteaux et al., 1988), but their physiological role is unknown. α-Synuclein knockout mice are normal, apart from exhibiting increased release of dopamine from nigrostriatal neurons under certain conditions, implying that the protein can negatively regulate dopaminergic neurotransmission (Abeliovich et al., 2000). Given potential redundancy between synucleins, this work was extended in triple knockout mice lacking α-, β- and γ-synuclein: here, a clear phenotype emerges of an age-dependent alteration in axonal morphology, neuronal dysfunction and decreased survival (Greten-Harrison et al., 2010).

Maintenance of protein complexes involved in synaptic release requires chaperone activity mediated by synucleins; these protein complexes are decreased in the αβγ-synuclein knockout mouse (Burré et al., 2010). Subtle overexpression of α-synuclein in mice (in a range similar to that seen clinically) impairs neurotransmitter release via defective synaptic vesicle recycling, in the absence of overt toxicity (Nemani et al., 2010). However, it remains to be seen whether this functional perturbation can lead to neuronal loss over the time course seen in PD.

α-Synuclein has been shown to bind to mitochondria, more so when overexpressed, impairing complex I function, decreasing respiration and increasing free radical production (Loeb et al., 2010; Chinta et al., 2010). Expression of α-synuclein in mammalian neurons (both *in vitro* and *in vivo*) leads to fragmentation of mitochondria (Nakamura et al., 2011) whilst in cultured cells and in *C. elegans*, α-synuclein also causes
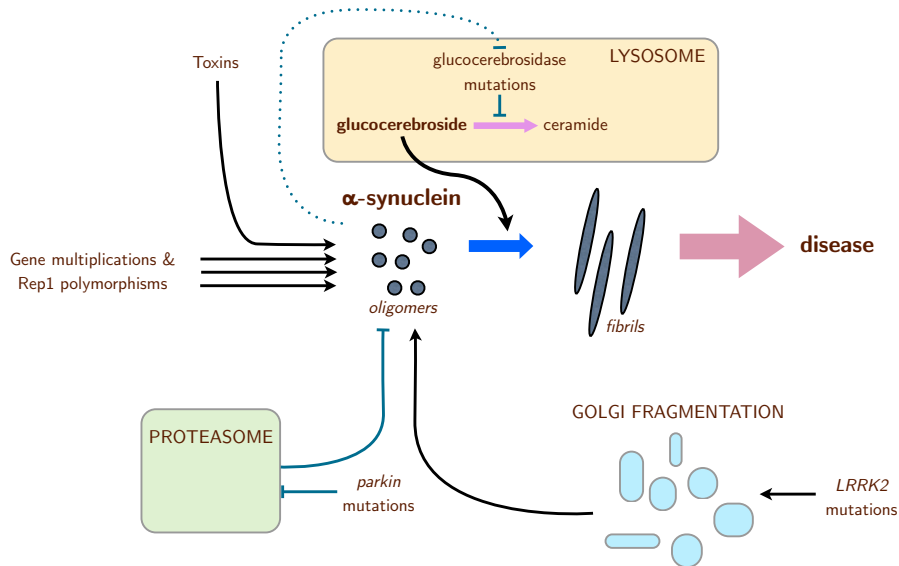
Figure 1.2: Multiple pathways promote accumulation and aggregation of α-synuclein. Gene multiplications and certain Rep1 polymorphisms can increase expression of α-synuclein directly. On the other hand, degradation of α-synuclein in the proteasome may be impaired by *parkin* mutations. Mutated LRRK2 can fragment golgi, disrupting vesicular trafficking and thereby increasing α-synuclein in the soma. Mutations in glucocerebrosidase cause accumulation of glucocerebroside, which stabilises oligomeric α-synuclein, enhancing fibril formation. In turn, α-synuclein impairs physiological glucocerebrosidase function. Multiple environmental toxins, including heavy metal cations, organic solvents and pesticides, can enhance misfolding and aggregation of α-synuclein. However, it is currently unclear what species of α-synuclein (oligomers or fibrils) are toxic to cells.

A

dysfunction of mitochondria (Kamp et al., 2010). These are pertinent findings given the importance of mitochondria in maintaining neuronal viability in PD (Knott et al., 2008; Henchcliffe and Beal, 2008). Mice overexpressing the disease-associated A53T *SNCA* mutation develop mitochondrial DNA damage and degeneration (Martin et al., 2006), and α-synuclein pathology in this model is exacerbated by exposure to paraquat (Norris et al., 2007). In contrast, dopaminergic neurons in α-synuclein knockout mice are resistant to the neurotoxin MPTP (Klivenyi et al., 2006).

Overexpression of α-synuclein has also been shown to impair autophagy, a major route for clearance of aggregate–prone intracytoplasmic proteins, whilst α-synuclein depletion enhances this pathway (Winslow et al., 2010). Overexpressing cells would also likely clear dysfunctional mitochondria less efficiently, increasing susceptibility to apoptotic stimuli. The combination of these perturbations, persisting over many decades, might be sufficient to cause neuronal death.

1.5.2 *Toxicity of α-synuclein*

Fibrillogenic monomers of α-synuclein form oligomeric intermediates which assemble into fibrils, and finally deposit in Lewy bodies (Schulz and Falkenburger, 2004). α-Synuclein has a strong tendency to self-aggregate *in vitro*. Therefore, increasing its expression would be expected to generate more of these aggregates (Uversky, 2007). However, a pivotal question is which of these species, if any, are toxic to neurons?

For example, there is a dissociation between presence of Lewy bodies and cellular loss: Lewy bodies are present in 10-15% of individuals over the age of 65 who die without clinical evidence of neurological illness, despite having an identical pattern of deposition to that seen in PD, although such cases may represent pre-clinical PD which would manifest given time (Gibb and Lees, 1988). Cytotoxicity in model

systems can occur without aggregated α-synuclein (Xu et al., 2002). Lentiviral expression of α-synuclein in rat nigrostriatal neurons results in selective dopaminergic toxicity, but without fibrillar inclusions, whilst missense mutations in *SNCA* (for example, A30P) increases oligomerisation of α-synuclein, but not fibril formation (Conway et al., 2000; Lo Bianco et al., 2002).

The mechanism of toxicity is not clear, but there are several hypotheses, for example through disruption of membranes via the formation of pores (Lashuel et al., 2002). Lewy body formation might, in fact, be an adaptive cellular response, protecting neurons from the damaging effects of oligomeric intermediates.

1.5.3 *Permissive templating of α-synuclein*

Transplantation of fetal dopaminergic neurons began over twenty years ago as a potentially curative treatment for PD (Bjorklund et al., 2003). Recently, several individuals with these transplants have come to autopsy, with surprising results. Lewy body pathology is observed in surviving nigrostriatal neurons, as expected. But in eight patients who have received this treatment, Lewy bodies were observed in the transplanted dopaminergic neurons as well (Kordower et al., 2008a; Li et al., 2008; Kordower et al., 2008b). There are two possible explanations for these findings:

1. Lewy body pathology arises *de novo in* these transplanted cells. However, these grafts have all been less than 14 years old at the time of autopsy, yet PD is a disease of old age. Is this not far too early for such pathology to develop?

2. Alternatively, pathology spreads from the diseased host neurons to the grafted cells, reminiscent of a prion-like process.

Prion diseases are characterised by spread of prion protein (PrP) from one organism to another. Healthy cellular PrP (designated PrP^C) is

ubiquitously expressed and has the same amino acid sequence as the disease-causing scrapie isoform (PrP^{Sc}) but a different secondary structure, being composed largely of α-helices whilst PrP^{Sc} is predominantly β-sheets. Disease is caused by a change in conformation of PrP^{C} to PrP^{Sc}, which can act as a template for recruitment of PrP^{C}, converting them into PrP^{Sc}. Aggregates of the disease isoform build up, and propagate between cells leading to disease progression (reviewed by Aguzzi et al. (2008)).

α-Synuclein is unstructured in aqueous buffers, whilst adopting a predominantly α-helical structure when membrane bound, which can become β-sheet when present at high concentration or in mutant form (Conway et al., 1998). α-Synuclein is present in cerebrospinal fluid and plasma of healthy subjects and patients with neurodegenerative diseases (El-Agnaf et al., 2006; Noguchi-Shinohara et al., 2009), and can be detected in media of neuronal culture models (Lee et al., 2005). More specifically, exosomes released by α-synuclein overexpressing SH-SY5Y cells contain α-synuclein and pharmacological inhibition of lysosomal function increases this release (Alvarez-Erviti et al., 2011).

Recent studies have provided direct evidence of cell-to-cell spread: neurons overexpressing α-synuclein can transmit the protein to neighboring neurons in culture, and to neural precursor cells in a transgenic model of PD-like pathology (Desplats et al., 2009) and also to postmitotic nigrostriatal neurons, in a direct model of the fetal transplantation clinical studies (Hansen et al., 2011). Oligomers of α-synuclein can recruit, and aggregate, α-synuclein endogenously expressed by primary cortical neurons, and this effect increases with time and also with concentration of the applied oligomers (Danzer et al., 2009). In other words, misfolded α-synuclein might operate as a template catalysing further misfolding events (Hardy, 2005).

Transmission of misfolded α-synuclein between cells provides a mechanistic basis for the findings of Braak et al. (2003) where α-synuclein pathology extends sequentially from the dorsal motor nucleus in the lower brainstem, to upper brainstem areas and from there

to the cerebral hemispheres. The authors speculate that PD pathology may arise first in the nose and foregut, which act as portals for entry of an unknown neurotropic pathogen, via inhalation or ingestion, and suggest that this pathogen may trigger misfolding of α-synuclein (Hawkes et al., 2007).

An alternative possibility is that an environmental toxin, rather than a pathogen, is responsible. Many potential neurotoxins, including metals, solvents, pesticides and herbicides have been linked to PD (reviewed by Uversky (2007)). Paraquat and rotenone enhance production of α-synuclein *in vivo,* whilst *in vitro*, fibrillation of α-synuclein is dramatically accelerated by these and other substances, including heavy metal cations and organic solvents. These can all induce structural perturbations in α-synuclein and stabilise partially folded structures, which are prone to form fibrils.

Increased *SNCA* expression could cause PD by augmenting the likelihood of α-synuclein misfolding, the quantity of exocytosed misfolded proteins, and the speed of nucleation in recipient cells. Age is the major risk factor for sporadic PD, and concentration of α-synuclein increases with age in neuronal cell bodies (Chu and Kordower, 2007). Therefore, in both *SNCA* multiplication and sporadic PD, initiation of disease relates to and appears to be dependent on the concentration of the pathogenic protein, perhaps through increasing the chances of a misfolding species emerging, which could form a scaffold for further proteins to misfold and aggregate.

α-Synuclein fibrillisation starts *in vitro* with a lag-phase during which soluble oligomers form a nucleus, but once the nucleus forms, aggregates grow rapidly (Wood et al., 1999). Therefore, the prediction would be that permissive templating is efficient and less dependent on the concentration of the protein than the initial misfolding event, such that the process becomes self-propagating. This would explain the variable age of onset of disease, even in triplication cases, given the stochastic nature of protein misfolding. Recent data suggests that prion propagation *in vivo* proceeds via two phases: an initial exponential

phase not dependent upon levels of PrP^C, followed by a plateau phase prior to clinical onset, the duration of which is shortened as endogenous PrP^C levels are increased (Sandberg et al., 2011). The authors suggest that toxicity is exerted by neither PrP^C nor PrP^{Sc} but via a toxic intermediate, generation of which requires conversion to take place and is therefore dependent on local availability of PrP^C. If a similar mechanism is at work in the synucleinopathies, the implication of increasing *SNCA* expression becomes clear: time to onset of disease is shorter.

1.6 IMPLICATIONS FOR DISEASE-MODIFYING PD THERAPIES

Neither the physiological nor the pathogenic roles of α-synuclein are fully understood. Nevertheless, the clinical, genetic and toxin studies described above speak to the importance of α-synuclein concentration, and cell-to-cell spread, in driving disease onset and progression. Therefore, strategies that seek to either deplete, or prevent spread, of α-synuclein ought to be clinically beneficial.

A recent report of an inducible α-synuclein transgenic mouse model of DLB showed that reducing α-synuclein expression triggered a reversal in pathological changes and improved behaviour and memory (Lim et al., 2011). This provides proof of concept data that α-synuclein depletion might not just slow disease progression, but in fact reverse it.

However, it is not yet clear how this depletion should be achieved. Several studies have employed RNA interference to successfully reduce α-synuclein expression in cells (Fountaine et al., 2008), rodents (Sapru et al., 2006; Lewis et al., 2008) and primates (McCormack et al., 2010), although reversal of pathological changes has not been demonstrated with this approach so far. Moreover, α-synuclein silencing caused nigral *degeneration* in rat (Gorbatyuk et al., 2010), precisely the opposite effect of that desired. The reasons for this are not certain,

and seem at odds with *SNCA* knockout mouse models that are relatively normal (Abeliovich et al., 2000). Nevertheless, given that *in vivo* levels of α-synuclein are likely to be tightly regulated, perhaps the goal should be normalisation of α-synuclein levels rather than full suppression.

There is also the wider problem of turning such antisense strategies into viable drugs. Problems with degradation of the introduced oligonucleotides, and off-target effects are commonly seen (Jones, 2011), notwithstanding the considerable difficulties of delivering such an agent into the brain.

Enhancing degradation of α-synuclein protein might be a viable possibility. Pharmacological upregulation of autophagy has been shown to help clear the protein, for example (Sarkar et al., 2007). Antibody-based strategies also look promising. Vaccination of human α-synuclein-expressing mice with human α-synuclein protein led to degradation of aggregates of human α-synuclein, a reduction in formation of new aggregates, and diminished neurodegeneration (Masliah et al., 2005). Indeed, the presence of autoantibodies directed against α-synuclein has recently been reported in PD patients, and antibody titres reduce with progression of disease, implying that immune-mediated clearance of α-synuclein may be a factor in determining disease onset (Yanamandra et al., 2011).

Much current work focuses on α-synuclein depletion as a possible therapeutic strategy. However, when we consider the ascending pathology noted by Braak et al. (2003), the spectrum of pathology seen in the multiplication kindreds, and the presence of Lewy bodies in grafted fetal dopaminergic neurons, then cell-to-cell protein propagation begins to take on a central role in the disease process. The mechanistic basis for this propagation has not yet been fully defined. Nor is it known whether it serves a physiological purpose. Nevertheless, blocking it is an attractive potential therapeutic target. This strategy may help preserve brain areas not yet affected by the pathological process, if potentially toxic forms of α-synuclein are pre-

vented from reaching them. It might also avoid potential side effects of excessive α-synuclein depletion. However, it remains possible that cellular release of α-synuclein might be a mechanism by which cells can lower concentrations of this protein before they become dangerously high. Therefore, it is conceivable that the combination of α-synuclein depletion with blockade of its propagation will be required to make a clinically detectable impact on disease progression. We therefore need strategies that normalise α-synuclein levels rather than fully deplete it, and are deliverable intrathecally. In addition, we need to understand precisely how, and importantly why, α-synuclein propagates from cell to cell, in order to appropriately target it.

1.7 THE ROLE OF LRRK2 IN PD

Mutations in *LRRK2* (leucine-rich repeat kinase 2) were established as an autosomal dominant cause of familial PD in 2004 (Paisan-Ruiz et al., 2004; Zimprich et al., 2004). *LRRK2* mutations are currently regarded as one of the commonest genetic causes of PD, accounting for 2 to 4% of all PD cases (Bonifati, 2006). The phenotype of PD caused by mutations in *LRRK2* is very similar to sporadic disease, with similar age at onset, clinical presentation, rate of progression, pathological features and response to L-dopa, suggesting that there may be a shared aetiology (Khan et al., 2005). Furthermore, genome wide association studies suggest that common variation at the *LRRK2* locus influences the development of sporadic PD: a European cohort study is supportive of a link (Simon-Sanchez et al., 2009) whilst a Japanese cohort study found a significant link (Satake et al., 2009). Taken together, studying the impact of *LRRK2* mutations should help us understand the pathogenesis of sporadic disease, given the strong similarities between the two.

LRRK2 encodes a member of the ROCO family of proteins, containing a ROC (Ras of complex proteins)/GTPase, COR (C-terminal of
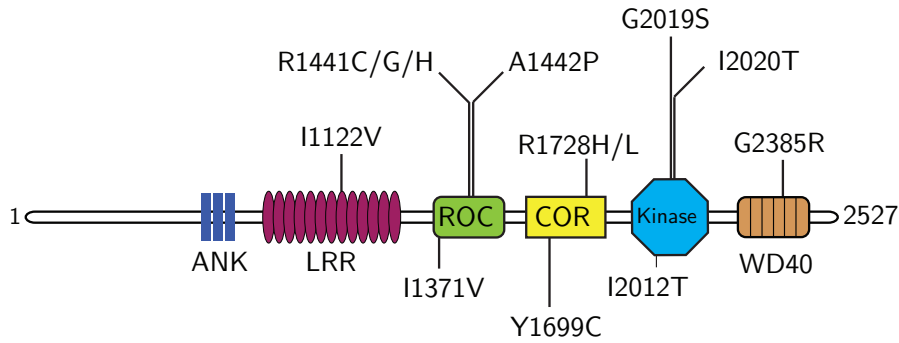
Figure 1.3: LRRK2 ideogram. Mutations associated with disease are shown. ANK, ankyrin repeats; LRR, leucine rich repeats; ROC, Ras of complex proteins; COR, C-terminal of ROC. Adapted from Hardy et al. (2009).

ROC) and a kinase domain, flanked by several protein-protein interaction motifs including a WD40 domain and Leucine Rich Repeats (Marin, 2006). Figure 1.3 shows an ideogram of LRRK2 depicting the domains and the sites of pathogenic mutations. The precise physiological role of LRRK2 is unknown, and mutations associated with PD can be found throughout the length of the gene, although there is a degree of clustering within the enzymatic domains (Paisán-Ruíz et al., 2008), and these appear to be the ones that exhibit penetrance (Ross et al., 2011). *In vitro* studies suggest that mutations in the GTPase domain and the COR domain decrease GTPase activity, whilst most mutations in the kinase domain increase kinase activity (reviewed by Cookson (2010)).

The three dimensional structure of full length LRRK2 is not known, although the crystal structure of the ROC domain suggests that LRRK2 is a dimer, supported by evidence from cellular studies (Deng et al., 2008; Greggio et al., 2008). LRRK2 associates with membranous structures including the mitochondrial outer membrane, as well as lysosomal vesicles and punctate structures within the perikarya, dendrites and axons (Biskup et al., 2006; Hatano et al., 2007). It is also found in association with Golgi apparatus, plasma membranes and synaptic vesicles.

Studies of LRRK2 in rat neurons suggest a physiological role in the regulation of neurite process morphology (MacLeod et al., 2006). Expression of G2019S LRRK2 in SH-SY5Y cells leads to neurite shortening associated with increased autophagic vacuole content, whereas RNA knockdown of autophagy-relevant proteins or interference with the MAPK/ERK signalling pathway reverses this phenotype (Plowey et al., 2008). LRRK2 interacts with parkin (recessive mutations in which cause juvenile parkinsonism) *in vitro* but not α-synuclein or tau (Smith et al., 2005). The ROC domain has been shown to be capable of interacting with β-tubulin, a key component of microtubules, and moesin (Jaleel et al., 2007; Gandhi et al., 2008). Of more apparent relevance is a possible interaction with α-synuclein: Qing et al. (2009) have shown that recombinant LRRK2 is capable of phosphorylating α-synuclein *in vitro*, and G2019S mutant LRRK2 even more so. *In vivo* studies are required to clarify all of these findings, but these data nevertheless suggest interactions with pathways already implicated in PD pathogenesis.

1.7.1 *Tau, tangles and tauopathies*

Although patients with mutations in *LRRK2* have in general a uniform phenotype that closely resembles sporadic PD, a remarkable feature of these cases is that they display highly variable pathology. Two cases from a clinically uniform R1441C kindred displayed respectively Lewy body pathology typical of PD and a Lewy body distribution similar to DLB, whereas a third case had no observable protein deposition (Zimprich et al., 2004). A fourth case displayed a different pathology altogether: neurofibrillary tangles (NFTs) in a pattern similar to that seen in progressive supranuclear palsy. Cases with the G2019S mutation have variably shown either Lewy body pathology, or NFT pathology (Rajput et al., 2006). This holds true for cases with the Y1699C mutation and a case with the I1371V mutation (Khan et al., 2005; Giordana

et al., 2007). Four members of the original Japanese kindred, carrying the I2020T mutation, displayed nigral cell loss without distinct pathology (Funayama et al., 2005). More recently, inclusions of TDP-43 (TAR DNA binding protein 43) have been found at post mortem in individuals with LRRK2 PD: Covy et al. (2009) report such inclusions in the temporal cortex (though not elsewhere) in two patients with tangle-predominant DLB, whilst Wider et al. (2010) report these inclusions in a patient with otherwise pure nigral degeneration. TDP-43 is a major constituent of intracellular inclusions seen in patients with frontotemporal lobar degeneration (Neumann et al., 2006).

NFTs are aggregates of the protein tau, encoded by *MAPT* (microtubule-associated protein tau, in full). In 1998, mutations in *MAPT* were linked to frontotemporal dementia with parkinsonism linked to chromosome 17 (FTDP-17), providing a direct link between tau and pathogenesis in these cases (Hutton et al., 1998). Just as the synucleinopathies (PD, DLB and MSA) are defined by intracellular aggregates of α-synuclein, the tauopathies – comprising PSP, corticobasal degeneration (CBD), and frontotemporal dementia (FTD) – are defined by tau deposition. The heterogeneous nature of LRRK2-associated pathology has led to the suggestion that LRRK2 may link tau and α-synuclein by operating upstream of their respective pathological cascades.

Tau is a microtubule-associated protein that is abundant within the central nervous system and exists as six alternatively spliced isoforms (Andreadis, 2005). Tau stabilises microtubules by promoting their polymerisation and suppressing their dissociation, and appears to have a stabilising role during axonal outgrowth (Ballatore et al., 2007). Suppression of tau expression decreases neurite formation, with ectopic expression of tau leading to growth of axon-like structures. Tau isoforms differ by the number of microtubule binding domains that are present. It is an abundantly phosphorylated protein: phosphorylation has been reported at 30 out of a possible 70 serine and threonine residues.

Akin to amyloid formation by α-synuclein, tau can aggregate to form paired helical filaments, which are deposited in NFTs. Several lines of evidence suggest that oligomeric tau is the toxic species, rather than NFTs themselves (Iqbal et al., 2005). NFT-bearing neurons can survive for decades and there is no apparent causal relationship between apoptotic morphology and tau deposition. In *D. melanogaster*, retinal degeneration is observed with tau expression alone, and neuronal death can be seen without NFTs (Wittmann et al., 2001). Suppressing tau expression in a mouse model of FTDP-17 improves memory function and stabilises neuronal numbers, despite the continued presence of tangles (Santacruz et al., 2005).

The role of phosphorylation is a critical aspect of the biology of tau. Increased phosphorylation of tau negatively regulates its binding to microtubules and tau is hyperphosphorylated in the paired helical filaments that form NFTs. MAPK activation due to oxidative stress leads to phosphorylation of tau (Zhu et al., 2000). Following hyperphosphorylation, tau dissociation from microtubules increases the concentration of soluble tau, enhancing its propensity to aggregate (Garcia de Ancos et al., 1993). Mutations in tau cause disease by impacting on alternative splicing, or point mutations that impair the ability of tau to bind to microtubules.

In addition to the pathological parallels between tau and α-synuclein, there is significant overlap at the genetic and clinical levels. Tauopathies often have parkinsonian features, whilst synucleinopathies can present with dementia (Galpern and Lang, 2006). Both tau and α-synuclein inclusions have been reported in some disease cases, with Lewy bodies and NFTs sometimes present in the same cell. In the Contursi kindred, carrying the A53T *SNCA* mutation, tau inclusions were observed in some individuals, in addition to Lewy bodies (Duda et al., 2002).

Furthermore, an increase in the overall burden of tau can also cause disease: the H1 haplotype (which increases transcription of tau) predisposes to tauopathies (Kwok et al., 2004). *In vitro*, α-synuclein binds tau, can stimulate its phosphorylation, and initiate its polymerisation

(Jensen et al., 1999; Giasson et al., 2003). Both proteins can synergistically aggregate to form homopolymers. There is also an interaction in animal models of disease: bigenic mice overexpressing α-synuclein and tau display exacerbated pathologies for both proteins compared to the monogenic equivalents (Giasson et al., 2003). Finally, a synergistic interaction between tau and α-synuclein has been shown in the development of cognitive impairment in PD patients, where the combination of the *MAPT* inversion polymorphism and a single nucleotide polymorphism (SNP) in *SNCA* doubles the risk of developing cognitive impairment, whereas either alone only marginally increases risk (Goris et al., 2007).

1.7.2 *LRRK2 and pathogenesis*

The G2019S mutation in the kinase domain of LRRK2 has been shown to increase its activity, whilst mutations in the ROC domain disrupt GTPase activity or increase its affinity for GTP (West et al., 2005; Lewis et al., 2007; Li et al., 2007). The Y1699C mutation in the COR domain has recently been shown to decrease GTPase activity as well (Daniëls et al., 2011). These studies are consistent with a model where the GTPase domain regulates the activity of the kinase domain, with mutations acting to increase the activity of the latter (West et al., 2007). However, not all the experimental data fits with this model: mutations outside of the kinase domain do not consistently raise kinase activity by *in vitro* assay (Greggio et al., 2006), and the G2385R mutation, a known risk factor for PD located in the WD40 domain, causes a partial loss of kinase function (Rudenko et al., 2012). It is possible that mutations in the COR domain alter the spatial relationship, and therefore the interaction, between the ROC and kinase domains, and that mutations in the protein/protein interaction domains change binding to substrates or regulatory proteins, but more structural data or physiological substrates are needed to examine this.

What is becoming clear is that the enzymatic activities of LRRK2 play a central role in disease. For example, LRRK2 mutants are less cytotoxic if the GTP binding or kinase activity of LRRK2 is artificially ablated (Greggio et al., 2006; Smith et al., 2006). Mirroring the aggregation seen with α-synuclein and tau, there is some evidence that LRRK2 may also aggregate and form inclusions. When *LRRK2* is overexpressed in some cells, the protein can form inclusion bodies that are exacerbated if carrying mutations, and LRRK2 has been found in Lewy bodies in sporadic PD (Greggio et al., 2006).

There are clear pathogenic links between mutations in *MAPT* or *SNCA* and familial PD. Furthermore, genetic variability at these loci are also associated with sporadic disease. Genome wide analysis of sporadic PD has demonstrated linkage to chromosome 17 in the *MAPT* region (Scott et al., 2001). The A0 *MAPT* allele (Pastor et al., 2000) and H1 haplotype (Martin et al., 2001; Healy et al., 2004) are overrepresented in the context of sporadic PD. Meanwhile, *SNCA* is a clear susceptibility gene for sporadic PD, as described in Section 1.4. Similarly, the *LRRK2* G2019S mutation is significantly more common in patients with sporadic PD than in controls (Hulihan et al., 2008), with an overall prevalence of 1% in cases of sporadic PD, and 4% in hereditary PD. Furthermore, the common genetic *LRRK2* variants G2385R and R1628P both increase the risk of developing sporadic PD in Chinese populations (Tan, 2007; Ross et al., 2008b).

Taken together, these findings suggest that the distinction between sporadic and familial disease is somewhat arbitrary. The extremes of fully penetrant genetic and apparently sporadic PD should be considered opposing ends of a spectrum. Most cases of PD will result from a combination of environmental and genetic factors, underlining the importance of genetic findings in understanding how sporadic disease develops. Intriguingly, as yet there is no documented link between LRRK2 and tauopathies or synucleinopathies presenting without pure parkinsonism, for example AD (Toft et al., 2005), PSP (Ross et al., 2006) or MSA (Ozelius et al., 2007). It is not known whether variation

in *LRRK2* alter the likelihood of developing these diseases – there is
no evidence for a direct autosomal dominant causative relationship
– but it would be possible to rationalise such a connection given the
unpredictable nature of LRRK2 PD pathology. Future genome-wide
association studies might bring some clarity to this issue.

1.7.3 *A pathogenic troika*

Individually, mutations in *SNCA* and *MAPT* lead to parkinsonism and
dementia characterised by protein deposition in Lewy bodies and NFTs
respectively, whereas mutations in *LRRK2* generate PD coincident with
α-synuclein or tau pathology. In light of the evidence linking LRRK2
kinase dysfunction to disease, an attractive hypothesis is that tau
and α-synuclein are downstream targets of this activity, linking in to
the dysregulation of the phosphorylation state of these proteins. As
yet, however, firm experimental evidence for this is lacking: there is
a report of abnormally deposited and phosphorylated tau in a rat
neuronal cell model (MacLeod et al., 2006), and LRRK2 appears to be
capable of phosphorylating α-synuclein at Serine 129 (G2019S mutated
LRRK2 even more so) in a transfected HEK 293T model (Qing et al.,
2009). Based upon the genetic evidence, where α-synuclein and tau
are capable of causing disease independent of mutations in *LRRK2*,
with tau also reacting to deposition of Aβ in AD, the data suggest that
there are separate, yet interlinked, pathways in operation (Figure 1.4).

One of the most perplexing aspects of LRRK2 pathobiology is how
identical mutations in the same kindred can generate different patholo-
gies. There are several hypotheses, which are not mutually exclusive,
for why this might occur, as follows.
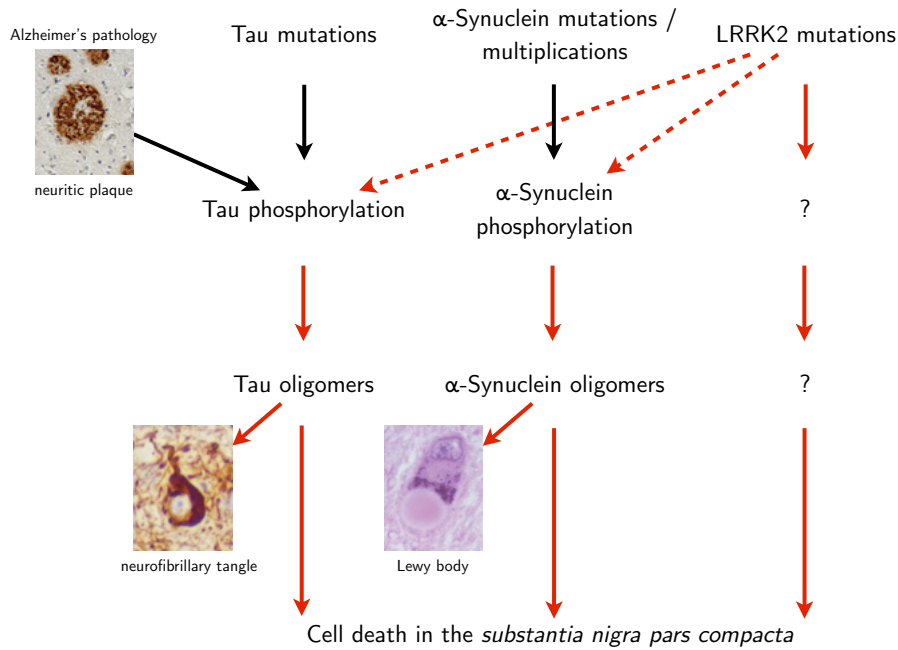
Figure 1.4: The parallel and interlinking pathways between tau, α-synuclein and LRRK2 neurodegeneration linked to parkinsonism and dementia, showing the potential crosstalk between LRRK2 and pathology associated with tau and α-synuclein dysfunction.

1.7.4 *Impact of genetics*

Outside of the context of LRRK2 disease, *MAPT* haplotypes and *SNCA* expression levels are known to alter the likelihood of developing corresponding tau or α-synuclein pathology, so the simplest explanation would be that genetic variability at these loci determine resulting pathology. The other possibility is that as yet undetermined gene or genes play a regulatory role, perhaps by providing an interface for crosstalk between the three pathways of LRRK2, tau and α-synuclein (Figure 1.4). So far, the number of LRRK2 cases that have come to autopsy is too small to study for potential genetic modifiers, but this should become tractable with time given the prevalence of mutations.

1.7.5 *Impact of environment*

Twin studies have suggested that non-genetic factors play a major
part in the development of PD. Epidemiological data have suggested
several possibly environment-linked factors that affect the likelihood
of developing PD, including pesticides, farming and head trauma
(Chade et al., 2006; Ascherio et al., 2006). There are also examples from
other neurodegenerative diseases. Repetitive head trauma can lead
to a dementing state both clinically and pathologically similar to AD,
termed dementia pugilistica (Schmidt et al., 2001). Subacute sclerosing
panencephalitis (SSPE), which presents with NFT pathology, can arise
as a rare late complication of infection with measles (Bancher et al.,
1996).

Therefore, different environmental factors might steer LRRK2 ei-
ther towards tau or α-synuclein pathology. There are two potential
difficulties with examining this hypothesis. Firstly, many of the epi-
demiological reports on PD do not describe the neuropathology of
the cases studied, and so it is currently tricky to build a model link-
ing specific pathologies with specific environmental insults. Secondly,
diseases with environmental links previously viewed as robust have
been called into question. For example, the parkinsonism-dementia
complex of Guam (NFT pathology) is now no longer felt to be due
to Cycad exposure (Steele and McGeer, 2008). Encephalitis lethargica
(another NFT disease) was originally thought to be a consequence
of influenza, because an outbreak occurred contemporaneously with
an outbreak of Spanish influenza in the early 20th century, though
opinion has since diverged (McCall et al., 2008). What is certain is
that it will require large numbers of cases of LRRK2 PD with neu-
ropathological correlation and extensive clinical and biographic details
to establish any environmental links with certainty.

1.7.6 *LRRK2 PD as a separate disease entity*

I have discussed evidence that suggests at least some mutations in *LRRK2* can dysregulate the protein's kinase activity. But LRRK2 may convey pathology via other mechanisms: for example, wildtype but not mutated LRRK2 can attenuate stress-induced cell death via activation of the ERK pathway in a cell model (Liou et al., 2008), building upon previous work which found that phosphorylation of proteins on the ERK pathway was reduced in leucocytes carrying the G2019S mutation (White et al., 2007).

These findings each shed light on separate, though not mutually exclusive, mechanisms through which LRRK2 might convey toxicity. One possible consequence is that the relative balance between LRRK2 gain of function (via kinase dysregulation) and loss of function (via ERK pathway inactivation for example) determines the pathology that results. The demonstration of phosphorylation and deposition of tau in diseases that are not classically regarded as neurodegenerative (e.g. secondary progressive multiple sclerosis (Anderson et al., 2008)) suggests that tau pathology might be a relatively generic, or default, pathway to neuronal death. On the other hand, α-synuclein pathology might require more stringent provocation. Therefore, one might predict that tau pathology results from LRRK2 loss of function, and α-synuclein pathology from LRRK2 gain of function. Genetic and environmental modifiers would determine which of these prevails.

However, how can we account for cases where no specific pathology is seen, for example in I2020T mutation cases? Perhaps in these circumstances neurons die before typical tau or α-synuclein pathology can be generated, with a predominance of protofibrils rather than mature aggregates, in which case a further prediction would be that these cases generally have a younger clinical onset of PD and a more rapid clinical course. Current epidemiological data are insufficient to draw conclusions on this.

An alternative possibility is that any observable neuropathology is an epiphenomenon, and that deranged LRRK2 drives neuronal death through a separate pathway. LRRK2 has also been linked to leprosy (Zhang et al., 2009) and Crohn's disease (Franke et al., 2010) via genome wide association studies. Furthermore, LRRK2 has been found to be genetically amplified or overexpressed in cases of papillary renal cell carcinoma and thyroid cancer (Looyenga et al., 2011). These studies certainly hint at LRRK2 dysfunction having a broad impact on cell regulation, potentially through multiple pathways.

Given evidence that neither tau nor α-synuclein accumulation and aggregation directly correlates with neuronal death, perhaps LRRK2 can steer pathology without the help of the other members of the troika. In any case, it does suggest that the correlation between clinical phenotype and genotype is more robust than that between phenotype and neuropathology. Returning to the therapeutic standpoint, clarification of which of these possibilities is pivotal, because these hypotheses suggest that attenuating dysregulated LRRK2 kinase activity may not be sufficient to limit development of PD, at least in some cases.

1.7.7   *The complexity of PD pathogenesis*

PD pathogenesis is not a simple, linear pathway, universally triggered by a single event. Instead, akin to cancerous cells developing malignant potential through accumulation of several carcinogenic mutations, there may be a requirement for multiple insults to occur before dopamine neuron loss ensues. These can be divided into neuronal stressors (e.g. oxidative) and diminished compensatory responses (e.g. impairment of the proteasomal pathway). The age-related increase in both PD prevalence, and LRRK2 penetrance, are consistent with this view.

There are three fundamental aspects of LRRK2 in particular that need to be clarified in order to understand its role in PD pathogenesis more completely:

1. the *in vivo* substrates of LRRK2, so that we can begin to work out which intracellular pathways it maps to,

2. the structure of LRRK2, so we can begin to comprehend how it interacts with these pathways,

3. the means by which LRRK2 modifies tau and α-synuclein biology specifically.

Understanding how the pathogenic mutations in LRRK2 impact upon these three characteristics should aid the development of mechanistic therapies for PD.

1.8 THE NEED FOR NEW CELL MODELS

The biggest barrier to research on neurological disease is the inaccessability of diseased tissue. Moreover, by the time PD manifests clinically most of the cells of interest – midbrain dopaminergic neurons – have already been lost (Kempster et al., 2010). Animal models allow the study of PD in an intact organism, and much of our understanding of the dopamine networks downstream of the substantia nigra has come from studying toxin or lesion models of PD (Carlsson et al., 1957; Langston et al., 1984). These models are very successful at modelling loss of cells in the substantia nigra or depletion of dopamine, but rely upon an acute insult to the nervous system and do not model the slow degeneration observed in PD (Westerlund et al., 2010).

Following the description of mutations linked to familial PD, a number of transgenic models have been created, including *D. melanogaster*, yeast and murine models of α-synuclein pathology (Feany and Bender, 2000; Outeiro and Lindquist, 2003; Masliah et al., 2005). These models have shed light on the pathogenic processes operating in PD, but

have been disappointing with regard to replicating the phenotype and pathology of the human disease (Dawson et al., 2010). Indeed, neither *D. melanogaster* nor *S. cerevisiae* has a gene that is homologous to human *SNCA*, limiting their potential as models of PD.

Cellular models can circumvent some of these issues, but existing primary and tumour cell models have major drawbacks. Primary neuronal cultures from mice or rats are difficult to maintain *in vitro* and do not self renew, and have an amino acid at position 53 of α-synuclein which in humans causes disease (Larsen et al., 2009). Transformed cell lines are readily amenable to genetic manipulation for study of proteins of interest. However, these cells carry mutations in genes that are involved in apoptosis and chromosomal rearrangements that can disrupt cell signalling pathways, and are phenotypically different from the cells affected by the disease process – all of which severely limits their use as a model system (Bottomley et al., 1969; Jakel et al., 2004; Gibbs and Singleton, 2006). A cellular environment that is so far removed from that seen in disease hampers attempts to identify genuine substrates of physiological and pathological LRRK2 activity for example. It should also be noted that many of the existing cellular models rely on poorly controlled overexpression of transgenes, a particular drawback when attempting to model a disease in which gene dosage is a critical aspect, as seen in *SNCA* multiplication kindreds (Eriksen et al., 2005).

1.9 PLURIPOTENT STEM CELLS OFFER A POSSIBLE SOLUTION

1.9.1 *The discovery of pluripotent stem cells*

Given that the zygote of multicellular animals differentiates into all the cell lineages of the embryo and ultimately the adult, it was theorised that cells must exist at early stages of development that have the potential to differentiate into a wide range of cell lineages, a feature

called pluripotency (from Latin *pluri* - many, and *potens* - having power). Evidence for such pluripotent cells came from studies with mouse teratocarcinomas – tumours that contain a large variety of differentiated cell types. The demonstration that transplantation of a single teratocarcinoma cell *in vivo* could result in a teratocarcinoma in the recipient animal established the presence of pluripotent tumour stem cells – stem referring to the property of self-renewal. These cells were named embryonal carcinoma (EC) cells (Kleinsmith and Pierce, 1964). They could be established in culture, and also had the ability to contribute to the formation of chimaeric mice (Papaioannou et al., 1975). By this time it was thought that EC cells might not be grossly abnormal cells, but rather normal early embryonic cells that find themselves out of context.

Evans and Kaufman (1981) were the first to report the establishment of defined early embryonic cells in culture, isolated from the inner cell mass (ICM) of delayed blastocysts. These shared all properties described for EC cells hitherto, in that they could be proliferated indefinitely in culture, they would not senesce and they would retain their pluripotency. Unlike EC cells, they also retained a normal karyotype. The term embryonic stem (ES) cell was coined.

The ability of these cells to contribute to chimaeric mice was subsequently demonstrated (Bradley et al., 1984). They chimaerised not just the soma, but also the germline, hence genetic manipulation of transferred ES cells could alter the genome of subsequent generations, permitting the development of transgenic animals (Evans, 2008).

It was over a decade later that cells with equivalent properties were derived from human embryos (Thomson et al., 1998), designated human ES or hES cells.

1.9.2   *Nuclear reprogramming*

In parallel with the work leading up to the discovery of ES cells, Sir John Gurdon showed that it was possible to generate new animals by transferring tadpole intestinal cell nuclei into enucleated eggs from the African clawed toad, *Xenopus laevis* (Gurdon, 1962). By some means yet to be fully worked out, the recipient egg had reprogrammed the nucleus from the donor differentiated cell, enabling the development of a normal embryo, genetically identical to the donor. These seminal findings paved the way for nuclear reprogramming (as this technique was called) to be applied to mammalian adult cells, with the cloning of Dolly the sheep (Wilmut et al., 1997).

The paths of nuclear reprogramming and ES cell biology crossed with a report in 2001 that thymocytes would acquire pluripotency on electrofusion with mouse ES cells (Tada et al., 2001). Therefore, ES cells also have the capability to reprogram nuclei – ES cells as well as eggs contain factors that induce pluripotency in somatic cells.

1.9.3   *Induced pluripotent stem cells*

The discovery that eggs and ES cells could reprogram differentiated nuclei led Shinya Yamanaka to hypothesise that it might be possible to induce pluripotency in somatic cells using factors that are responsible for maintaining the pluripotent cell state (Yamanaka, 2009). Over several years, his lab assembled a list of factors that are either specifically expressed in mouse ES cells, or have important roles in these cells. By 2004, a total of 24 candidate genes had been curated.

Through an intelligent process of elimination, this list was swiftly wittled down to just four genes that, when overexpressed in fully differentiated mouse cells, could convert them into a pluripotent stem cell state, a groundbreaking result reported in 2006 (Takahashi and Yamanaka, 2006). The cells produced were termed induced pluripotent

stem cells (iPS cells or iPSCs). Those four factors were *Oct4*, *Sox2*, *c-Myc* and *Klf4* – all transcription factors known to have important roles in the pluripotency gene network. The first reports of the generation of human iPSCs came the following year from several groups working independently: Yamanaka's team achieved reprogramming of human somatic cells with the same four factors that worked in mouse (Takahashi et al., 2007b); Jamie Thomson's group, working on the same problem almost in parallel, found that a slightly different combination (*Oct4*, *Sox2*, *Lin28* and *Nanog*) also works (Yu et al., 2007); George Daley's group supplemented the Yamanaka four factor cocktail with SV40 large T and *hTERT* (Park et al., 2008b).

1.9.4 *A new model system*

iPSC technology thus makes it feasible to take fully differentiated cells from humans and reprogram them to adopt a pluripotent state. When applied to the modelling of disease, the ramifications of this become clear: the specific cells affected by disease can be generated that bear the *same gene mutations that cause the disease*. For example, midbrain dopaminergic neurons bearing mutations in *SNCA* or *LRRK2* could be generated from patients with PD caused by these mutations. This technology has the potential to revolutionise our understanding of PD precisely because it provides the opportunity to generate and study disease-affected cells directly from patients.

The iPSC-based approach to disease modelling was rapidly adopted and by the end of 2009 had been employed to generate cell models for several neurological conditions. Dimos et al. (2008) published an early study demonstrating that it is feasible to generate iPSCs and thence motor neurons from an elderly patient with amyotrophic lateral sclerosis (ALS) carrying a mutation in *SOD1*, although a cellular phenotype was not reported. Soldner et al. (2009) generated iPSC lines from five patients with sporadic PD; dopaminergic neurons could be

differentiated from all cell lines examined. Ebert et al. (2009) generated two iPSCs from a patient with spinal muscular atrophy and Lee et al. (2009) described an iPSC model of familial dysautonomia.

Although few if any of these reports described clear phenotypic differences between cells derived from patients and healthy controls, they provided important proof of principle that cells affected by disease could indeed be derived from patients.

1.10 THESIS STRUCTURE

This thesis begins by describing two studies in a fibroblast model of PD caused by mutations in *LRRK2*. The first study provides preliminary data on abnormal phosphorylation of 4E-BP (a component of the mTOR pathway), and the second describes microarray analysis of gene expression in *LRRK2* mutation and control fibroblasts.

The next part of the thesis describes the different strategies that were employed to attempt reprogramming of fibroblasts into iPSCs. I then describe methods used to characterise iPSCs generated from members of the Iowa *SNCA* triplication kindred. The final section documents the approach used to direct differentiation of these iPSC lines into midbrain dopaminergic neurons. This includes the demonstration that neurons derived from a PD patient with triplication of *SNCA* contain twice as much α-synuclein protein as those from a healthy relative. This doubling of α-synuclein recapitulates the cause of PD in members of this kindred. The advantages and limitations of this model system are discussed, in the context of the strong parallels that exist between disease due to multiplication of *SNCA*, and sporadic PD. The thesis concludes with an outline of potential future directions for this work.

Part II

FIBROBLASTS

In this section, I describe two studies in Parkinson's disease patient fibroblasts with mutations in *LRRK2*. The first examines a potential substrate of LRRK2 kinase activity, and the second examines genome-wide gene expression in these fibroblasts. Potential limitations of using fibroblasts as a model of a neurological disease are discussed.

LRRK2 FIBROBLAST STUDIES

2.1 INTRODUCTION

As outlined in Chapter 1, mutations in *LRRK2* are currently regarded as one of the commonest genetic causes of PD (Bonifati, 2006) and phenotypically, PD caused by mutations in *LRRK2* is very similar to sporadic disease (Khan et al., 2005). Furthermore, genome wide association studies suggest that common variation at the *LRRK2* locus influences the development of sporadic PD (Simon-Sanchez et al., 2009; Satake et al., 2009). Therefore, studying the impact of *LRRK2* mutations should help us understand the pathogenesis of sporadic disease.

LRRK2 contains a ROC (Ras of complex proteins)/GTPase domain, a COR (C-terminal of ROC) domain and a kinase domain, flanked by several protein-protein interaction motifs including a WD40 domain and Leucine Rich Repeats (Marin, 2006). The precise physiological role of LRRK2 is not understood, and pathogenic mutations are clustered within the enzymatic domains (Paisán-Ruíz et al., 2008). *In vitro* studies suggest that mutations in the GTPase domain and the COR domain decrease GTPase activity, whilst most mutations in the kinase domain increase kinase activity (reviewed by Cookson (2010)). The presence of these enzymatic domains, and the alteration of enzymatic activity secondary to pathogenic mutations, has prompted the suggestion that LRRK2 can act as a signaling node within cells, with the protein-protein interaction domains functioning as scaffold areas to recruit targets to an active protein complex (Hsu et al., 2010b). Specifically, LRRK2 has been implicated in several signalling pathways including

ERK signalling and the mTOR pathway (Hsu et al., 2010a; Imai et al., 2008).

In order to try and identify phenotypic differences specific to LRRK2 mutation fibroblasts, I carried out experiments in fibroblasts obtained from patients with LRRK2 PD. Results of such investigations have the potential to help shed light on the pathogenic impact of these mutations, and guide future experiments on iPSC-derived neurons.

Two experiments on fibroblasts are described in this chapter: the study of the mTOR pathway member 4E-BP as a potential phospho-substrate of LRRK2, and a comparison of gene expression in LRRK2 mutation and control fibroblasts.

2.1.1 *4E-BP as a putative substrate of LRRK2*

Studies in transfected HEK 293T cells and a *D. melanogaster* model have suggested 4E-BP as a putative target of human LRRK2 and *D. melanogaster* LRRK kinase activity respectively (Imai et al., 2008). 4E-BP is a downstream target of mammalian target of rapamycin (mTOR), which is a central regulator of cell growth and proliferation and acts mainly through the modulation of protein synthesis. It does this in part by regulating protein translation, which permits cells to respond swiftly to intrinsic and environmental stress. The PI3K and Akt pathways integrate a wide range of signals from within and outside the cell to modulate mTOR activity (reviewed by Hay and Sonenberg (2004)).

4E-BP negatively regulates cap-dependent protein translation via direct sequestration of eIF4E, part of the translation initiation complex. Phosphorylation of 4E-BP causes its dissociation from eIF4E thereby relieving inhibition. Thus the proposed phosphorylation of 4E-BP by LRRK2 would prompt eIF4E liberation and allow an increase of cap-dependent protein translation (Figure 2.1).
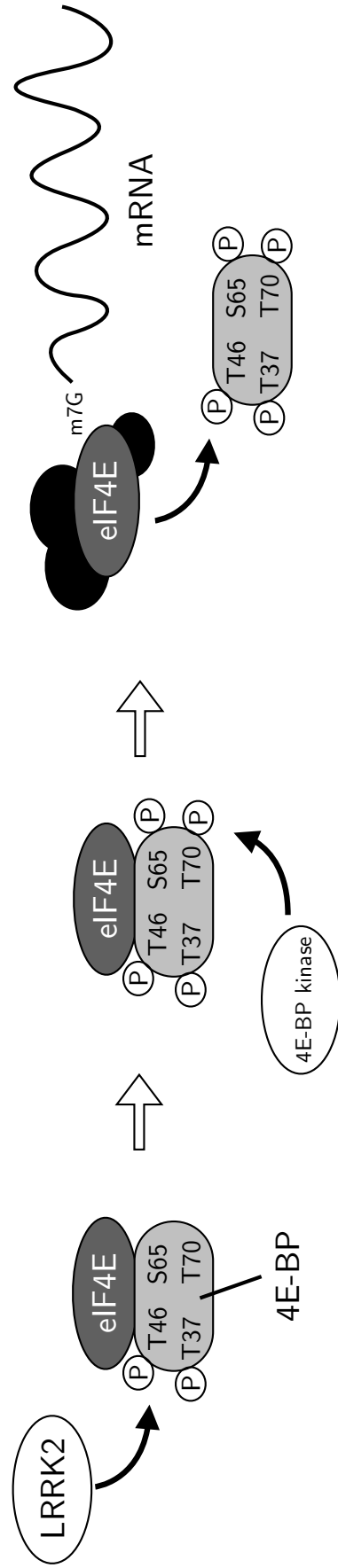
Figure 2.1: Putative interaction between LRRK2 and 4E-BP. Phosphorylation of 4E-BP at T37/T46 residues by LRRK2 enables subsequent phosphorylation at T70 and S65. Fully phosphorylated 4E-BP then separates from the mRNA cap-binding protein eIF4E, leading to the formation of an initiation factor complex enabling protein translation. Adapted from Imai et al. (2008).

Imai et al. (2008) show that overexpression of eIF4E is sufficient to increase sensitivity to oxidative stress and dopaminergic neuronal loss in *D. melanogaster*, and that co-expression of 4E-BP suppresses this loss, suggesting that the 4E-BP/eIF4E complex is important here. Increase in eIF4E levels, and mutations in *LRRK2* that increase kinase activity, would be expected to upregulate protein translation. That this would lead to neuronal death may seem paradoxical. Imai et al. (2008) hypothesise that unchecked protein translation in the context of cell stress, being an energy intensive process, could upset the energy balance and redox status of cells. It could also increase the likelihood of protein misfolding events, simply by increasing the number of proteins being produced. In contrast, inhibition of eIF4E in *C. elegans* reduces protein synthesis, lowers oxidative stress and increases lifespan (Syntichaki et al., 2007).

Here, I describe a study that seeks to ask whether the findings described by Imai et al. (2008) can be reproduced in patient fibroblasts. I provide preliminary data that 4E-BP is hyperphosphorylated in the presence of disease-causing LRRK2 mutations, but not at the residues predicted by the *D. melanogaster* model (Imai et al., 2008).

2.1.2   *Regulation of gene expression by LRRK2*

Another possible mechanism of LRRK2 pathogenesis involves an interaction with microRNAs (miRNAs) which are evolutionarily conserved non-coding RNAs that regulate gene expression (Ambros, 2004).

In *D. melanogaster*, pathogenic LRRK2 has been shown to antagonise two specific miRNAs: *let-7* and *miR-184* (Gehrke et al., 2010). These miRNAs normally repress the translation of *E2F1* (which lies downstream of cyclin E, a key regulator of cell cycle progression) and *DP* mRNAs, and this repression is relieved when *LRRK2* is mutated. Gehrke et al. (2010) demonstrated that overproduction of *E2F1* and *DP*

was critical for LRRK2 pathogenesis. So, *LRRK2* mutations may impact upon downstream gene expression, via *E2F1*-mediated transcription.

Aside from this direct modulation of gene expression, *LRRK2* mutations might indirectly alter gene expression via disrupting signalling pathways.

In this chapter, I test the hypothesis that mutated LRRK2 will alter gene expression, by comparing global gene expression in fibroblasts cultured from PD patients carrying mutations in *LRRK2* with fibroblasts from healthy control subjects. This study provides data that mutated LRRK2 does not significantly alter global gene expression at a level detectable with the microarray platform employed. The limitations of such a study in a non-neuronal cell type are discussed.

2.2 METHODS

2.2.1 *Fibroblast derivation*

Fibroblast cultures were isolated from PD patients with *LRRK2* mutations and healthy controls (summarised in Table 2.1) following approval of the study by the ethics board of the Royal Free Hospital, London, UK and informed written consent from the individuals concerned.

Fibroblasts provided by Dr Jan-Willem Taanman, UCL Institute of Neurology

Skin punch biopsies (forearm) were cultured in 5 cm² sterile Petri dishes at 37ºC in 5% CO_2 in 2 ml DMEM supplemented with 10% Fetal Bovine Serum (FBS), penicillin (50 U/ml) and streptomycin (50 μg/ml) until fibroblasts were seen to migrate from the skin explants (Sly and Grubb, 1979). Media volume was increased by 0.5 ml every 2 days. When plates were confluent, fibroblasts were lifted from dishes by trypsinising with TrypLE (Invitrogen) and transferred to 10 cm² dishes for culturing. Samples were designated anonymous identifiers following collection.

Biopsies performed by Dr Daniel Healy, Royal Free Hospital

MUTATION	LRRK2 DOMAIN	*n*
R1441G	ROC	2
Y1699C	COR	1
G2019S	Kinase	8
Controls	–	11

Table 2.1: Patient and control fibroblast samples used.

2.2.2 *Protein extraction and Western blot*

Six fibroblast lines (one each of R1441G, Y1699C and G2019S and three age matched controls) were seeded into three wells of a six-well plate at a density of approximately 20,000 cells/cm² (200,000 cells/well). Media was replaced 24 hours later, and after a further 24 hours cells were lysed (Cell Signaling Lysis buffer, Complete protease inhibitor and Halt phosphatase inhibitor) in 100 μl buffer per well.

Protein concentration was determined with BCA Protein Assay kit (Pierce) according to manufacturer's instructions, and equalised with addition of lysis buffer. Lysates were denatured via boiling with Nupage sample buffer supplemented with DTT (dithiothreitol), and groups of replicates were run on separate Nupage Bis-Tris 4-12% gels in MES buffer for 70 mins at 150 V, then transferred in Tris-glycine methanol to PVDF membrane (Millipore). Membranes were blocked with 5% milk solution in phosphate buffered saline (PBS) for 1 hr prior to probing overnight with primary antibodies to β-actin mouse monoclonal AC-74 (Sigma) (1:5000 dilution) in tandem with the following 4E-BP antibodies that recognise phosphorylated motifs, as individual experiments:

- Serine 65 (Cell Signaling #9451, rabbit polyclonal, 1:1000),

- Threonine 37/46 (Cell Signaling #9459, rabbit polyclonal, 1:1000),

- Threonine 70 (Cell Signaling #9455, rabbit polyclonal, 1:1000).

Membranes were then probed with relevant horse radish peroxidase (HRP) secondary antibodies and then washed three times in PBS supplemented with 1% Tween. Chemiluminescence was determined with the Pierce Pico Kit (Thermo Scientific). Membranes were exposed to Kodak biomax film and developed on a Fujifilm developer as per manufacturers instructions.

4E-BP blots were then stripped according to the following protocol: blots were incubated with stripping buffer (2% SDS, 50 mM Tris-HCl, 100 mM 2-mercaptoethanol, pH 6.8) for 15 to 30 mins at 50°C with gentle shaking, then rinsed multiple times in TBS-Tween, until 2-mercaptoethanol odour had dissipated. Blots were then reprobed for total 4E-BP independent of phosphorylation (Cell Signaling #9452, rabbit polyclonal, 1:1000). Blots were quantitated using ImageJ (NIH).

2.2.3 *RNA extraction*

For collection of RNA, cultures of the 11 control and 11 LRRK2 mutation cell lines described in Table 2.1 were brought to equivalent passage by serial thawing and replating (final passage = 7). Cells were then plated in 6 cm plates and at equal density (500,000 cells/dish). Following 24 hrs growth, RNA was extracted using the RNeasy kit (Qiagen) according to manufacturer's instructions.

2.2.4 *Gene expression microarray*

Illumina Human HT-12 Arrays were used according to manufacturer's instructions, starting with 500 ng of total RNA for each sample which was then subject to quality control using RNA integrity number (RIN), performed prior to analysis (Schroeder et al., 2006).

Microarrays were run by AROS AS, Denmark

Arrays were read on an Illumina Bead array reader confocal scanner. Differential gene expression values were calculated with the Illumina Custom algorithm within the Illumina BeadStudio software suite.

Expression data was subjected to quantile normalisation and differential expression values calculated on sets of biological replicates. The threshold for significance for individual genes was set at $\pm$ 1.5 fold expression between conditions and $P < 0.05$. Cluster analyses were derived using the Illumina Beadstudio software suite. Expression data from this study are MIAME compliant and have been deposited in the GEO database (accession number GSE25580).

2.3 RESULTS

2.3.1 *Mutated LRRK2 increases 4E-BP phosphorylation*

Three mutation lines (one each of R1441G, Y1699C and G2019S) and three age matched control lines were compared. No differences in 4E-BP phosphorylation between mutation and control lines were detected at residues Threonine 37, 46 or 70 (Figure 2.2). However, a robust hyperphosphorylation was seen at residue Serine 65 across all three replicates of each of the mutation lines, when compared to wildtype lines (Figure 2.3).

Ratio of total 4E-BP to actin was not significantly different between lines (ANOVA and Kruskal-Wallis, $P > 0.05$). Ratios of Serine 65-phosphorylated 4E-BP (Ser65-4E-BP) to total 4E-BP were not significantly different between mutation lines (ANOVA and Kruskal-Wallis, $P > 0.05$) but taken as a group, Ser65-4E-BP was significantly higher in the mutation group compared to the control group (Student's t-test, $P < 0.0001$) (Figure 2.4).

2.3.2 *Mutated LRRK2 does not alter gene expression in fibroblasts*

One case (Y1699C mutation) and one control were excluded as outliers – given that they clustered separately to, and far from, the other samples – which is an accepted approach to improve signal-to-noise
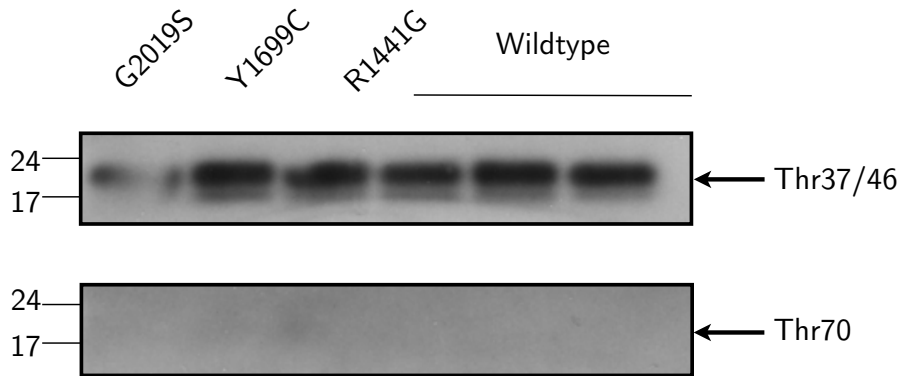
Figure 2.2: Western blot of Phospho-4E-BP (Thr70 and Thr37/46). No difference in phosphorylation of 4E-BP was observed between mutation and control fibroblast lines at these residues.
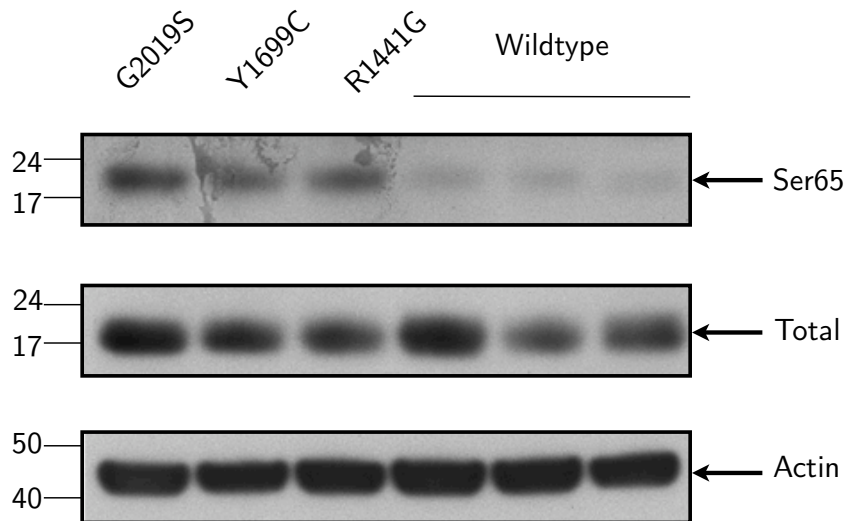
Figure 2.3: 4E-BP is hyperphosphorylated at Ser65 in *LRRK2* mutation fibroblasts. Representative western blot.

(b) Quantification of Phospho-4E-BP (Ser65).
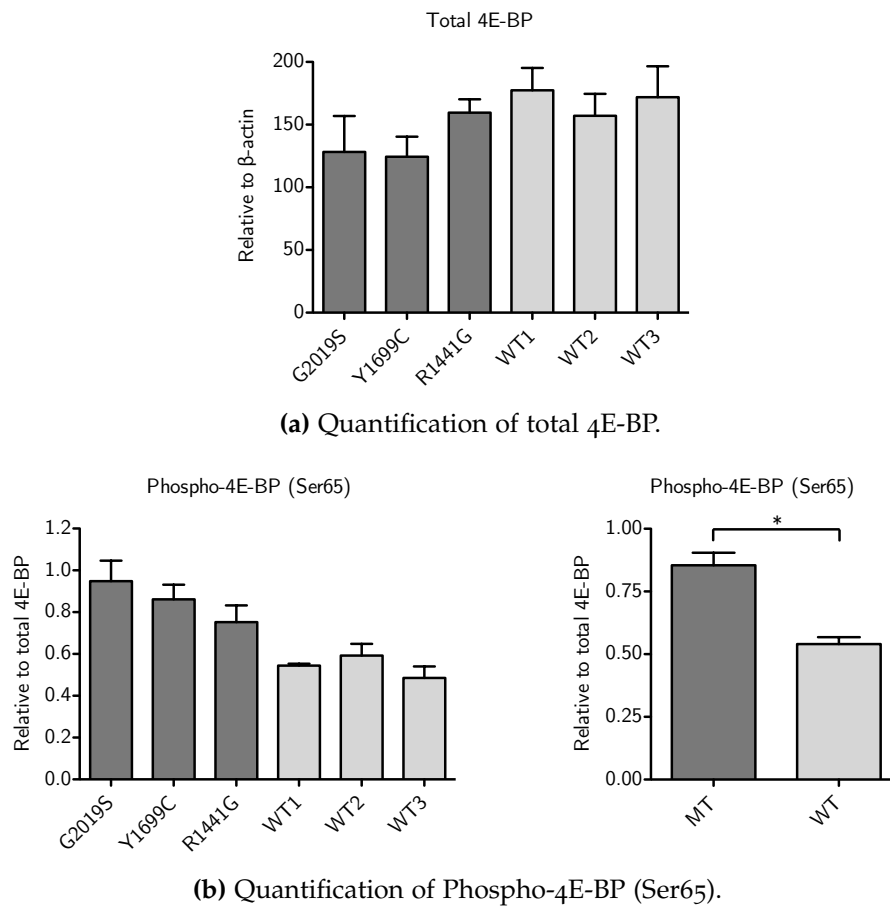
Figure 2.4: (a) ImageJ quantification shows that total 4E-BP is not significantly different between fibroblast lines. Error bars are standard deviations of technical replicates, $n = 3$. **(b)** ImageJ quantification of pSer65-4E-BP corrected for total 4E-BP (left panel). Grouped results comparing mutation lines (MT) and wildtype lines (WT) (right panel) demonstrate significantly higher phosphorylation in MT compared to WT (Student's t-test, $P < 0.0001$).

ratio (Kauffmann and Huber, 2010). Results from the remaining cases ($n = 10$) and controls ($n = 10$) were filtered to show probes detected (> 0.95) and marginal detections ($0.9 - 0.95$), and then filtered on error (standard deviation < 0.5 within cases or controls). Mann-Whitney unpaired testing ($P \leq 0.05$) was performed comparing the overall gene expression profile between these cases and controls.

These results were filtered on fold change (> 1.5) yielding six genes with altered expression: *LOC647673*, *TMEM200A* and *IGFBP3* were seen to increase whilst *CXCL12*, *FGF9*, and *RPESP* showed a decrease in expression. However, none of these alterations survived correction for multiple testing (Benjamini-Hochberg).

A scatter plot of cases (y-axis) versus controls (x-axis) is shown in Figure 2.5 with 1.5-fold change from equivalent expression indicated by green bounding lines.

2.4 DISCUSSION

The main aim of these experiments was to determine whether fibroblasts display an altered phenotype in the presence of mutated LRRK2.

2.4.1 *4E-BP phosphorylation study*

Although preliminary, the 4E-BP phosphorylation data presented herein are consistent with the findings from Imai et al. (2008) that 4E-BP is phosphorylated by LRRK2. Imai et al. (2008) report that LRRK2 expression in HEK 293T cells phosphorylates 4E-BP at Thr37/46 and Ser65, and that phosphorylation of d4E-BP was reduced in $dLRRK^{(-/-)}$ flies. They suggest that 4E-BP phosphorylation in general is augmented by transfecting cells with mutant LRRK2 (I2020T), and report that some pathogenic mutations in LRRK2 (R1441G and I2020T but
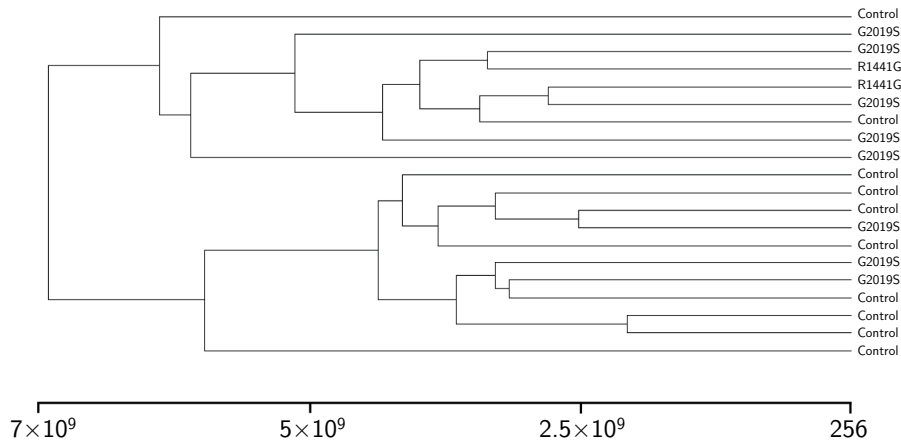
(a) Gene expression dendrogram.
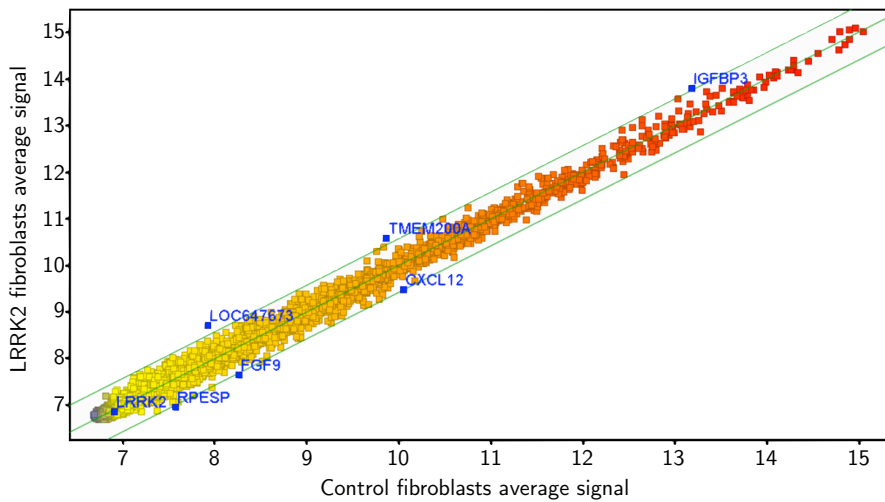
(b) Gene expression scatterplot.

Figure 2.5: *LRRK2* mutations do not significantly alter gene expression in
patient-derived fibroblasts. **(a)** Unsupervised cluster analysis pro-
duces a dendrogram where the mutation and control fibroblast
samples intermingle with each other. **(b)** Gene expression scat-
terplots compare gene expression in mutation versus control
fibroblasts. Outer bounding lines (in green) denote 1.5-fold ex-
pression change. Genes shown are those that reach significance
prior to Benjamini-Hochberg correction. *LRRK2* is also shown.
No changes in gene expression survived correction for multiple
testing.

not Y1699C) exhibit higher kinase activity at Thr37/46 than wildtype LRRK2 under starvation (serum-free) conditions.

Here, I report that 4E-BP is hyperphosphorylated at Ser65, but not Thr37/46 or Thr70, in patient fibroblasts with *LRRK2* mutations (G2019S, Y1699C and R1441G) compared to fibroblasts from healthy controls. The reason for this discrepancy might be due to the difference in cell type (fibroblasts rather than HEK 293T cells) and expression of LRRK2 (endogenous rather than inducibly expressed).

The consequences of this difference are not clear – 4E-BP is thought to be phosphorylated at multiple sites in a hierarchical fashion (Gingras et al., 2001) so the functional impact of hyperphosphorylation at one or other phosphosite may not necessarily be different. Imai et al. (2008) hypothesise that phosphorylation at Thr37/46 can facilitate subsequent phosphorylation at Thr70 and Ser65 *in vivo* by other kinases, or possibly by LRRK2.

Nevertheless, the data presented here suggest that cultured fibroblasts from patients with LRRK2 PD might have a detectable phenotype, which warrants further investigation. As a counterpoint, and subsequent to the work presented here, Kumar et al. (2010) described 4E-BP phosphorylation by LRRK2 *in vitro*. They reported that, whilst LRRK2 can indeed phosphorylate 4E-BP, its autophosphorylation is stronger under conditions of molar excess of 4E-BP, and cannot be reproduced in HEK 293T cells overexpressing LRRK2, suggesting that 4E-BP is not a good substrate for LRRK2 – at least in this system.

The caveat with the 4E-BP study described herein is that it included only a limited number of lines, and they were assessed without modulation of either the mTOR pathway, or of LRRK2 kinase activity. However, one advantage over the Kumar et al. (2010) study is the use of patient-derived cells expressing LRRK2 at endogenous levels, rather than a cancer cell line with artifical overexpression. The next step would be to repeat these experiments in the remaining disease and control lines, including provocation of the mTOR pathway (through inducing cell stress via serum withdrawal and insulin stimulation) to

assess 4E-BP phosphorylation in a dynamic context. Also, it would be important to establish whether 4E-BP hyperphosphorylation has the predicted effect of increasing cap-dependent protein translation.

2.4.2 *Gene expression analysis*

The results of the gene expression microarray study uncovered several genes that appeared to exhibit altered expression in the presence of mutations versus controls. However, none of these alterations proved to be significant when corrected for multiple testing, and all were of a modest size (less than a two-fold change in expression). Based upon these data, there is no significant difference in gene expression between the grouped *LRRK2* mutation fibroblasts and the control samples. *LRRK2* expression level was also found to be no different between cases and controls. These data were incorporated into a published study (Devine et al., 2011) along with data from two additional gene expression microarray experiments performed by collaborators: a comparison of occipital cortex from G2019S mutation carriers and controls, and a comparison of HEK 293T inducible LRRK2 wildtype and mutation cell lines. No significant alterations in gene expression were found in these two additional experiments either, corroborating the dataset obtained from the fibroblasts.

These findings have been substantiated by a recent comparison of gene expression in putamen from patients with IPD, LRRK2 PD and neurologically healthy controls (Botta-Orfila et al., 2012). Gene expression was not found to be significantly altered in LRRK2 PD putamen compared to controls. In contrast, differences were indeed detected when IPD putamen was compared to control tissue – pathway analysis found that genes involved in synaptic transmission and cell signalling cascades were affected.

Alterations in expression of genes due to *LRRK2* mutations have been observed in two model systems. One probed expression in

mononuclear cells isolated from G2019S mutation carriers and controls, and found altered expression of genes involved in proteasomal and mitochondrial function in the presence of mutations (Mutez et al., 2011). The other compared gene expression in multiple tissues from LRRK2 knockout and G2019S transgenic mice to equivalent tissue from wildtype mice (Nikonova et al., 2012). Subtle though significant differences in expression were found in knockout animals relative to wildtype controls in cortex, striatum and kidney of knockout animals, but only striatum of G2019S animals. In contrast, highly significant differences were observed in cortex, striatum, kidney and muscle when tissues from G2019S and knockout mice were directly compared. Ribosomal and glycolytic pathways were upregulated in G2019S tissue, whilst genes related to membrane-bound organelles, oxidative phosphorylation, mRNA processing and endoplasmic reticulum were downregulated in these tissues.

There are a number of factors that might help account for the differences between these separate studies. Firstly, peripheral blood mononuclear cells have a higher relative expression of LRRK2 compared to fibroblasts (Jan-Willem Taanman, unpublished observations) which might account for the different data obtained in this system. Any impact of mutations upon gene expression could be dependent on levels of LRRK2 expression raising this impact above background variation between diverse patient genotypes. Given the relatively low expression levels of LRRK2 in the patient fibroblasts, it is perhaps not surprising that an alteration in overall gene expression in the mutant lines versus the controls was not observed. It should be noted that neither cell type has been linked to the disease process in PD, and so *a priori* one would not expect a major impact of mutations upon gene expression in either system.

A second factor to consider is the specific conditions in which the mRNA has been isolated. The study presented herein was carried out in fibroblasts having spent several passages in tissue culture. In contrast, the primary cells analyzed by Mutez et al. (2011) were iso-

lated directly from patients and not subjected to culture conditions. The culturing of these cells may result in selective pressure against expression of *LRRK2* at a level where a pathogenically linked expression phenotype is observed. However, disease and control lines do not show any difference in level of *LRRK2* expression, suggesting that this form of selection is unlikely. Alternatively, such a phenotype might be silent in standard cell culture conditions, and require additional cell stressors (e.g. oxidative stress or serum starvation) to be revealed.

Thirdly, the general background noise in the different systems must be considered. When analysing brain tissue for example, differences in postmortem delay, sample preparation, age of the individual and comorbidities can all have a bearing on RNA quality and gene expression. Differences due solely to *LRRK2* mutations therefore need to be strong enough to avoid being drowned out by this noise. Put another way, the brain tissue analysis in Devine et al. (2011) suggests that any differences in gene expression due to *LRRK2* mutations are outweighed by differences due to sample heterogeneity.

The results of this study have specific implications for the use of *LRRK2* patient fibroblasts as a model for the disease process. Human fibroblasts harbouring pathogenic mutations have previously been used as a model system for neurological disorders including PD (Hoepken et al., 2008). In the case of *LRRK2* mutation fibroblasts, the data here suggest that the focus of model development should be on generating human neuronal systems to examine *LRRK2* mutations.

In the next part of this thesis, I will describe the generation of such a neuronal model, utilising induced pluripotent stem cell technology.

Part III

INDUCED PLURIPOTENT STEM CELLS

In this section, I describe the strategies that were employed to reprogram human fibroblasts into induced pluripotent stem cells. I then document the methods used to demonstrate that cells obtained via successful reprogramming are indeed pluripotent.

REPROGRAMMING METHODOLOGY

3.1 INTRODUCTION

The previous chapter presented data on possible phenotypes in LRRK2 PD patient fibroblasts. However, these data are hard to reconcile: on the one hand, preliminary data is described suggesting a possible alteration of phosphorylation of 4E-BP, a downstream component of the mTOR pathway, in LRRK2 fibroblasts. In contrast, gene expression profiling suggests that the overall expression profile of the disease and control fibroblasts is not significantly different.

Perhaps the problem here is that we are studying a neuronal disease in a non-neuronal cell type. Ideally, we would have a human neuronal cell model in which to study these mutations. In this chapter I will outline the methods that I have used to generate induced pluripotent stem cells (iPSCs) from patient fibroblasts as progress towards this goal.

Initial testing of reprogramming methods was carried out on fibroblasts from healthy subjects and fibroblasts with mutations in LRRK2. However, whilst this part of the project was underway, fibroblasts were obtained from members of the Iowa kindred, a large pedigree with an early onset, rapidly progressive autosomal dominant PD caused by triplication of the *SNCA* locus, encoding α-synuclein (described in Section 1.3.1) (Singleton et al., 2003). These fibroblasts were felt to form a more promising basis for an iPSC project, because *SNCA* triplication iPSCs and their neuronal progeny should serve as a good test case of the iPSC disease modelling paradigm. The fully penetrant, early onset nature of *SNCA* triplication PD ought to maximise the chances of observing phenotypic differences between disease and control iPSC-

derived cells. Therefore, subsequent reprogramming attempts were made exclusively with these fibroblasts.

The reprogramming strategies available at this time (mid 2009) followed the same strategy as Yamanaka's original papers (Takahashi and Yamanaka, 2006; Takahashi et al., 2007a) i.e. delivering a set of four genes encoding transcription factors to target cells. Most commonly, retroviral vectors were employed to achieve this, the advantage being that these will integrate into the target cell genome, so that when a strong promotor is used, high levels of transgene expression will ensue through multiple cell divisions (required for completion of the reprogamming process (Hanna et al., 2009)). This facilitates a high reprogramming efficiency. However, there are three potential problems:

1. Transgenes can disrupt the target cell genome through random integration, which may have unpredictable consequences on cell behaviour.

2. Transgenes cannot be removed following completion of reprogramming, and therefore have the potential to reactivate, which may limit the differentiation potential of the iPSCs in which they reside.

3. Furthermore, although not the aim of this project, retention of potentially oncogenic transgenes in reprogrammed cells would make them unfit for therapeutic purposes.

Given all of these potential drawbacks with retroviral reprogramming, much work was being conducted to develop methods of reprogramming that avoid insertion of genetic material into the target cell genome, or would allow such inserted material to be removed seamlessly once reprogramming had been completed.

A survey of the methods used for reprogramming human fibroblasts published by November 2009 is shown in Table 3.1. Successful reprogramming of mouse embryonic fibroblasts to iPSCs had also
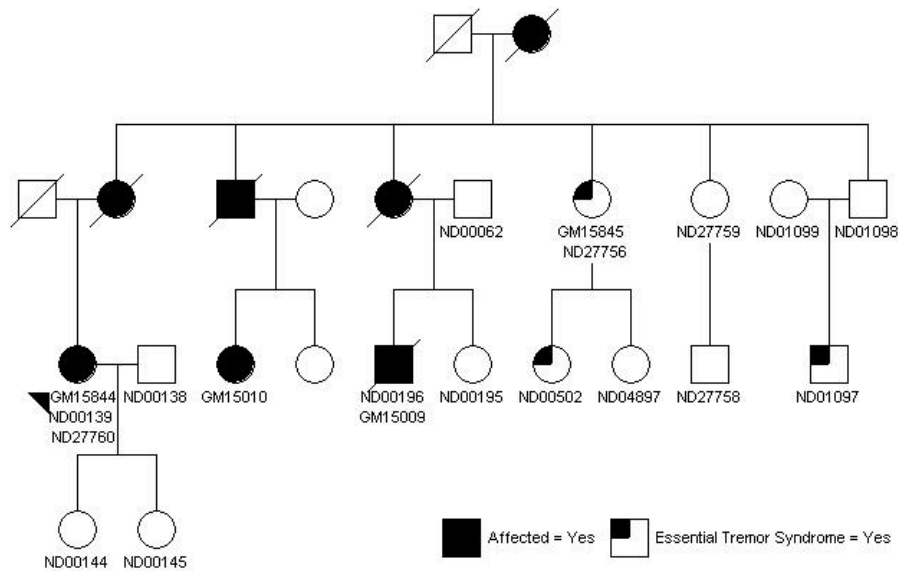
Figure 3.1: Abridged pedigree of the Iowa kindred. Arrow, proband; circles, female; squares, male; crossed, deceased. The proband's daughter (ND00144) also provided fibroblasts for this study. Image derived from the Coriell Cell Repositories website (http://ccr.coriell.org/), where both fibroblast lines have been deposited with open access.

been described utilising recombinant proteins (Zhou et al., 2009), but this was still technically very challenging. Later advances in reprogramming methodology using mRNA (Warren et al., 2010) or miRNA (Anokye-Danso et al., 2011) were not published at the time.

3.2 CLINICAL DETAILS OF PROBAND

An abbreviated pedigree of the Iowa kindred is shown in Figure 3.1. At 44 years of age, the proband was fired from a clerical job because she was "unable to work and think fast enough". She was treated for depression, with some benefit in mood, but the slowness persisted. Within a year and a half thereafter, she noted occasional activation tremor. She had nightmares, which she acted out; she had given her spouse injuries including a black eye during one such episode.

Clinical details provided by Dr Katrina Gwinn, National Institute of Neurological Disorders and Stroke

REFERENCE	DELIVERY	FIBROBLASTS	MEF FEEDERS	HESC MEDIA	DNA
Takahashi et al. (2007b)	infection	800,000 per dish	Day 6	Day 7	mouse retrovirus
Park et al. (2008a)	infection	50,000 per well	Day 5	Day 6 + Y27632	retrovirus (+ *hTERT* & *SV40LT*)
Tateishi et al. (2008)	infection twice	800,000 per dish	Day 5	Day 6	retrovirus
Huangfu et al. (2008)	two to four infections	1000,000 per well	Day 31	Day 1 + VPA	*mOct4* & *mSox2* retrovirus
Dimos et al. (2008)	infection twice	30,000 per well	Day 6	Day 7 + TSA	retrovirus
Liao et al. (2008)	infection	500,000 per dish	Day 2	Day 2	lentivirus (+ *LIN28* & *NANOG*)
Lowry et al. (2008)	infection twice	N/A	Day 7	Day 7	retrovirus
Yu et al. (2009)	nucleofection	~100,000 per well	Day 1	Day 2	episomes
Kaji et al. (2009)	lipofection	~70,000 per well	Gelatin	Day 1 + Dox	piggyBAC
Gai et al. (2009)	infection twice	1,000,000 per dish	Day 7	Day 8	lentivirus
Maehr et al. (2009)	infection twice	100,000 per well	Gelatin	Day 4 + VPA	mouse retrovirus
Zhou and Freed (2009)	infection twice	~500,000 per dish	Day 6	Day 7	adenovirus
Ye et al. (2009)	infection	100,000 per well	Day 5	Day 6 + VPA	retrovirus

Table 3.1: Summary of published human fibroblast reprogramming methods available by November 2009. All reports utilise four-factor reprogramming, unless stated otherwise. Cell numbers are plated in wells of 6-well plates, or 10cm dishes, as stated. VPA, valproic acid; TSA, trichostatin A.

At age 46, she presented to a tertiary care center with these complaints; she was taking hormone replacement therapy and sertraline at the time of presentation. She and her spouse felt that her thinking would fluctuate, as would her motor abilities, in a matter of days or even hours. She had spontaneous visual and auditory hallucinations. She also noted that she felt dizzy when moving from a sitting to a standing position.

Multiple medications were initiated including carbidopa/levodopa with moderate benefit in bradykinesia: donepezil reportedly improved the fluctuations in cognition, clonazepam helped the REM sleep behavior disorder (RBD) symptoms, and midodrine was helpful for orthostasis. Her cognition at the time of evaluation mandated that she be with a 24-hour caregiver to prevent accidents and wandering. Her weight decreased from 130 to 100 lbs over the first two years of her illness.

On examination, sitting blood pressure was 98/67 mmHg, and pulse 81 bpm: standing blood pressure 86/60 mmHg, pulse 90 bpm. Folstein Mini-mental status examination (MMSE) (Folstein et al., 1975) score was 13/30, with particular difficulty on recall and sequential tasks. She scored 14 on the Controlled Oral Word Association test (Ruff et al., 1996) and 16 on the Beck Depression inventory (Beck and Beck, 1972). She had marked constructional difficulties (see Figure 3.2). She could not count backwards from 100, 20, or 12. She had marked anosmia, scoring only 14/40 on the University of Pennsylvania Smell Identification Test (UPSIT) (Doty et al., 1988). There was marked hypophonia, saccadic pursuits, and moderately masked facies. She had difficulty with rapid alternating movements. Gait was shuffling. She took several steps backwards to prevent herself from falling on the pull test.

Over the subsequent decade, she has become bedridden. At the time of her clinical assessment prior to skin biopsy at age 54, she was severely rigid, occasionally following faces with her eyes but mute to commands and without spontaneous vocalisations or verbalisations.

January 2000   July 2002   February 2003
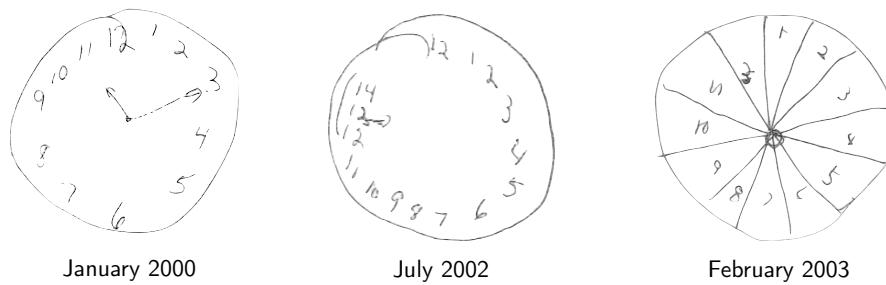
Figure 3.2: Progressive worsening of the proband's constructional apraxia over a three year period.

She was no longer able to eat by mouth and was tube-fed. She had complete incontinence of bowel and bladder and required full-time care.

3.3 METHODS

3.3.1 *Fibroblast derivation*

Skin biopsies were collected from the proband (age 54 at collection) and her unaffected daughter (age 30 at collection). Fibroblasts were cultured and expanded according to the methods given in Section 2.2.1. Skin punch biopsies (forearm) were cultured in 5 cm² sterile Petri dishes at 37ºC in 5% CO_2 in 2 ml DMEM supplemented with 10% FBS, penicillin (50 U/ml) and streptomycin (50 µg/ml) until fibroblasts were seen to migrate from the skin explants (Sly and Grubb, 1979). Media volume was increased by 0.5 ml every 2 days. When plates were confluent, fibroblasts were lifted from dishes by trypsinising with TrypLE (Invitrogen) and transferred to 10 cm² dishes for culturing. Fibroblasts from the patient were designated AST (alpha-synuclein triplication) and the daughter NAS (normal alpha-synuclein).

Biopsies performed by Prof Henry Houlden, UCL Institute of Neurology

Fibroblasts provided by Dr Jan-Willem Taanman, UCL Institute of Neurology

3.3.2   *Retroviral reprogramming – Daley method*

Reprogramming of human fibroblasts was attempted following the protocol as described in Park et al. (2008a). The four human reprogramming factors inserted into the pMIG vector backbone are available from Addgene:

- pMIG-hOCT4 #17225,

- pMIG-hSOX2 #17226,

- pMIG-hKLF4 #17227,

- pMIG-hcMYC #18119.

pMIG is a vector containing pMSCV (murine stem cell virus promotor) and GFP (green fluorescent protein) separated by an IRES (internal ribosome entry site).

The following protocol is carried out at category 2 biosafety, given that oncogene-carrying retrovirus is produced with the ability to infect human cells. HEK 293T cells are used as the packaging cell line.

3.3.2.1   *Viral packaging*

The retrovirus genome is comprised of the following three open reading frames that encode for viral proteins:

- group-specific antigen (*gag*) encodes core and structural proteins,

- polymerase (*pol*) encodes reverse transcriptase, protease and integrase,

- envelope (*env*) encodes retroviral coat proteins.

Viral packaging uses a cell line that is readily transfectable with separate plasmids carrying these genes to form viral particles capable of infecting target cells. Crucially, these plasmids lack the Ψ (Psi) packaging signal that is required for their uptake into viral particles, and they are therefore replication-incompetent. Instead, genes destined for

packaging are inserted into a separate plasmid containing Ψ which is also transfected into the packaging cells.

In this protocol, *VSV-g*, which encodes envelope proteins for the Vesicular Stomatitis Virus (VSV), is also added to generate pseudo-typed viral particles. These particles are capable of infecting a broader range of target cell species. The incorporation of *VSV-g* also increases stability of the viral particles and allows them to be concentrated via ultracentrifugation.

DAY 0:

- 2,000,000 HEK 293T cells are seeded in $5\times$ 10cm dishes per retrovirus (i.e. 20 plates in total for each round of packaging) and incubated at 37°C, 5% CO_2 overnight.

- Cells are permitted to grow to approximately 70% confluency.

DAY 1:

- Once HEK 293T cells are at 70% confluency, media is replaced with fresh HEK 293T media.

- For each plate, 20 µl FuGENE 6 transfection reagent and 300 µl media are mixed and incubated at room temperature for 5 mins.

- Add DNA to the transfection mix: 2.5 µg retroviral vector, 0.25 µg VSV-g and 2.25 µg Gag-Pol.

- Mix and incubate at room temperature for 15 mins.

- Then add this mixture dropwise to each plate, and swirl the media to ensure an even mix.

- Incubate at 37°C, 5% CO2 for 48 hrs.

DAY 3:

- Retrovirus-containing media is collected and passed through 0.45 µm filter unit.

- Filtered media is placed in a 38.5 ml Beckman polyallomer centrifuge tube (catalogue #326823), placed in autoclaved metal centrifuge buckets and balanced to within 0.01 g, then centrifuged at 70,000 g, 4°C for 90 minutes using a Beckman XL-90 ultracentrifuge.

- Supernatant is then removed and the viral pellet covered in 1 ml DMEM with gentle shaking.

- The pellet is then stored overnight at 4°C to allow it to dissolve.

DAY 4:

- Pipette DMEM up and down gently with a 100 μl pipette tip until pellet is completely dissolved.

- Carry out viral titration.

3.3.2.2 *Viral titration*

METHOD 1:

- Make a tenfold serial dilution of the viral preparation (from undiluted to 10^{-6}) in PBS.

- Coat a 24-well plate with poly-L-lysine to aid cell adherence.

- Add 500 μl per well, incubate for 15 mins at room temperature, then remove liquid.

- Seed 100,000 HEK 293T cells in each well in 500 μl PBS + 0.2% EDTA.

- Immediately add 20 μl of each viral dulution to the cells, mix gently and the incubate at 37°C.

- GFP fluorescence should become visible 24 hours after infection (and can be checked with a fluorescent microscope).

- Grow cells for 48 hrs. Wash cells twice with PBS to eliminate leftover virus in the media.

- Resuspend in PBS + 0.2% EDTA (ethylenediaminetetraacetic acid) by pipetting up and down.

- Determine the percentage of GFP-labelled cells by FACS. Calculate biological titre ($BT = TU$ / ml, transducing units) according to the following formula:

$$TU = \frac{P \times N}{100 \times V} \times \frac{1}{DF}$$

where

TU	transducing units
P	% GFP+ cells
N	number of cells at time of transduction
V	volume of dilution added to each well
DF	dilution factor

METHOD 2:

- HEK 293T cells are plated at 75,000 cells per well of a 12-well plate with 1 ml medium and incubated at 37°C, 5% CO2 overnight.

- To five wells, add aliquots of the vector to be titrated: use 50 μl and 25 μl of undiluted stock, and 100 μl, 50 μl and 25 μl of a 1:50 diluted stock.

- The remaining wells are left uninfected to serve as controls.

- Incubate at 37°C, 4% CO_2 for 48 hours.

- Prior to FACS, remove the medium, wash once with 2 ml PBS, and add 500 μl of 0.25% trypsin/EDTA.

- Incubate for 5 mins at 37°C. Pipette up and down with a 1000 μl pipette tip to break up clumps.

- Transfer to a FACS tube containing 500 μl PBS.

- Determine the percentage of GFP-positive cells.

- Calculate the titre in *TU* according to the formula:

$$TU = \frac{P \times N \times 1000}{V}$$

- For accurate titre calculations, the number of GFP+ cells in two adjacent wells must be close to the expected 1:2 ratio.

3.3.2.3 *Fibroblast transduction*

DAY 1:

- Plate out fibroblasts at 10,000 cells/well of a 6-well plate.

- Incubate at 37°C for 6 hrs to allow to sit down.

- Replace media with retroviral infection media (MEMα plus additives).

- Add virus at multiplicity of infection (MOI) of 5.

- Incubate for 24 hrs.

DAY 2:

- Aspirate media.

- Wash cells three times with PBS.

- Replenish media.

DAY 4:

- Coat dishes with 0.1% gelatin, incubate for at least 30 mins at 37°C, and seed with inactivated MEFs (2,000,000 cells per 6-well plate).

DAY 5:

- Transfer infected fibroblasts onto MEFs. Add 0.2% trypsin/EDTA, incubate for 2 to 3 mins at 37°C, inactivate with DMEM with fetal calf serum, spin down for 2 mins at 200 g and then transfer to MEF-coated dishes (1:2 split. Each well of 6-well plate transferred to 2 wells).

DAY 6:

- Change media on fibroblasts to hESC media. This first media change is supplemented with Y27632 to promote survival of individual cells with hESC properties.

DAY 8:

- Change media to fresh hESC media (KO-DMEM, 20% KSR, 2 mM L-glutamine, 1× non-essential amino acids, 50 mM 2-mercaptoethanol, 50 U/ml penicillin, 50 mg/ml streptomycin (all from Invitrogen), and 20 ng/ml FGF2 (Peprotech)), and every second day after that.

DAY 30 - 40:

- Observe for colonies and pick accordingly.

3.3.3   *Transposon-based reprogramming*

This method uses the piggyBAC transposon system to deliver the transgenes to the target cells. The original publications that used this method described generation of iPSCs from mouse embryonic fibroblasts and human fetal fibroblasts, but not adult human fibroblasts (Kaji et al., 2009; Woltjen et al., 2009). The following plasmid combinations were trialled:

Plasmids kindly provided by Dr Keisuke Kaji, Institute for Stem Cell Research, Edinburgh

- Doxycycline-inducible expression:

    - PB-TetO-MKOS-imOrange (Tetracycline operator element – *c-Myc*, *Klf4*, *Oct4*, *Sox2* separated by 2A peptides – mOrange marker),

    - PB-pCAG-rtTA (pCAG-driven expression of tetracycline reverse transcriptional activator),

    - pCyl43 (piggyBAC transposase).

- Constitutive expression:

> – PB-pCAG-superMKOS-imOrange (pCAG-driven expression of reprogramming factors and mOrange marker),
>
> – pCyl43 (piggyBAC transposase).

- GFP control plasmid was included in all experiments.

IMR-90 fibroblasts (#CCL-186 from ATCC) were transfected with each plasmid combination using Fugene HD (Roche), Lipofectamine LTX (Invitrogen) or Nupherin (Biomol) at a range of reagent:DNA ratios according to manufacturer's instructions, in triplicate. Suspension transfection was also attempted, as described by Zhang et al. (2007).

Separately, IMR-90 fibroblasts were electroporated with each plasmid combination using an Amaxa nucleofector (Lonza Biosciences), according to manufacturer's instructions.

Combinations of transfection and electroporation, and multiple transfections on consecutive days, were also attempted.

3.3.4 *Episomal reprogramming*

The approach used here is as described in Yu et al. (2009). The plasmids were obtained from Addgene:

- pEP4 E02S ET2K (*OCT4*, *SOX2*, *SV40LT*, *KLF4* separated by IRES) (Addgene #20927)

- pEP4 E02S CK2M EN2L (*OCT4*, *SOX2*, *KLF4*, *c-Myc*, *NANOG* and *LIN28* separated by IRES) (Addgene #20924)

3.3.4.1 *Electroporation*

DAY 1:

- Plate feeder layer: irradiated MEFs in $2\times$ 6-well plates at 1,400,000 cells per plate.

- Nucleofect 1,000,000 patient fibroblasts with 10.5 µg of episomal DNA (3.2 µg pEP4 E02S ET2K + 7.3 µg pEP4 E02S CK2M EN2L)

using program U-23 and Human MSC Nucleofector kit (cat #VPE-1001) with an Amaxa Nucleofector (Lonza Biosciences). Approximately 10% survival expected.

- Plate nucleofected cells into all 12 wells of 2× 6-well plates of irradiated MEFs in MEF media.

DAY 2:

- feed with hESC media supplemented with 20 ng/ml FGF2 every second day.

DAY 10:

- feed with MEF-CM supplemented with 20 ng/ml FGF2 every second day.

DAY 25:

- observe plates and pick colonies if present.

3.3.5 *Retroviral reprogramming – Yamanaka method*

The four main reprogramming factors described in the original iPSC papers (Takahashi and Yamanaka, 2006; Takahashi et al., 2007b) were employed. The plasmids are also available from Addgene:

Plasmids kindly provided by Dr Alison Thomson, Roslin Institute

- pMXs-Oct4 #13366

- pMXs-Sox2 #13367

- pMXs-cMyc #13375

- pMXs-Klf4 #13370

The protocol used here is similar to that described by Ohnuki et al. (2009) with the major difference being that, in the published protocol, virus is packaged with a tropism restricted to murine cells. The murine viral receptor is first transfected into target fibroblasts so that they can

be infected by the virus produced. This is mainly for safety reasons, because it avoids the need to generate virus that is capable of infecting human cells. In contrast, in the protocol detailed below, virus with a tropism encompassing human cells is generated under category 2 level biosafety.

Human fibroblasts and mouse embryonic fibroblasts (the latter serving as positive control) were seeded in three wells each (100,000 cells per well) of 6-well plates. These were transfected into Platinum-A cells (Cell Biolabs #RV-102) with Lipofectamine 2000 (Invitrogen) to package viral particles.

Target fibroblasts (100,000 cells) were transduced with virus in the presence of 6 ng/ml polybrene (Millipore #Tr-1003-G) twice on consecutive days, then lifted with Accutase (Invitrogen) a day later and replated on irradiated SNL feeders (available from European Collection of Cell Cultures, ECACC).

The day after re-plating, media was switched to hESC media supplemented with 0.5 mM valproic acid (VPA) – a histone deacetylase inhibitor shown to accelerate and improve the efficiency of reprogramming (Huangfu et al., 2008). Colonies were mechanically picked after approximately 20 days and maintained on SNL feeders in hESC media without VPA. Established iPSC lines were maintained in hESC media containing 10 ng/ml FGF2.

3.3.5.1 *Viral packaging and fibroblast transduction*

DAY 1:

- Coat four 10cm dishes with 1.2 ml poly-D-lysine, incubate RTP for 2 hrs.

- Wash three times with PBS.

- Seed 3,600,000 Plat-A cells per plate in 12 ml DMEM + FBS without antibiotics.

DAY 2:

- One hour before transduction, change medium to Optimem, 12 ml/dish.

- Dilute 16 μg DNA with 1.5 ml Optimem.

- Dilute 60 μl Lipofectamine 2000 in 1.5 ml Optimem, incubate RTP for 5 mins.

- Mix DNA + Lipofectamine together, incubate RTP for 20 mins.

- Add mixture to appropriate dish.

DAY 3:

- Change media to DMEM + FBS, 6 ml per plate.

- Seed fibroblasts: 100,000 in each of three wells of a 6-well plate.

DAY 4:

- Collect and combine 4 viral supernatants, filter 0.45 μm.

- Add to cells to be transduced (24 ml total, ~4 ml per well, 6-well format).

- Supplement with 8 μg/ml polybrene per well.

    - Two of three wells of each target lines (third being untransfected control),

    - One MEF positive control.

- Replenish media on transfected cells.

DAY 5:

- Repeat steps of DAY 4 and discard packaging cells.

- Seed feeders (irradiated SNL or MEF): 900,000 per 10 cm dish, four dishes in total.

DAY 6:

- Lift transduced fibroblasts with Accutase (no need for ROCK inhibitor).

- Count and seed cells on 10 cm dish of feeders (range 60,000 to 500,000 cells per dish).

- Freeze down remainder.

DAY 7 − 21:

- Change media on plates to hESC media + 0.5mM VPA + 20 ng/ml FGF2.

- Replace media alternate days thereafter, until colonies form.

- Then, withdraw VPA and feed daily with hESC media.

3.3.5.2 *Colony picking and expansion*

Once colonies are visible in the dish by eye (~ 2 to 4 mm in diameter), they are ready to be picked. Only those colonies that have a clearly demarcated border separating them from surrounding feeder cells will have completed reprogramming, i.e. those with hESC colony appearances. Colonies with an indistinct border are likely to be c-Myc transformed or partially reprogrammed fibroblasts that will fail to generate viable iPSC lines.

- Plate out fresh feeders in 24-well format the day prior to picking and transferring colonies.

- Demarcate appropriate colonies to be picked under microscopic visualisation.

- In the tissue culture hood, aspirate sufficient media from the plate leaving a thin film of media remaining.

- Score round the edge of the colony using a P200 micropipette tip and a Gilson pipette, holding it perpendicular to the plate, to separate it from the surrounding feeder layer.

- Take up a few microlitres of media into the pipette tip, then aspirate the colony into the tip, and gently place in a dedicated well of the the new 24-well plate.

- Repeat for each viable colony, using one well per colony.

- The day after colony transfer, withdraw VPA and feed daily with hESC media thereafter.

- Once colonies have expanded to near confluence, or there are signs of early differentiation, or the feeder cells are dying, the colony should be transferred to fresh feeders, potentially to individual wells of 6-well plates, which is the format that I have used to maintain iPSC lines in culture.

3.4 RESULTS

3.4.1 *Retroviral reprogramming – Daley method*

One of the first laboratories to generate iPSCs from human cells was that of George Daley in Boston (Park et al., 2008b). His was also the first group to publish a full protocol on how to generate human iPSCs (Park et al., 2008a) and we were generously given the set of plasmids containing the four reprogramming factors that they used in their studies. Therefore, this was the first approach that I used to try and generate iPSCs from human fibroblasts. The method begins by using HEK 293T cells to generate (package) retrovirus containing each of the four reprogramming transgenes. The viral supernatants are then spun down to concentrate the virus. These transgenes also express GFP, which is used to titre the virus as described in Section 3.3.2.2. The process of titration via FACS is shown in Figure 3.3.

Initial attempts used HEK 293T cells to package the virus according to the published protocol, using separate plasmids encoding *VSV-g* and *gag-pol*. Despite multiple and extensive rounds of packaging
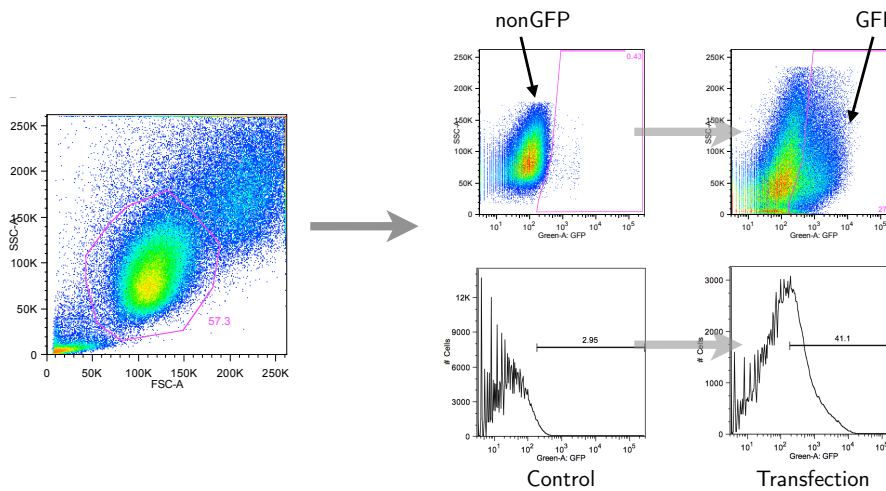
Figure 3.3: FACS titration of viral vectors. HEK 293T cells are infected with serial dilutions of concentrated viral supernatant, viable cells gated (shown in left panel) then analysed by FACS for expression of GFP, and compared to uninfected control cells.

with several fresh batches of HEK 293T cells and reagents, viral titres remained very low. At best, by pooling viral supernatant from a large number of plates of packaging cells, virus could be produced, but at a titre at least 10-fold lower than required.

Packaging was then switched to the Phoenix Ampho cell line (Cell Biolabs), which already encodes *VSV-g* and *gag-pol*. Efficiency was anticipated to increase, because only one plasmid (the transgene) needs to be added to the cells in order to package viral particles bearing the gene of interest. This did improve packaging efficiency hugely. Nevertheless, viral packaging of these vectors gave titres of less than 1 million TU/ml at best. At multiplicity of infection (MOI) = 5, at least 500 µl of concentrated viral supernatant (of a total of 1000 µl generated by the packaging protocol) would be needed to attempt to reprogram 100,000 fibroblasts. Furthermore, viral supernatant produced by Phoenix ampho cells was more toxic to cells than supernatant taken from HEK 293T cells, an effect noted during viral titration. Either this was due to the direct result of a higher concentration of virus being produced, or due to empty viral particles (i.e. transgene free) that are continuously produced by the Phoenix Ampho cells.

Multiple attempts were made to reprogram control human fibroblasts with appropriate titres of virus, but were not successful. Infected fibroblasts did take on a granular appearance (possibly due to the presence of viral inclusions, implying that infection had occurred), however hESC-like colonies did not emerge.

3.4.2   *Transposon-based reprogramming*

By this time, Keisuke Kaji in Edinburgh had published successful generation of iPSCs from mouse and embryonic human fibroblasts using transposons (Kaji et al., 2009; Woltjen et al., 2009). Transposons are DNA sequences that can move (or transpose) themselves to another location within the genome. Transposons can be seamlessly removed (excised) from the genome, in contrast to retrovirally-delivered transgenes which integrate into the host genome and remain there. This is potentially advantageous for disease modelling with iPSCs because it avoids continued or ectopic transgene expression which can limit the differentiation potential of iPSCs (Hotta and Ellis, 2008). Therefore, this was the next approach attempted.

However, despite multiple attempts with several DNA delivery strategies, including transfection with multiple reagents, electroporation, various combinations of both electroporation and transfection, and repeated rounds of transfection, this was ultimately not successful. Representative images of the most successful attempts at DNA delivery are shown in Figure 3.4. In short, adequate DNA delivery was not achieved.

3.4.3   *Episomal reprogramming*

The next approach that was explored was James Thomson's method using episomes (Yu et al., 2009). Episomes are the eukaryotic equivalent of bacterial plasmids – generally closed DNA molecules that
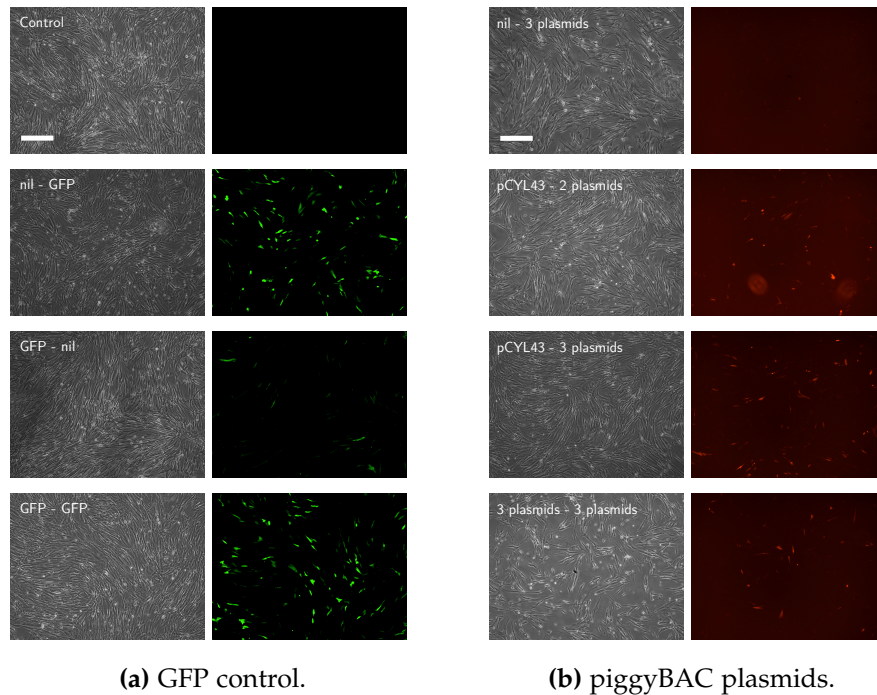
(a) GFP control.

(b) piggyBAC plasmids.

Figure 3.4: The most efficient DNA delivery method used was a combination of nucleofection and transfection. The fibroblasts tolerated this approach, however there were still very few mOrange-positive cells generated by this method. Representative images shown. Scale bar, 100 μm.
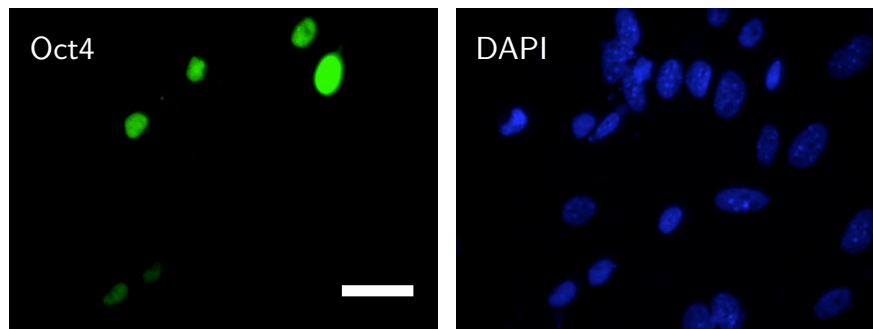
Figure 3.5: Immunofluorescence for Oct4 in IMR-90 fibroblast electroporated with episomes described in Yu et al. (2009). DNA delivery was poor at best (10 to 15% of cells, with the aim being close to 100%). Representative images shown. Scale bar, 50 μm.

replicate autonomously in the cytoplasm. Yu et al. (2009) successfully generated human iPSCs using a combination of two episomes carrying *OCT4*, *SOX2*, *c-Myc*, *KLF4*, *LIN28*, *NANOG*, *hTERT* and *SV40LT*, each gene being separated by an internal ribosome entry site (IRES). The potential advantage with this method is that it has the potential to be entirely integration-free. Although episomes can integrate, they can also be spontaneously lost: subcloning of successfully reprogrammed cell lines can identify clones where this loss has occurred or where integration has not taken place.

Both episomes are relatively large (almost 20 kb), in part because they both carry multiple transgenes. This perhaps explains why the major difficulty with this approach was achieving sufficient DNA delivery to cells. Nevertheless, a handful of colonies with phase-bright edges did appear after one reprogramming cycle (Figure 3.6), however these failed to expand in culture. One colony (Figure 3.7) did have hESC-like appearances, including cell morphology (high nuclear:cytoplasmic ratio) and reasonably distinct colony border. However, this did not expand and persist well in culture either.
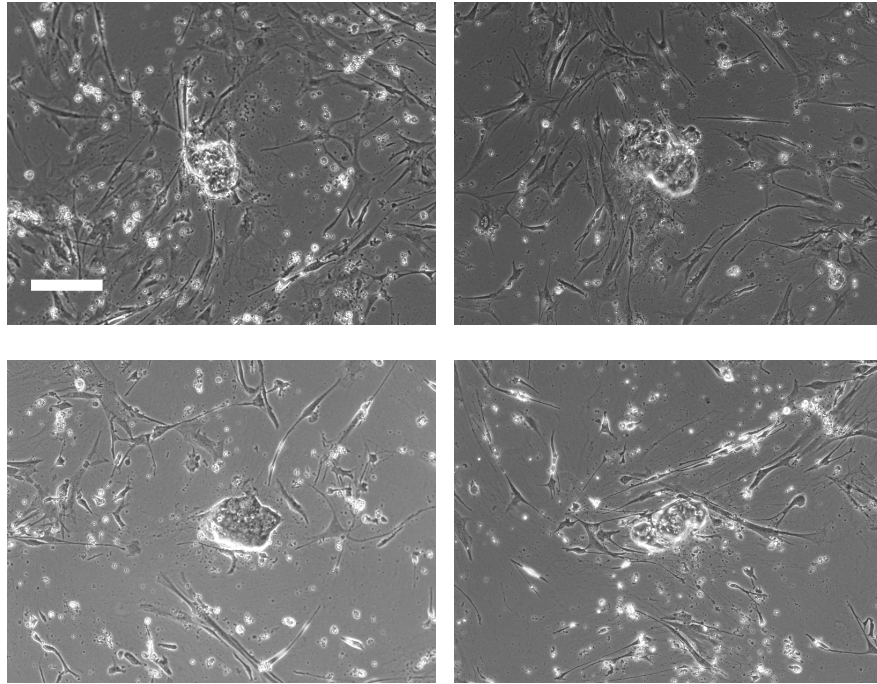
Figure 3.6: Colonies generated from episomal-based reprogramming, shown at day 14 post electroporation (Amaxa). These have phase bright edges, but failed to thrive in culture, and did not generate cell lines. Representative images shown. Scale bar, 100 μm.
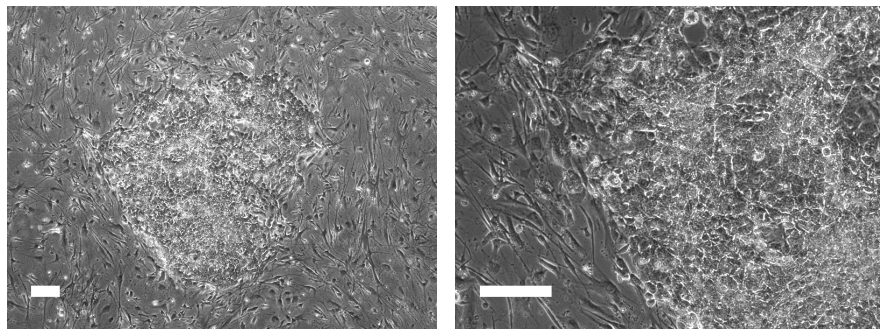
Figure 3.7: Episomal transfection did generate one colony that was successfully expanded in culture, and initially had hESC-like appearances. However, this cell line did not survive in culture for more than a few passages. This was likely a partially reprogrammed, or c-Myc-transformed, cell colony. Scale bar, 100 μm.

PHENOTYPE	AGE	GENDER	GENOTYPE	LINE
Early onset PD	54	F	SNCA triplication	AST
Unaffected	30	F	Daughter	NAS
Unaffected	82	F	Unrelated	UNF
Unaffected	78	M	Unrelated	UNM

Table 3.2: Patient and control fibroblast lines used for reprogramming.

3.4.4 *Retroviral reprogramming – Yamanaka method*

In complete contrast to the methods described above, this approach worked extremely well. Two separate rounds of reprogramming were carried out using this method, yielding colonies with hESC-like appearances from a total of four parent fibroblast lines. Fibroblasts from the affected individual with *SNCA* triplication, an unaffected first-degree relative and two further control individuals were used (summarised in Table 3.2).

Pictures of *de novo* iPSC colonies are shown in Figure 3.8. These colonies, with distinct borders and hESC morphology, are in contrast to other colonies also generated that lack distinct borders and have a 'heaped up' appearance (Figure 3.9). Initial characterisation focussed on iPSC lines from the three parent fibroblast lines shown in Table 3.3, whilst subsequent characterisation (detailed in Chapter 4) concentrated on AST and NAS iPSC lines.

3.5 DISCUSSION

The initial methodological difficulties gave way to a robust and efficient method of reprogramming once the originally reported method was adopted (documented in detail in Ohnuki et al. (2009)). The fact that this original approach is so efficient is perhaps due to the route by which it was discovered: this reprogramming method was inevitably
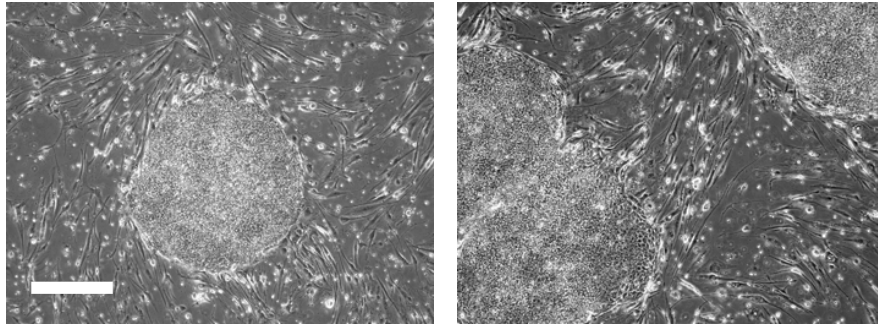
(a) Colonies derived from NAS fibroblasts.
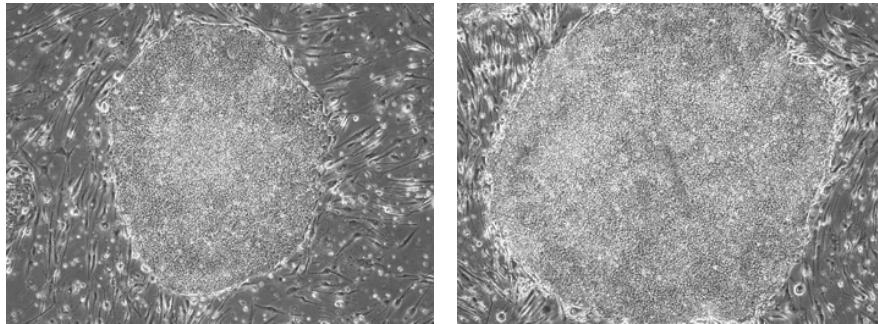
(b) Colonies derived from AST fibroblasts.

Figure 3.8: Phase contrast images of NAS and AST fibroblasts and *de novo* iPSC colonies on SNL feeder cells at day 20 post-viral transduction. Scale bar, 100 μm.
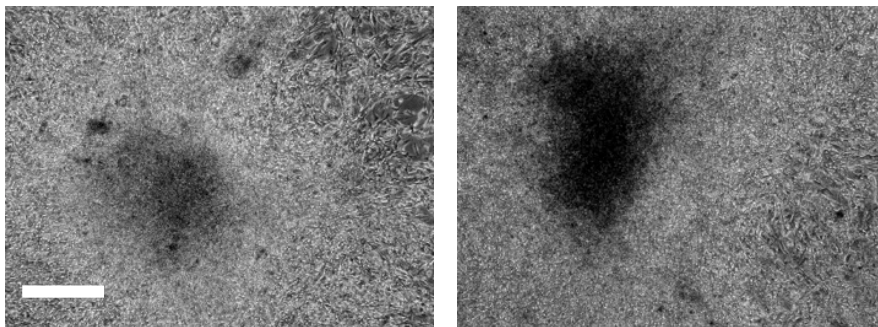
Figure 3.9: Non-iPSC colonies. Note heaped appearance and lack of distinct (phase-bright) border. Scale bar, 100 μm.

PARENT LINE	PASSAGE	COLONIES	VIABLE LINES
AST	3	13	7
NAS	8	25	9
UNF	4	21	4
UNM	5	24	5

Table 3.3: Viable iPSC lines generated via retroviral reprogramming using the Yamanaka vectors.

an efficient one if it were to permit iPSC generation via a screen of hand-curated genes (Takahashi and Yamanaka, 2006).

The approach adopted by George Daley's group (Park et al., 2008b) differed from Yamanaka's method in one critical respect: the promotor used to drive transgene expression in transduced fibroblasts. They opted for the murine stem cell virus (pMIG) promotor, rather than the Maloney virus (pMXs) promotor used by Yamanaka. At the time (2007) this made sense – this was before successful reprogramming of human cells had been reported, and it was perhaps believed by Daley's group that this might, in part, be due to insufficient transgene expression in emerging iPSCs. Hence, they opted for a stem cell promotor which would yield high expression in cells with pluripotent identity, but unfortunately expression in fibroblasts would be lower, making the reprogramming process less efficient.

The transposon-based and episomal methods described have the advantage that the genes used for reprogramming can be excised once reprogramming is complete (piggyBAC transposon (Kaji et al., 2009)) or may not integrate at all (Thomson episomes (Yu et al., 2009)). However, major difficulties were unfortunately encountered with appropriate DNA delivery. Given that patient-derived fibroblasts are a finite and precious resource, the reprogramming method employed had to be efficient, hence the return to a retroviral method which worked successfully.

The next chapter describes the demonstration of the hallmarks of pluripotency in the iPSC lines derived from the patient and the unaffected relative.

CHARACTERISATION OF INDUCED PLURIPOTENT STEM CELLS

4.1 INTRODUCTION

In Chapter 3, I discussed the various approaches that were used to try and generate iPSCs. The only robust and reproducible method found was original approach used by Takahashi and Yamanaka (Ohnuki et al., 2009). Multiple iPSC lines were generated from four separate fibroblast lines. The first step was to identify iPSC clones, from each parent fibroblast line, that could form stable lines capable of being maintained in prolonged culture (shown in Table 3.2).

The next stage was to determine whether these putative iPSC lines were indeed pluripotent. The original description of iPSCs used several methods to demonstrate that the novel cell type generated had properties similar to ESCs (Takahashi and Yamanaka, 2006). The overall question was how closely the novel cell type (iPSC) recapitulated the two key features of ESC behaviour: pluripotency, and self-renewal.

4.1.1 *Confirmation of pluripotency*

The following characterisation was carried out by Takahashi and Yamanaka (2006):

ENDOGENOUS PLURIPOTENCY GENE EXPRESSION: an indicator of completion of reprogramming is that the cell's endogenous pluripotency genes (e.g. *Oct4*, *Sox2*, *Nanog*) are switched on. This is determined via quantitative RT-PCR for these genes.

BISULPHITE GENOMIC SEQUENCING: key pluripotency genes were checked for promoter demethylation which is an indication of endogenous genes being switched on.

IMMUNOCYTOCHEMISTRY: for surface antigens specfically expressed in ESCs such as SSEA4 and TRA-1-81, and proteins that are present in the pluripotent state e.g. Nanog.

GENE EXPRESSION MICROARRAY: transcriptional profiles of iPSCs and ESCs are determined to see how closely they resemble each other.

EMBRYOID BODY FORMATION: to establish that iPSCs can differentiate into elements of all three germ layers *in vitro*.

TERATOMA FORMATION: to demonstrate that iPSCs can form elements of all three germ layers *in vivo*.

CHIMAERA FORMATION: regarded as the most stringent test of pluripotency, that cells can contribute to the formation of an embryo, and ultimately give rise to cells in the germ line. This test cannot be conducted with human ESCs due to ethical reasons that are self-explanatory.

4.1.2 *Confirmation of self-renewal*

TELOMERASE ACTIVITY: a defining characteristic of ES cells is the persistence of telomerase activity, which prevents the shortening of telomeres with cell division, hence enabling these cells to evade senescence.

KARYOTYPE ANALYSIS: to ensure that aneuploidies and other chromosomal abnormalities have not been acquired during the reprogramming process, nor during routine passage in culture.

4.1.3 *Characterisation of human iPSCs*

The characterisation outlined above is necessarily thorough and complete because this was the first report of a novel cell type. Subsequent reports of the generation of human iPSCs did not include chimaera formation for obvious reasons (Yu et al., 2007; Takahashi et al., 2007b; Park et al., 2008b), but did recapitulate the other characterisation methods listed above.

In this chapter, I will detail the methods used to characterise the iPSC lines described in Chapter 3. I also discuss additional characterisation that was carried out to confirm that the patient-derived iPSCs retained triplication of *SNCA*.

4.2 METHODS

4.2.1 *Transgene silencing and marker gene expression*

RNA was obtained from separate iPSC lines using the RNeasy Plus kit (Qiagen) according to manufacturer's instructions. cDNA was generated via Superscript III (Invitrogen), and qPCR reactions were carried out with SYBR Green (Qiagen) on a Lightcycler 480 (Roche), with primer pairs specific to mouse *Oct4*, *Sox2*, *Klf4* and *c-Myc* (see Section A.1).

Transgene silencing data provided by Dr Fatima Cavaleri, Insitute for Stem Cell Research, Edinburgh

Results were normalised to human *TBP* using the comparative C(T) method (Schmittgen and Livak, 2008) and compared to equivalent values determined from fibroblasts three days post-viral transduction (positive control), Shef4 hESCs (negative control) and non-transduced human fibroblasts (negative control). cDNA was generated from neuralised iPSCs by the same method, and qPCR reactions were carried out with the Universal Probe Library (UPL) system (Roche) and normalized to *GAPDH*. All primers are available in Section A.1.

4.2.2 *Immunocytochemistry*

Cells were fixed in 4% paraformaldehyde at room temperature, or 100% methanol at -20°C for 15 mins, then blocked and permeabilised with blocking buffer (2% goat serum, 0.1% Triton-X in PBS) overnight at 4°C before probing with the following primary antibodies (overnight in blocking buffer at 4°C):

- OCT4 (Santa Cruz #5279, mouse IgG2b, 1:200),

- TRA 1-81 (Biolegend #330701, mouse IgMϰ, 1:600),

- SSEA4 (DSHB, mouse IgG3ϰ, neat),

- NANOG (Abcam #ab21624, rabbit IgG, 1:1000).

Appropriate AlexaFluor-488 and AlexaFluor-596-labelled secondary antibodies (Molecular Probes) were used, with DAPI counterstaining, prior to imaging with an Olympus IX51 inverted fluorescent microscope.

4.2.3 *Embryoid body formation*

iPSC colonies from separate lines were mechanically lifted intact and seeded en bloc onto low attachment dishes (Sterilin #121V) and grown in 20% KSR medium (hESC media without FGF2) for seven days (feeding alternate days) after which they were plated onto tissue culture-treated plasticware coated with 0.1% gelatin and allowed to differentiate for a further seven days in DMEM with 10% FCS. RNA was then extracted, and examined by qRT-PCR for expression of *MSX1*, *PAX6*, and *AFP* – marker genes representative of each of the three germ layers (detailed in Section A.1).

4.2.4 *SNCA triplication screening*

Genomic DNA was obtained from individual cell lines using the DNA blood and tissue kit (Qiagen) according to manufacturer's instructions, including treatment with RNase A to remove contaminating RNA. Dosage of *SNCA* was then assessed with SYBR Green qPCR on a Rotorgene unit (Qiagen) using primers specific for exons 1 and 4 of *SNCA* and β2-microglobulin (*B2M*) and β-globin (*HBB*) as diploid control genes (Ahn et al., 2008) (detailed in Section A.1).

4.2.5 *SNP microarray*

DNA was extracted from fibroblasts and iPSC lines using the DNeasy Blood and Tissue Kit (Qiagen, UK) according to the manufacturer's instructions.

Microarrays were run by AROS AS, Denmark

DNA was quantified spectroscopically (NanoDrop, Thermo Scientific, UK) and 4 μl of 50 ng/μl gDNA and whole-genome amplified DNA samples were marked on the Illumina Infinium Omni1-Quad BeadChip (Illumina) according to the manufacturer's instructions. The BeadChips were scanned using an iScan (Illumina) with an AutoLoader (Illumina).

GenomeStudio v.1.8.X (Illumina) was used for analysing the data and generating SNP calls which were created using the HumanOmni1-Quad_v1-0_B cluster file provided by Illumina as a reference. This data has been deposited on GEO (accession number GSE28366).

4.2.6 *Gene expression microarray*

Total RNA was extracted from fibroblasts and iPSC lines using the RNeasy Plus kit (Qiagen, UK) according to the manufacturer's instructions.

Microarrays were run by AROS AS, Denmark

Following the evaluation of RNA quality by capillary electrophoresis (Agilent 2100 Bioanalyzer and RNA 6000 Nano Kit, Agilent Technologies, UK), 200 ng of total RNA was used as starting material for the cDNA preparation. All steps starting from the first and second strand cDNA synthesis, the In Vitro Transcription reaction to generate cRNA and the second round of cDNA synthesis were performed using the Ambion®WT Expression Kit (Ambion, UK) according to the manufacturer's instructions.

Samples were then processed using the Affymetrix GeneChip Whole Transcript Sense Target Labelling Assay and hybridised to the Affymetrix Exon 1.0 ST and U133 Plus 2.0 Arrays following the recommended Affymetrix protocols.

Hybridised arrays were scanned on GeneChip Scanner 3000 and visually inspected for hybridisation artefacts. The data has been deposited on GEO (accession number GSE28365).

4.2.7 *Gene expression microarray analysis*

Exon Array data generated from fibroblast lines ($n = 2$) and iPSC lines ($n = 4$) were evaluated for uniform hybridisation intensity, abnormal background signals and sample outliers using Affymetrix Expression Console (Affymetrix). All arrays were preprocessed using RMA quantile normalisation with GC background correction in Partek's Genomics Suite v6.5 (Partek Incorporated, USA). Only probe sets containing a minimum of three probes, unique hybridisation and designed against genes annotated within Entrez Gene (www.ncbi.nlm.nih.gov/entrez/query.fcgi?db=gene) as documented in the most recent Netaffx annotation file (HuEx-1_0-st-v2 Probeset Annotations, CSV Format, Release 31) were included in the analysis.

Gene level summary signals were generated by calculating the median expression value of all probe sets annotated to a single gene. Principal component analysis (PCA), unsupervised hierarchical clus-

Microarray analysis performed by Dr Mina Ryten, UCL Institute of Neurology

tering, Student's *t*-testing and gene expression scatterplot analyses were performed in Partek Genomics Suite v6.5 (Partek Incorporated, USA).

Gene set enrichment analysis (GSEA) was performed using GSEA v2.0.6 (Broad Institute, Cambridge, MA, USA) using gene set permutation and a Triplication Gene Set, which was defined as all genes present within the triplication region (as identified on SNP array assessment) (Subramanian et al., 2005). Following removal of batch effects, iPSC data analysed using Affymetrix U133 Plus 2.0 Arrays were compared via Principal Components Analysis with the following data sets, all publicly available via GEO: GSE16190, GSE19902, GSE22499, GSE26451, GSE7179, GSE7879, GSE8590 and GSE9440.

4.3   RESULTS

4.3.1   *Transgenes are silenced in a subset of iPSC lines*

Given that incomplete silencing of the reprogramming transgenes can limit the differentiation potential of iPSC lines (Hotta and Ellis, 2008) a pivotal step in screening iPSC lines for disease modelling is to determine transgene silencing by quantitative RT-PCR for transgene expression. A total of seven AST and nine NAS iPSC lines were established that could be maintained and expanded in culture. Cell lines with the strongest retroviral silencing have been shown to differentiate more efficiently and is indicative of complete reprogramming (Hotta and Ellis, 2008). Therefore, all lines were examined for transgene silencing relative to fibroblasts three days post-viral transduction (acting as a positive control) (Figure 4.1).

The first batch of reprogrammed cell lines had variable levels of transgene silencing. Whilst the majority of NAS iPSC lines exhibited good levels of transgene silencing, AST iPSC lines did not (Figure 4.1a). Additional AST clones were generated by thawing cells that had been

frozen at the colony picking stage. This non-clonal mixture of cells was plated at low density yielding several dozen new colonies from which five new clones were derived (AST9 – 14 in Figure 4.1b). When transgene expression was examined, only one of these clones (AST13) demonstrated efficient silencing. In order to generate additional AST iPSC lines with efficient silencing, a second round of AST reprogramming was carried out using higher titre virus by Dr Tilo Kunath, yielding a further 13 lines (lines AST18 – 30 in Figure 4.1b).

The cell lines with the lowest observed levels of transgene expression were chosen for further analysis. All chosen iPSC lines exhibited good hESC colony morphology and growth characteristics, and have been passaged more than 60 times, with more than 12 months in continual culture.

4.3.2 *Pluripotency genes are switched on in iPSC lines*

Colonies from NAS and AST iPSC lines demonstrated robust expression of the pluripotency markers OCT4, SSEA4, TRA-1-81 and NANOG (Figure 4.2). Endogenous expression of the pluripotency genes *OCT4*, *SOX2*, *NANOG* and *REX1* was reactivated in all iPSC lines examined (Figure 4.3). The *OCT4* and *SOX2* primers do not recognise the mouse *Oct4* and *Sox2* transgenes used to reprogram the cells. No significant differences between AST and NAS iPSC lines were observed with respect to expression of key pluripotency genes.

4.3.3 *Embryoid bodies can be generated from iPSCs*

Embryoid bodies derived from a sample of patient and control iPSC lines expressed *MSX1* (a marker of mesoderm), *PAX6* (ectoderm) and *AFP* (endoderm) (Figure 4.4). No major differences were observed in the ability of the iPSC lines to differentiate into the three germ layers.
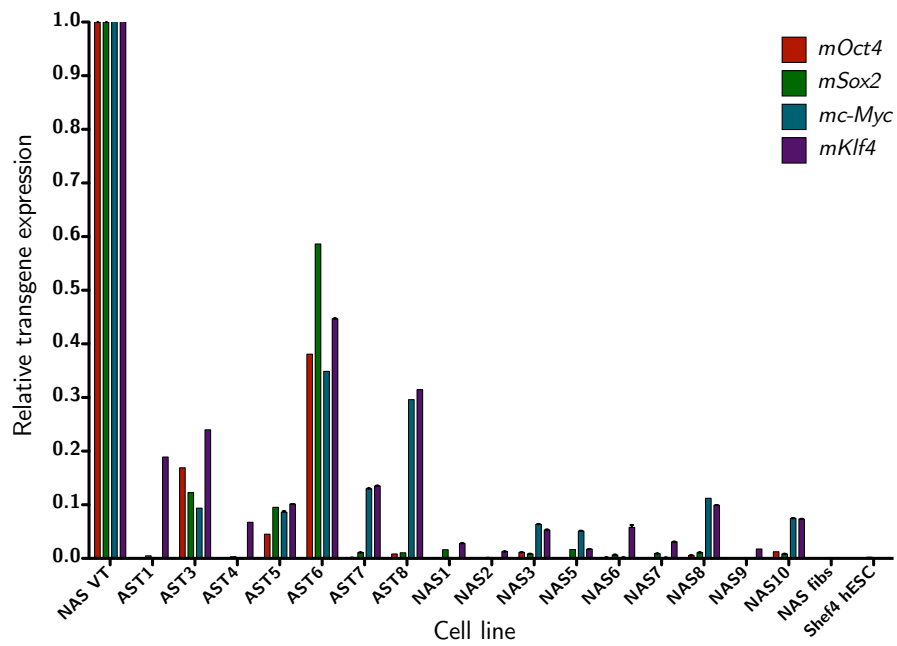
(a) Reprogramming batch 1.
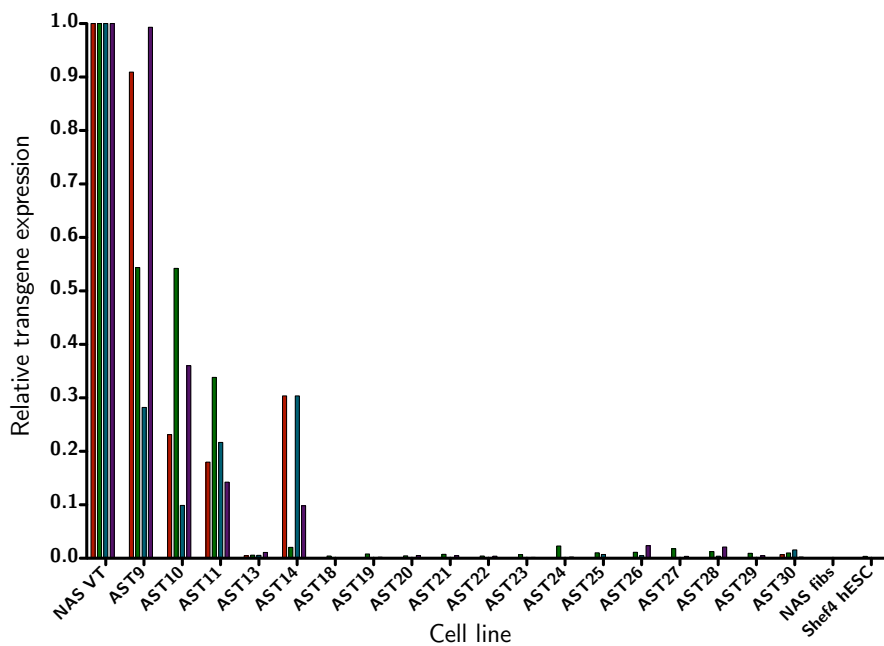
(b) Reprogramming batch 2.

Figure 4.1: Quantitative RT-PCR for retroviral transgene expression of the four reprogramming factors (*Oct4*, *Sox2*, *c-Myc*, *Klf4*). Expression in iPSC lines was normalised to transgene expression of NAS fibroblasts 3 days post viral transduction (NAS VT). Also shown are negative controls: untransduced fibroblasts (NAS fibs) and human ESCs (Shef4).
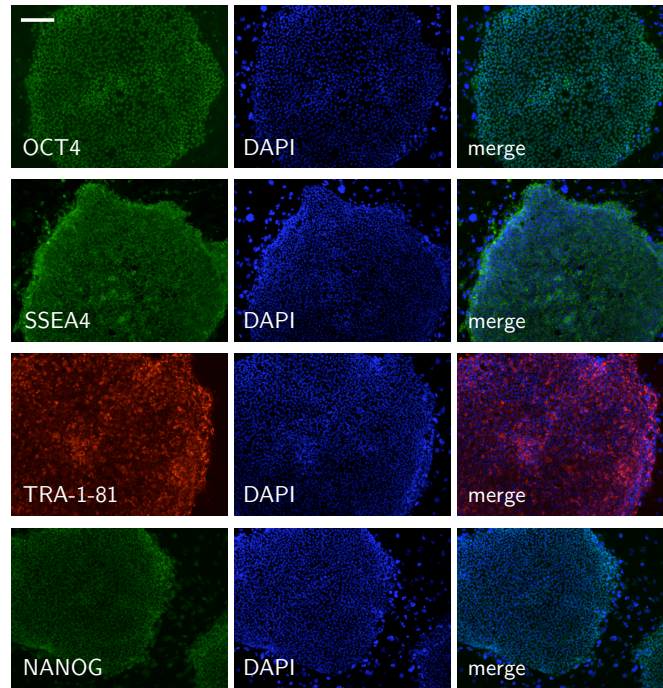
(a) NAS iPSC colonies.
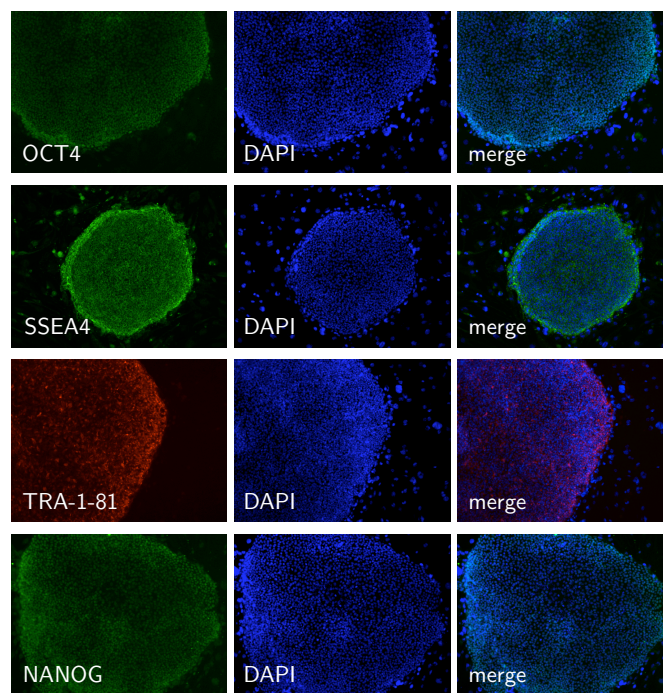
(b) AST iPSC colonies.

Figure 4.2: Representative iPSC colonies derived from **(a)** NAS fibroblasts and **(b)** AST fibroblasts stained positive for the pluripotency markers OCT4, SSEA4, TRA-1-81 and NANOG. Scale bar, 100 μm.
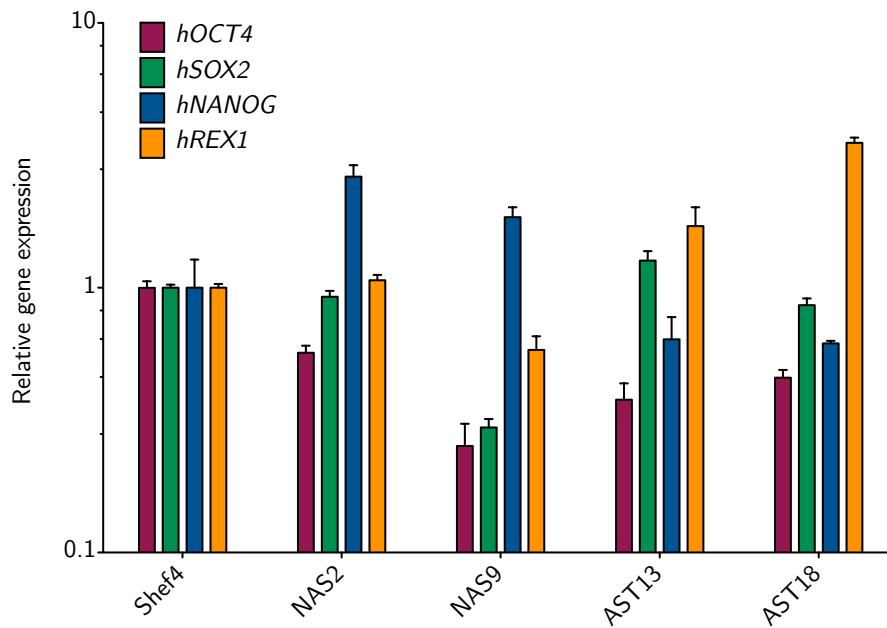
Figure 4.3: Endogenous expression of *OCT4*, *SOX2*, *NANOG* and *REX1* in two AST and two NAS iPSC lines, normalised to expression in human ESCs (Shef4), found a similar expression profile in all lines examined. Expression of these genes was absent in human fibroblasts (not shown). Error bars represent standard deviation of technical replicates, $n = 3$.
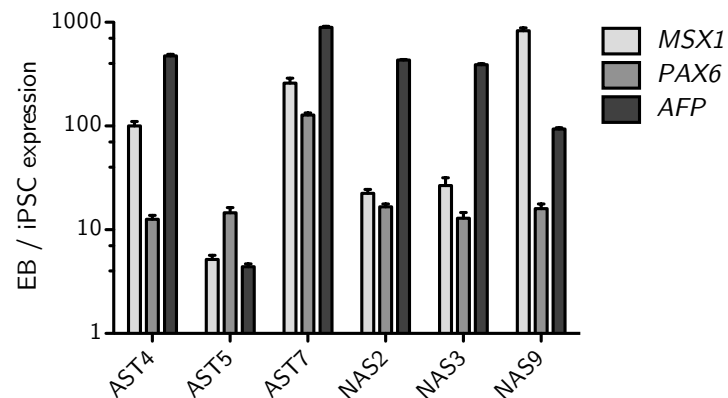
Figure 4.4: Embryoid bodies (Day 14) from three AST and three NAS iPSC lines were analysed for expression of *MSX1* (mesoderm marker), *PAX6* (ectoderm) and *AFP* (endoderm) and compared to expression in the same iPSC clones. Error bars represent standard deviation of technical replicates, $n = 3$.

(a) Fibroblasts.

(b) iPSCs.
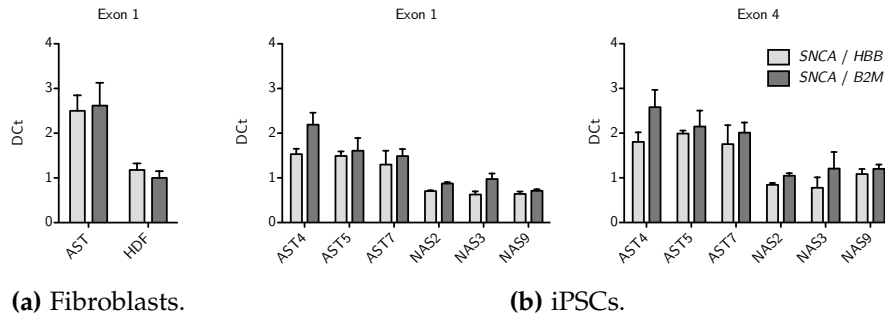
Figure 4.5: Quantitative genomic PCR for *SNCA* exons 1 and 4 demonstrates doubling of gene dosage in patient-derived AST iPSC lines when compared to NAS iPSC lines. Representative data shown from a sample of AST and NAS iPSC lines. *SNCA* was normalised to β-globin (*HBB*) and β2-microglobulin (*B2M*). Error bars represent standard deviation of technical replicates, $n = 3$.

4.3.4 *Triplication region is retained intact*

SNCA gene dosage was re-examined in the AST iPSC lines to confirm they retained the triplication: genomic qPCR for *SNCA* exons 1 and 4 confirmed that AST iPSC lines had twice as many *SNCA* alleles as NAS iPSC lines (Figure 4.5).

Genomic DNA samples from the two participants, the two fibroblast lines and four iPSC lines were further analysed on genome-wide SNP arrays. This analysis confirmed that those samples derived from the unaffected relative were normal at Chr4q22 whilst the triplicated region was retained intact in all samples derived from the patient (Figure 4.6).

The triplication region (originally defined in Singleton et al. (2003)) was refined further. The size was determined to be 1.505 Mb, spanning from chr4:89,375,425 to 90,880,891 (Figure 4.7).

(a) Unaffected relative (NAS).   **(b)** PD patient (AST).
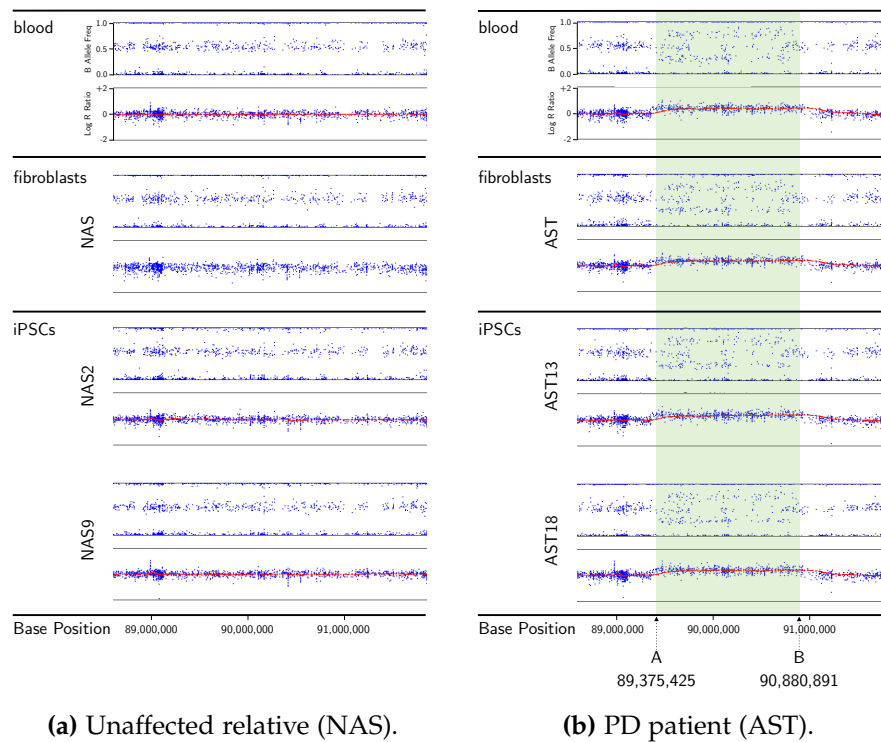
Figure 4.6: Triplication region is maintained in patient-derived fibroblasts and iPSCs. SNP profiles of chromosome 4q22 in DNA from unaffected relative blood, fibroblasts and iPSCs demonstrates that this region is normal whilst the same region analysed in DNA from patient blood, fibroblasts and iPSCs confirms that the triplication region is present and is retained during reprogramming.
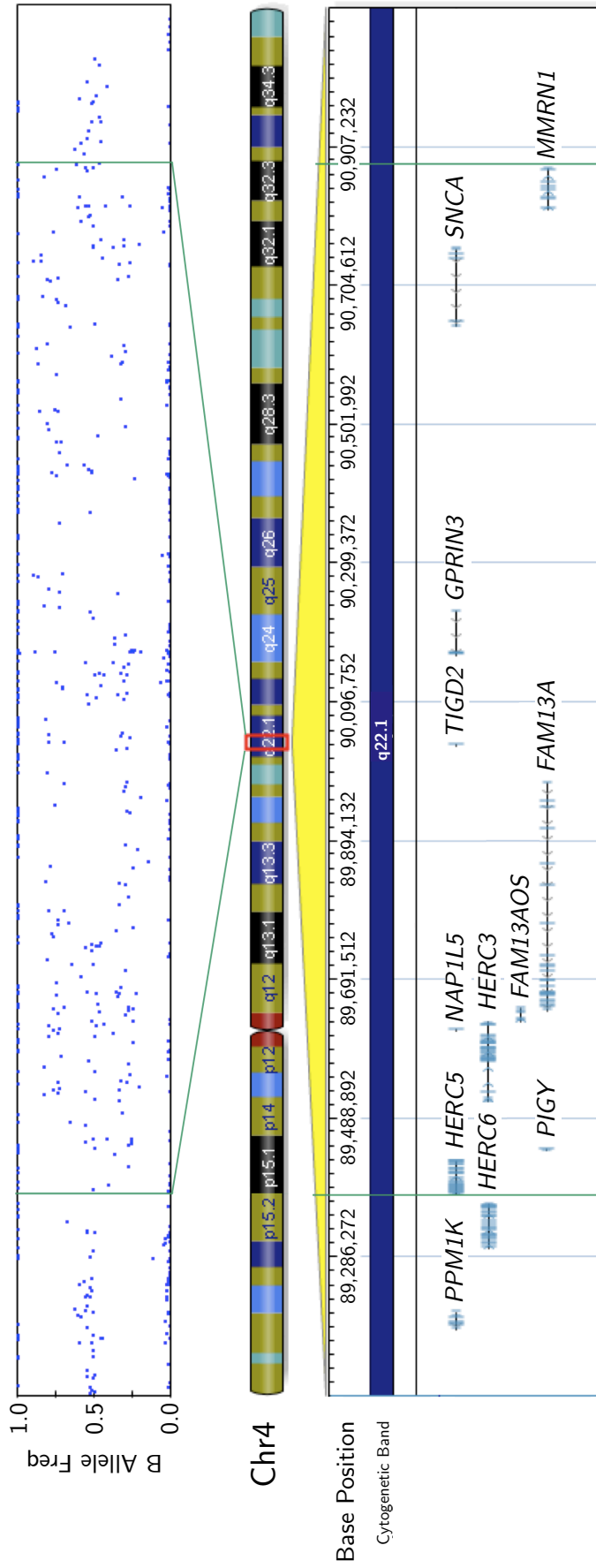
Figure 4.7: The triplication region is defined as chr4:89,375,425 to 90,880,891, spanning the following genes: *HERC5, PIGY, HERC3, NAP1L5, FAM13AOS, FAM13A, TIGD2, GPRIN3, SNCA* and *MMRN1. LOC644248* is also in the triplication region but not yet defined by RefSeq.
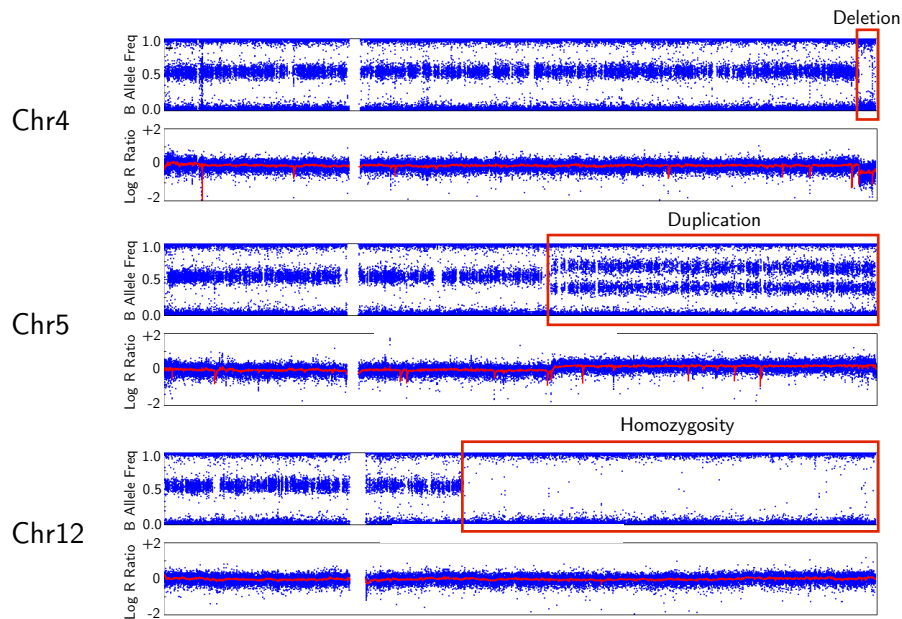
Figure 4.8: Genome-wide SNP analysis of NAS9 iPSCs identified the following chromosomal abnormalities: a small deletion at the end of Chr4q, a duplication of part of Chr5q and an extended run of homozygosity occupying most of Chr12q.

4.3.5 *NAS9 acquired chromosomal abnormalities*

SNP data was used as a virtual karyotyping method to survey the rest of the genome for chromosomal integrity in these cell lines. Two PD iPSC lines (AST13 and AST18) and one control iPSC line (NAS2) did not acquire any chromosomal aberrations following reprogramming and after more than 25 passages in culture. In contrast, one control iPSC line, NAS9, contained a duplication of a large part of chromosome 5q, an extended run of homozygosity in chromosome 12q, and a small deletion at the end of chromosome 4q (Figure 4.8).

Chromosomal abnormalities of this nature are consistent with published reports of iPSCs where this has been specifically examined (Mayshar et al., 2010). However, such analysis had not been reported in the iPSC disease models published at the time (mid 2011).

SAMPLE 1	SAMPLE 2	PI-HAT
Blood DNA (AST)	AST fibroblasts	0.9999
AST fibroblasts	AST13 iPSCs	0.9998
AST fibroblasts	AST18 iPSCs	0.9998
Blood DNA (NAS)	NAS fibroblasts	0.9999
NAS fibroblasts	NAS9 iPSCs	0.9797
NAS fibroblasts	NAS2 iPSCs	0.9999
Blood DNA (AST)	Blood DNA (NAS)	0.5

Table 4.1: Pi-hat analysis confirms origin of iPSC lines.

4.3.6 *Pi-hat analysis confirms origin of iPSC lines*

Pi-hat analysis (described in Dolan et al. (1999)) was used to make comparisons between SNP data sets from each sample. This analysis confirmed that AST and NAS iPSCs were indeed derived from the PD patient and unaffected relative, respectively (shown in Table 4.1). A value of 1 for Pi-hat means that the samples are identical. A value of 0.5 means that they share 50% identity and would be expected for first-degree relatives.

4.3.7 *Gene expression profile of iPSCs*

Gene expression profiling was carried out on the AST and NAS fibroblasts and four iPSC lines (NAS2, NAS9, AST13 and AST18). Scatter plots comparing gene expression of iPSCs and fibroblasts with that of hESCs found that the expression profile of hESCs was more similar to iPSCs than the fibroblast cell lines (Figure 4.9).

No significant differences (at false discovery rate of 0.05) in genome-wide gene expression between human ESCs and iPSCs or NAS iPSCs as compared to AST iPSCs could be detected.
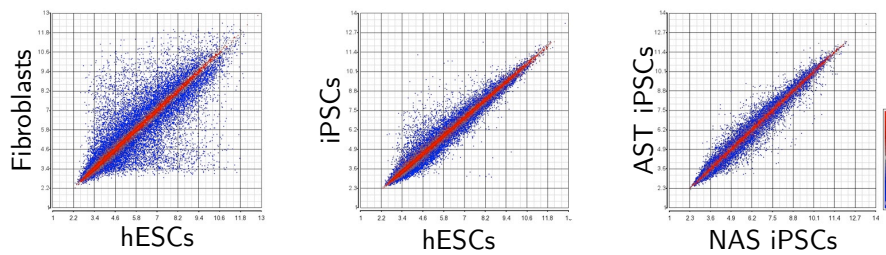
Figure 4.9: Scatterplots demonstrate that global gene expression of iPSCs is more similar to hESCs than to fibroblasts and there are no significant differences in global gene expression between AST and NAS iPSCs.
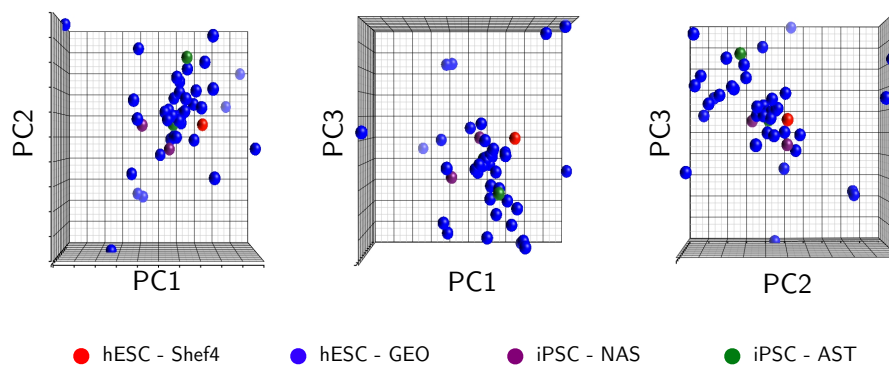
Figure 4.10: Multiple views of a PCA plot, following batch effect removal, comparing iPSC gene expression to all hESC data sets on the Affymetrix U133 Plus 2.0 platform that are publicly available. The iPSCs intermingle within the hESC landscape in all three dimensions, and are indistinguishable from the hESC data sets shown.

As a stringent test to further confirm that these iPSC lines exhibited a pluripotent expression profile, a comparison of global gene expression was made with all publicly available hESC gene expression data sets using the same platform (Affymetrix U133 Plus 2.0). A total of 59 samples from eight separate submissions (GEO database accesion numbers GSE16190, GSE19902, GSE22499, GSE26451, GSE7179, GSE7879, GSE8590 and GSE9440) were included. The resulting PCA plots demonstrate that the expression profiles of the iPSC lines described are indistinguishable from established hESC lines (Figure 4.10).

4.3.8   *Summary of iPSC characterisation*

A summary of characterisation of iPSC lines generated in this project is shown in Table 4.2. For completeness, details of neuronal characterisation are also included (discussed in Chapter 5). The following lines were generated but not characterised beyond transgene silencing: AST1, AST3, AST6, AST8 – 11, AST14, AST19, AST20, AST23 – 30, NAS1, NAS5, NAS6, NAS7, NAS8, NAS10.

4.4   DISCUSSION

In this chapter, I describe the characterisation of sets of iPSC lines that have been generated from two parent fibroblast lines, one of which harbours a triplication of the *SNCA* locus. All the described iPSC lines display robust transgene silencing, pluripotency gene expression and marker profiles, and ability to generate embryoid bodies with components of all three germ layers. The lines derived from the patient fibroblasts have the *SNCA* triplication intact, determined by PCR on genomic DNA and SNP profiling.

Teratoma formation was not assayed. Teratoma formation is regarded as a gold-standard of pluripotency, but is expensive to carry out and requires use of animals, therefore strong justification would be required to use it. In fact, this assay is not necessarily predictive of differentiation potential in culture. Some iPSC lines are capable of forming teratomas, but fail to differentiate into motor neurons in standard assays (Boulting et al., 2011). Furthermore, it has been reported that incompletely reprogrammed cells can also form teratomas (Chan et al., 2009). Global transcriptional profiling is now considered a more sensitive indicator of pluripotency and differentiation potential (Muller et al., 2011; Bock et al., 2011). Therefore, this was the method adopted here.

CELL LINES	TRANSGENE SILENCING	PLURIPOTENT MARKERS	SNCA DOSAGE	EB	SNP ARRAY	EXPRESSION ARRAY	NEURAL DIFF.	NEURAL MARKERS	PROTEIN ANALYSIS
AST4	Partial	•	•	•					
AST5	Partial	•	•	•					
AST7	Partial	•	•	•					
AST13	Full				•	•	•	•	•
AST18	Full				•	•	•	•	•
AST21	Full						•		
AST22	Full						•		
NAS2	Full	•	•	•	•	•	•	•	•
NAS3	Full	•	•	•			•		
NAS9	Full	•	•	•	•	•	•	•	•

Table 4.2: Summary of characterisation conducted on the iPSC lines generated. EB, embryoid bodies. Neural diff., neural differentiation.

SNP profiling identified several chromosomal abnormalities in NAS9 iPSCs (Figure 4.8). To date, this level of chromosomal analysis is not routine in published iPSC disease models. Furthermore, hESCs and hiPSCs have been shown to exhibit different potentials for lineage specification, and chromosomal abnormalities do not correlate with these differences (Osafune et al., 2008; Boulting et al., 2011), suggesting that the functional impact of these abnormalities may not necessarily be detrimental to disease modelling.

In summary, *bona fide* iPSC lines have been generated that exhibit the hallmarks of pluripotency. Given that the patient-derived iPSC lines retain the triplicated region intact, this collection of lines should serve as a useful model of PD.

In the next chapter, I discuss methods used to direct differentiation of these cells into cultures enriched for midbrain dopaminergic neurons, and describe characterisation that has been carried out on these cultures so far.

Part IV

NEURONS

In this section, I describe the strategy used to direct the differentiation of induced pluripotent stem cells into cultures enriched for midbrain dopaminergic neurons. I then describe the characterisation that has been carried out on these neuronal cultures.

NEURALISATION AND NEURONAL CHARACTERISATION

5.1 INTRODUCTION

Once iPSC lines have been generated and characterised in terms of pluripotency, the next step is to direct their differentiation into cells of interest – in this case, midbrain dopaminergic neurons.

Previous neural induction protocols have relied upon embryoid body formation or stromal feeder co-culture, which have the drawbacks of undefined culture conditions and low yield (Kawasaki et al., 2000). Recent advances include the development of a feeder-free monolayer culture method of inducing neural differentiation under defined conditions, via dual inhibition of SMAD signalling (Chambers et al., 2009). This approach uses the combination of Noggin (an inhibitor of BMP) and SB431542 (an inhibitor of Lefty/Activin/TGFβ pathways) to achieve robust neural differentiation. Here, Dorsomorphin (a further BMP inhibitor) has been employed as a partial substitute for Noggin, to improve efficiency and reduce costs (Yu et al., 2008).

The dual SMAD inhibition protocol has been employed to generate floor plate tissue from human ESCs (Fasano et al., 2010). Genetic lineage mapping studies in the mouse have shown that midbrain floor plate has neurogenic potential, and is the source of ventral midbrain dopaminergic neurons (Ono et al., 2007). Fasano et al. (2010) demonstrated directed differentiation of human ESCs into floor plate tissue via initial dual SMAD inhibition in conjunction with early high dose Sonic hedgehog (SHH) signalling. They also found that suppression of Dkk-1, a WNT inhibitor, enhanced floor plate generation at the expense of anterior neurectoderm. Since this protocol was found to

generate floor plate of the most anterior identity, the caudalising agent WNT-1 was used to make floor plate with midbrain identity.

Hence, the approach used here was to commence neural differentiation with dual SMAD inhibition for one day, followed by SHH, Wnt-1 and Dkk-1 blocking antibody treatment. Once floor plate differentiation had occurred, the protocol was switched to one for the maturation of midbrain dopaminergic neurons from neural progenitors derived from hESCs (Perrier et al., 2004) (see Figure 5.1 for a schematic of the entire neuralisation process).

5.2 METHODS

5.2.1 *Dual SMAD differentiation protocol*

PREPARATION:

- iPSC cultures are incubated for 1 hr in hESC media containing 10 µM ROCK inhibitor (Y27632, Ascent)

- iPSC colonies are then dissociated using Accutase (Invitrogen) for 20 mins, then titriated with a 5 ml stripette, to generate single-cell suspensions.

- Suspensions are passed through a 40 µm filter (BD Biosciences) to remove any cell clumps.

- Wash twice with hESC media.

- The suspension is then differentially plated on gelatin ($1\times$ 10 cm dish for each pair of wells from a 6-well plate) for 1 hr at 37°C in hESC media in the presence of 10 µM Y27632, to remove feeders and stroma.

- Non-adherent (iPS) cells are aspirated, spun down and resuspended in MEF-CM (R&D Systems) with 10 ng/ml FGF2 and ROCK inhibitor.
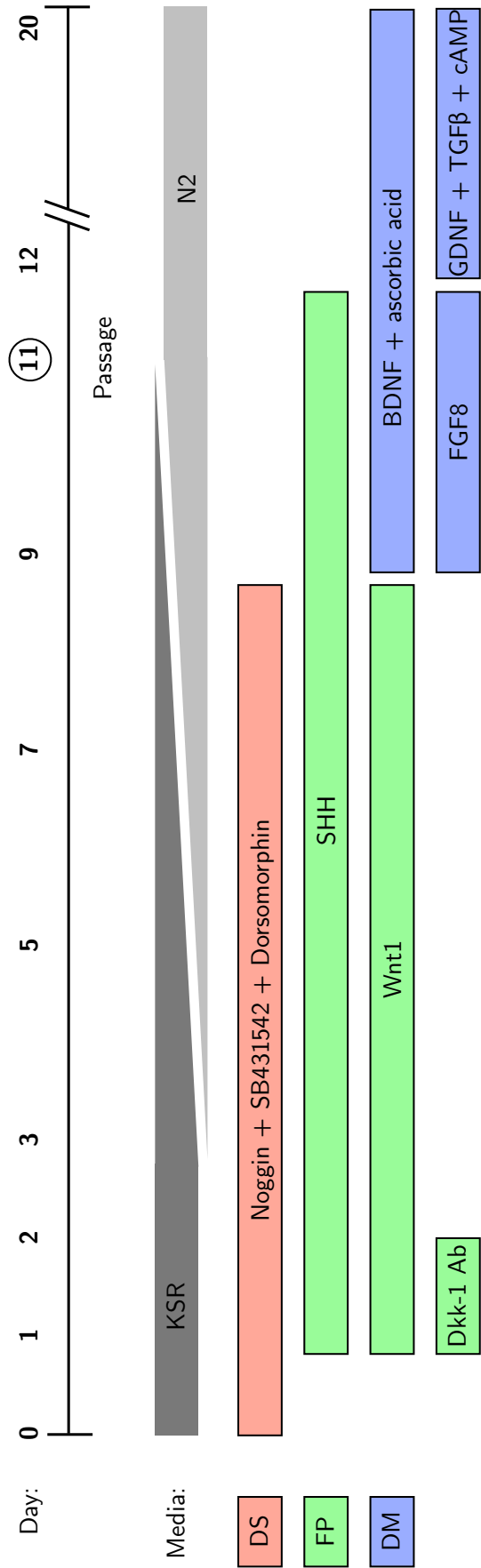
Figure 5.1: Schematic of the dual SMAD inhibition / floor plate protocol used to promote differentiation of iPSCs to a midbrain dopaminergic neuronal fate. DS, dual SMAD inhibition; FP, floor plate induction; DM, dopaminergic maturation.

- Plate on Matrigel (R&D Systems) at a density of 18,000 to 25,000 cells/cm² (a high plating density encourages differentiation into PAX6+ cells).

- Next day, media changed (Y27632 withdrawn) and cells allowed to expand for three days or until nearly confluent.

DAY 0:

- Once nearly confluent, switch to KSR medium (hESC medium minus FGF2) supplemented with 50 ng/ml Noggin (Peprotech), 10 μM SB431542 (Tocris) and 2 μM Dorsomorphin (Tocris) to make NSBDM medium.

DAY 1:

- Supplement NSBDM with 200 ng/ml SHH C24II (R&D Systems) and 50 ng/ml Wnt1 (Peprotech).

- On this day only, add Dkk-1 blocking antibody (100 ng/ml, R&D Systems).

DAY 3:

- Change media: NSBDM + SHH + Wnt1.

DAY 5:

- KSR media containing these ligands is cross tapered with N2B27 media (Stem Cell Sciences) containing the same ligands over 7 days (75% KSR and 25% N2B27 first day, 50% of each third day, and 25% KSR with 75% N2B27 fifth day).

DAY 7:

- Change media: 50% KSR, 50% N2B27 supplemented with Noggin, SB435432, Dorsomorphin, Shh and Wnt1.

DAY 9:

- Change media: 25% KSR, 75% N2B27 supplemented with Noggin, SB435432, Dorsomorphin, Shh and Wnt1.

5.2.2 *Dopaminergic neuronal differentiation protocol*

The full protocol is presented schematically in Figure 5.1.

DAY 1 − 8: Same as for Section 5.2.1.

DAY 9:

- Change media: 25% KSR, 75% N2B27 supplemented with 20 ng/ml BDNF (Peprotech), 0.2 mM ascorbic acid (Sigma) and 100 ng/ml FGF8 (Peprotech).

DAY 10:

- Prepare poly-L-ornithine/laminin coated dishes by coating plates with polyornithine (15 μg/ml) and storing at room temperature overnight.

- Next day (DAY 11) wash wells three times with PBS, then coat with laminin (1 μg/ml) in PBS and store in incubator for at least 2 hrs.

- When ready to use, aspirate wells and allow to dry for around 5 mins before adding cells.

DAY 11:

- Wash wells once with HBSS, then add fresh HBSS (3 ml per well) and keep at room temperature for 60 mins (in the tissue culture hood).

- Cells will become spheroid and not lift, but will be easily lifted with gentle use of a cell scraper.

- Then, use a 5 ml stripette to gently break up some of the larger clumps.

- Spin at 1300 rpm for 5 mins to pellet cells.

- Resuspend in 100% N2B27 + Shh (200 ng/ml), BDNF (20 ng/ml), ascorbic acid (0.2 mM), FGF8 (100 ng/ml).

DAY 12:

- Change media: 100% N2B27 supplemented with BDNF (20 ng/ml), ascorbic acid (0.2 mM), 10 ng/ml GDNF (Peprotech), 1 ng/ml TGFβ3 (Peprotech) and 0.5 mM dibutyryl-cAMP (Merck).

- Thereafter, refresh media with same ligands on alternate days.

DAY 20 ONWARDS:

- Analyse cells for morphology, gene expression and protein levels.

5.2.3 *Immunocytochemistry*

Cells were fixed in 4% paraformaldehyde at room temperature, or 100% methanol at -20°C for 15 mins, then blocked and permeabilised with blocking buffer (2% goat serum, 0.1% Triton-X in phosphate buffered saline) overnight at 4°C before probing with the following primary antibodies (also overnight in blocking buffer at 4°C):

LMX1B antibody kindly provided by Prof Yu-Qiang Ding, Tongji University

- TUJ-1 (R&D systems #MAB1195, mouse IgG2A),

- TH (R&D systems #MAB1423 clone TH-2, mouse IgG1),

- LMX1B (Rabbit polyclonal from Dai et al. (2008), 1:2000),

- α-synuclein (BD Transduction Laboratories #610787, mouse IgG1).

Appropriate AlexaFluor-488 and AlexaFluor-596-labelled secondary antibodies (Molecular Probes) were used at 1:1000, along with DAPI counterstaining, prior to imaging with an Olympus IX51 inverted fluorescent microscope or Leica DM IRE2 confocal microscope.

5.2.4 *Neuronal marker expression*

RNA was obtained from individual neuralised iPSC lines using the RNeasy Plus kit (Qiagen) according to manufacturer's instructions. cDNA was generated via Superscript III (Invitrogen), and qPCR reactions were carried out with the Universal Probe Library (UPL) system (Roche) and normalized to *GAPDH* or *MAPT*. All primers are available in Section A.1.

5.2.5 *Gene expression microarray analysis*

Gene expression microarrays from iPSC-derived neurons were run in tandem with RNA obtained from fibroblasts and iPSC lines, and analysed as described in Section 4.2.7.

5.2.6 *Protein analysis*

Fibroblast cells, neuronal cells differentiated from AST and NAS iPSCs and control SH-SY5Y cells were harvested in radio immunoprecipitation (RIPA) buffer (Cell Signaling Technologies) and protein concentrations estimated by BCA assay (Thermo Scientific) according to manufacturer's instructions.

Samples were diluted to equivalent protein concentration and then 20 μg denatured by the addition of $4\times$ sample buffer (Invitrogen) supplemented with 2-mercaptoethanol and boiled at 100°C for 10 mins, loaded onto 12% Bis Tris Acrylamide gels (Invitrogen) and proteins separated by SDS-PAGE.

Following transfer to cellulose or PVDF membrane, blots were probed for:

- α-synuclein (BD Transduction Laboratories #610787),

- β-actin (Sigma-Aldrich #A1978).

Blots were then imaged using either ECL (Pierce) and Kodak film, or the Odyssey imaging system (LiCor Biosciences).

5.2.7 *α-Synuclein secretion*

To quantify α-synuclein release by neurons, 48 hr conditioned media samples from neuralised cultures (individual wells of a 6-well plate) were concentrated with Amicon Ultra-15 Centrifugal Filter Units (Millipore). Released α-synuclein was assessed using an α-synuclein ELISA kit (USCN Life catalogue #E91222Hu) as per manufacturer's instructions.

5.3 RESULTS

5.3.1 *Dual SMAD inhibition generates neuronal precursors*

Preliminary neuralisations were conducted using the dual SMAD protocol in isolation. This established that the iPSC lines could be successfully directed to differentiate into neuronal progenitors. Immunocytochemistry from examples are shown in Figure 5.2.

5.3.2 *Dopaminergic neuralisation protocol generates TH+ neurons*

Eight AST and six NAS iPSC lines were subjected to the floor plate-dopaminergic differentiation protocol. Five AST lines and four NAS lines produced viable neurons that could be analysed. After 20 to 31 days, differentiated iPSCs were examined for tyrosine hydroxylase (TH – the rate limiting enzyme in the biosynthetic pathway to dopamine, used as a marker of dopaminergic neuronal identity) and neuron-specific class III β-tubulin (TuJ1 – used as a marker of pan-neuronal identity) and all showed robust expression of these markers, shown in Figure 5.3.

(a) day 9 iPSCs.

(b) day 13 hESCs.
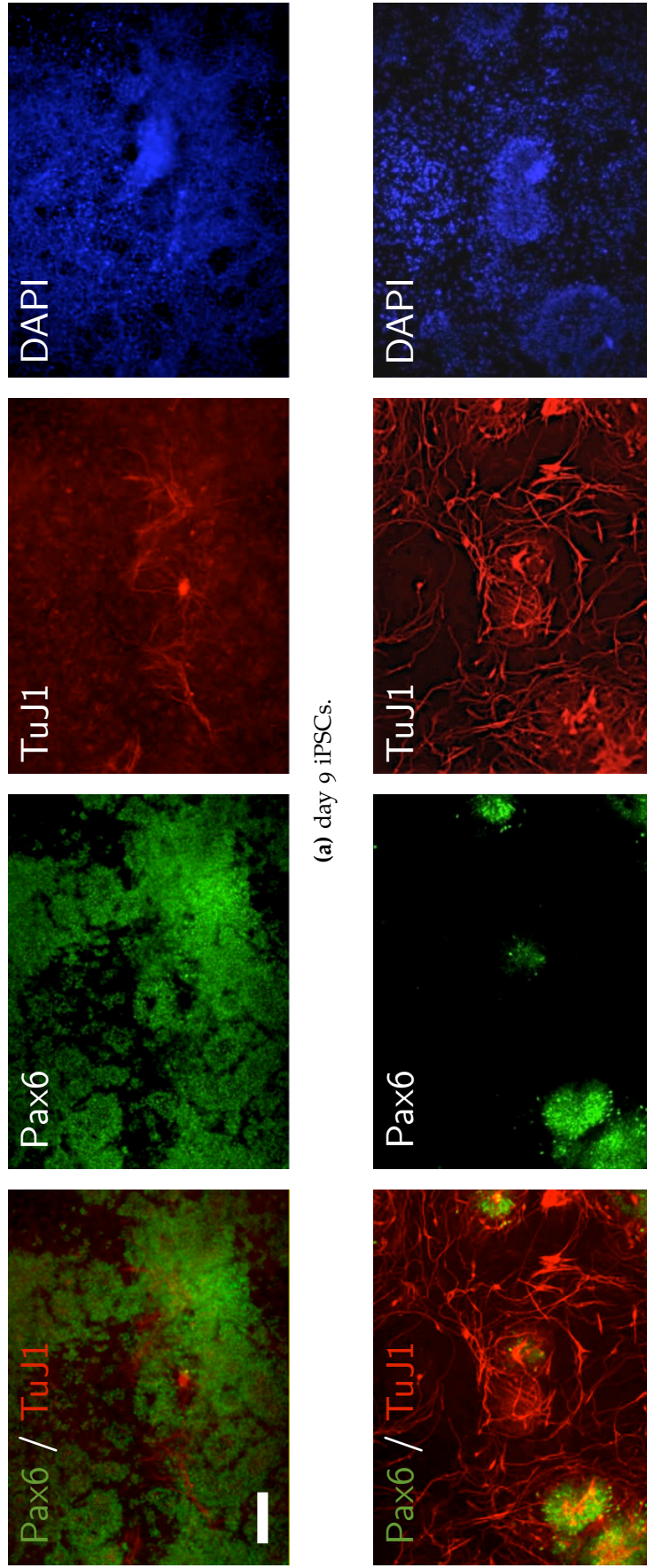
Figure 5.2: Immunocytochemistry of dual SMAD inhibition neuralisation. By day 9, widespread Pax6 expression can be seen throughout the cultures. By day 13, Pax6 expression has regressed, whilst TuJ1 expression becomes prominent. Pax6 is a marker of neuronal progenitors and TuJ1 is a marker of neuronal identity. Scale bar, 100 µm.

(a) Neuralised NAS iPSCs.

(b) Neuralised AST iPSCs.
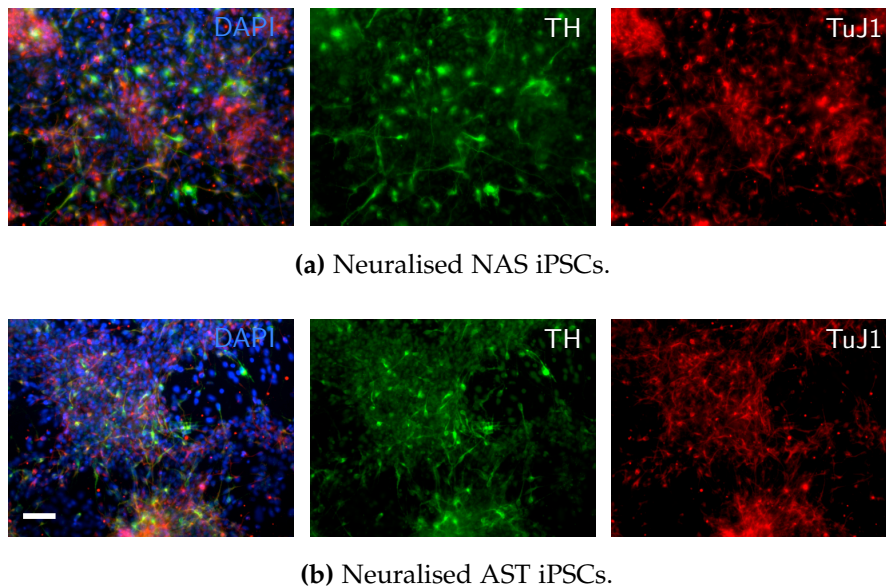
Figure 5.3: Immunocytochemistry of neuralized NAS and AST iPSCs for TuJ1 (red) and tyrosine hydroxylase (TH – green) shows robust differentiation into dopaminergic neurons. Scale bar, 100 μm.

Blinded cell counts were performed on micrographs fluorescently labelled for TH and TuJ1, which demonstrated that AST iPSCs yielded 37% (SD 9.5) TH-positive cells as a proportion of TuJ1-positive cells whilst NAS iPSCs yielded 28% (SD 6.8), which is not significantly different ($P = 0.26$) (Figure 5.4).

The midbrain identity of these TH-positive neurons was confirmed by co-immunolabelling with the ventral midbrain marker LMX1B (Dai et al., 2008) (Figure 5.5).

5.3.3 *Transcriptome analysis shows enrichment for triplication genes*

Gene expression profiling was carried out on the AST and NAS fibroblasts, four iPSC lines (AST13, AST18, NAS2, and NAS9) and eight neuronal cultures (Day 23 and Day 31 of the 4 iPSC lines). Principal component analysis and hierarchical clustering found that the three groups of cell samples clustered separately, with the iPSCs most closely associated with a control hESC line, Shef4 (Figure 5.6).
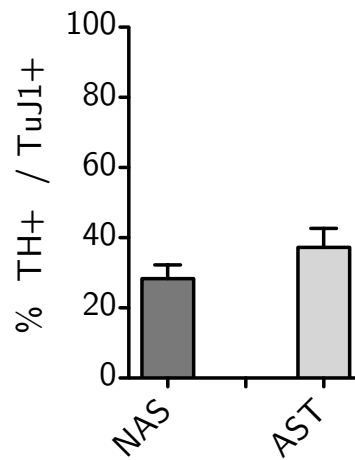
Figure 5.4: Counts of TH+ neurons, expressed as a percentage of TuJ1+ neu-
rons ($n = 1955$ total), found no significant difference in efficiency
of dopaminergic differentiation between AST and NAS iPSCs.
Error bars represent standard deviation of biological replicates,
$n = 3$.
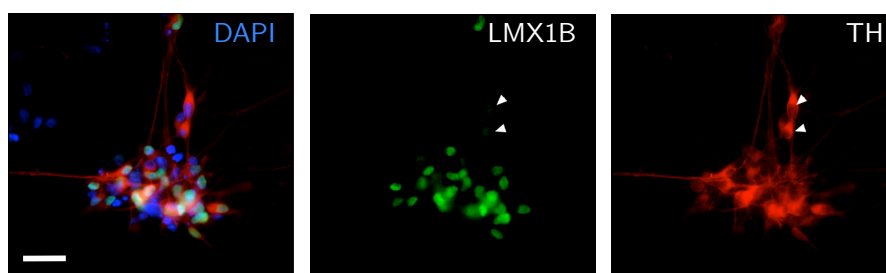
Figure 5.5: LMX1B (green) is expressed in the majority of TH-positive (red)
neurons (>80%). A minority of TH+ cells are negative for LMX1B
(arrowheads). Scale bar, 100 µm.
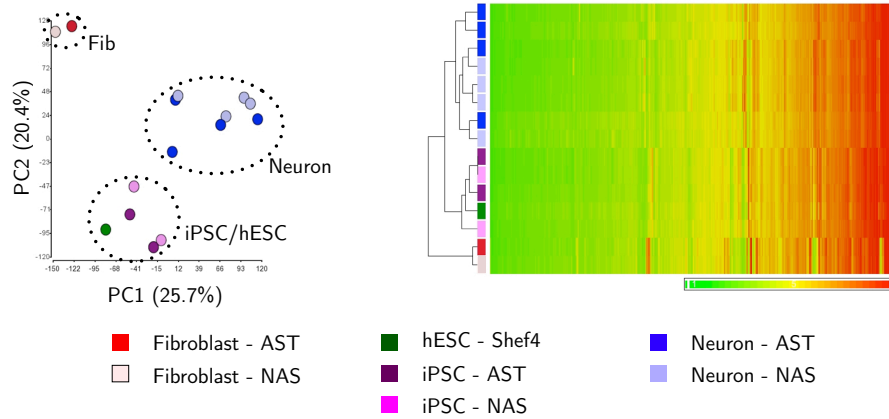
Figure 5.6: Comparison of gene expression profiles of fibroblasts, iPSCs and neurons. **(a)** Principal component analysis and **(b)** hierarchical clustering show that iPSCs cluster with hESCs, while fibroblasts and neurons cluster separately. There is no clear separation between AST and NAS-derived cells at this level of analysis.

Following the creation of a triplication gene set (defined as all genes within the triplication region, shown in Figure 4.7), Gene Set Enrichment Analysis (GSEA) was used to demonstrate a highly significant enrichment (nominal $P < 0.0001$) of this set within AST as compared to NAS neurons (Figure 5.7). Although significant enrichment (nominal $P < 0.05$) of the Triplication Gene Set could be demonstrated in AST versus NAS iPSCs, no significant enrichment could be detected in AST versus NAS fibroblasts (nominal $P = 0.09$). Statistical significance (nominal P value) of the enrichment score was estimated by using an empirical gene set-based permutation test procedure, as described in Subramanian et al. (2005).

5.3.4   *Neuronal markers reveal clonal variation*

To further confirm the midbrain dopaminergic identity of the cultured neurons, expression analysis of the following neuronal markers was performed: *LMX1A*, *NURR1*, *TH* and *DAT* (Figure 5.8). A range of expression of these genes was observed, not linked to genotype. This

(a) Fibroblasts.   **(b)** iPSCs.
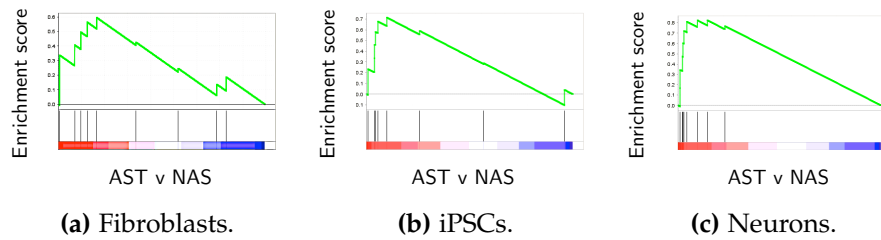
Figure 5.7: Gene set enrichment analysis of the ⋯ ⋯
significant enrichment in AST iPSCs ⋯ ⋯
rons (nominal $P < 0.0001$) but not fib⋯ ⋯ .
Enrichment score P-values are estin⋯ ⋯
gene set-based permutation test pro⋯⋯⋯ (⋯⋯⋯⋯⋯⋯⋯
2005).

Figure 5.8: Quantitative RT–PCR analysis for midbrain dopaminergic neu-
ral markers (*LMX1A*, *NURR1*, *TH* and *DAT*) in AST and NAS
neuronal cultures. To control for efficiency of neuralisation, ex-
pression was normalised to the pan-neuronal marker *MAPT*.
Error bars represent standard deviation of technical replicates,
$n = 3$.

may reflect clonal variation, or efficiency of neuralisation which has
been previously observed in iPSCs (Hu et al., 2010).

5.3.5 *Triplication region is retained in patient neurons*

Genome-wide SNP analysis of AST iPSC-derived neuronal cultures
confirmed that the triplication region had remained intact during
differentiation (Figure 5.9).
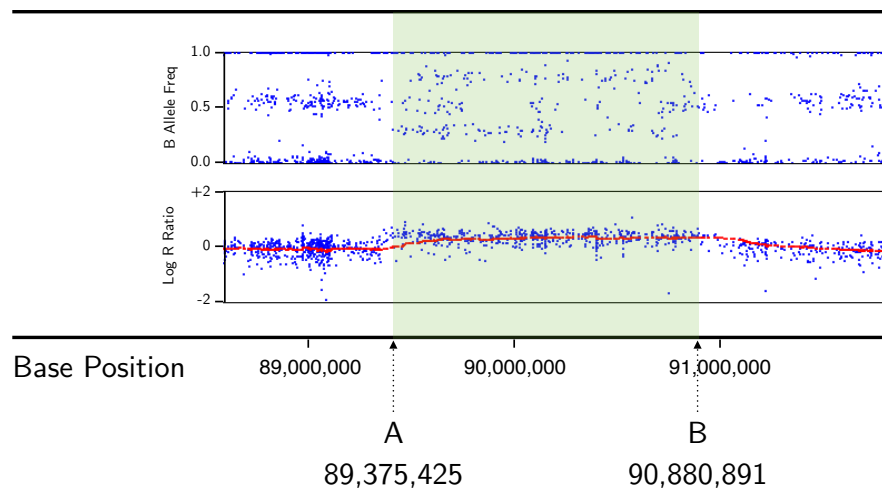
Figure 5.9: SNP analysis of AST-derived neurons confirms that the triplication region is retained intact following neuronal differentiation.

5.3.6 α-*Synuclein is present in iPSC-derived neurons*

α-Synuclein protein could be detected in all iPSC-derived neuronal cultures (Figure 5.10). Considerable heterogeneity of expression of α-synuclein was observed, which may reflect different neuronal subtypes or different stages of neuronal maturity (Zhong et al., 2010). However, α-synuclein was found to be expressed in all TuJ1+ cells. In contrast, it was not detectable in fibroblasts by immunocytochemistry or western blot (Figure 5.11).

5.3.7 α-*Synuclein protein is doubled in patient neurons*

To determine whether AST neurons recapitulate the elevated *SNCA* expression observed in postmortem brain tissue in patients from this kindred, and to confirm the microarray results, additional neuronal differentiations were conducted with quantitative RT-PCR analysis of *SNCA*. AST-derived neurons expressed approximately double the quantity of *SNCA* mRNA as NAS-derived neurons, when controlling for efficiency of neuralisation by normalising to the pan-neuronal marker *MAPT* (Figure 5.12).
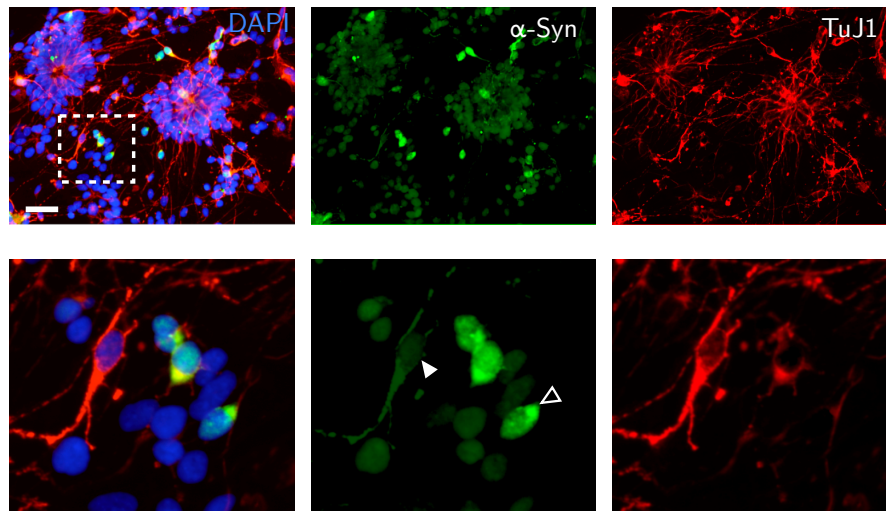
(a) NAS iPSC-derived neurons.
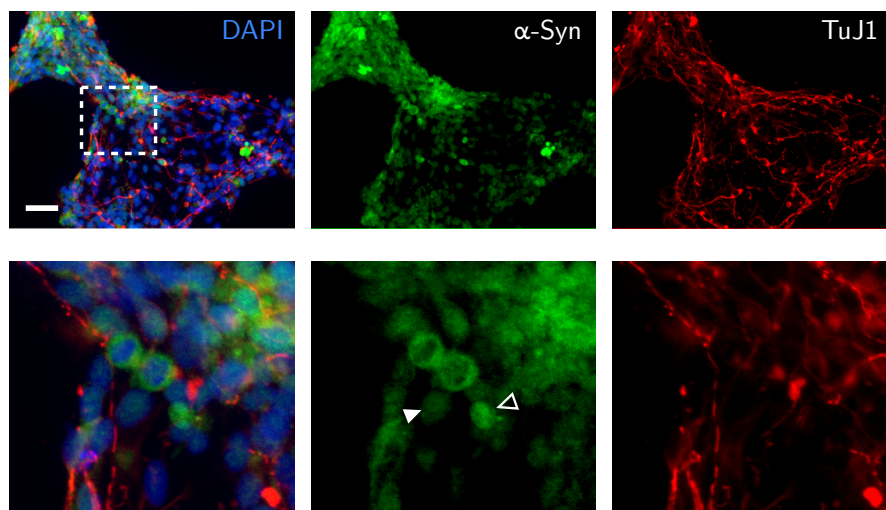
(b) AST iPSC-derived neurons.

Figure 5.10: Expression of α-synuclein was observed in all TuJ1+ neurons derived from **(a)** NAS and **(b)** AST iPSCs. The majority of cells expressed low levels of α-synuclein (filled arrowheads) whereas 3 – 7% of TuJ1+ cells expressed a high level of protein (open arrowheads). Scale bar, 100 µm upper panels, 400 µm lower panels.

(a) Western blot.

(b) Immunocytochemistry.
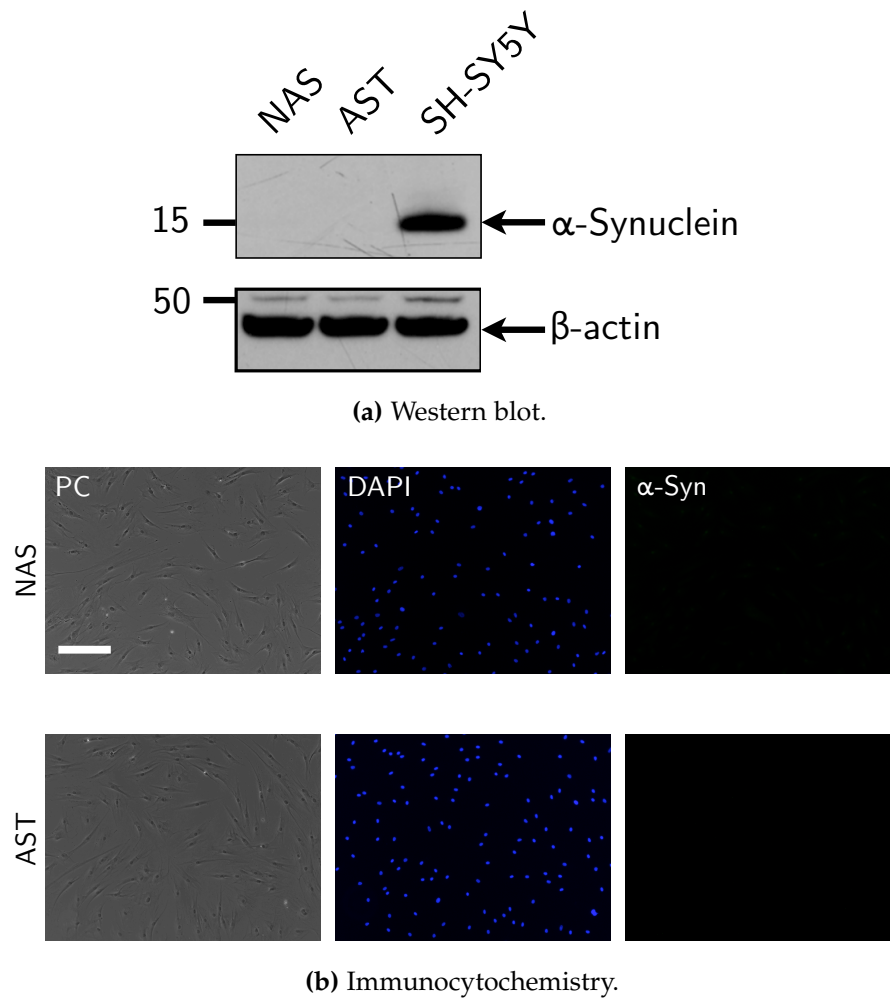
Figure 5.11: α-Synuclein protein is not detectable in fibroblasts by either **(a)** western blot (provided by Dr Patrick Lewis) or **(b)** immunocytochemistry (using the same antibody mixtures and microscope settings for imaging neurons). For the western blot in **(a)**, lysate of SH-SY5Y neuroblastoma cells transfected with an α-synuclein expressing plasmid was used as a positive control, and β-actin as a loading control. Scale bar, 100 μm.
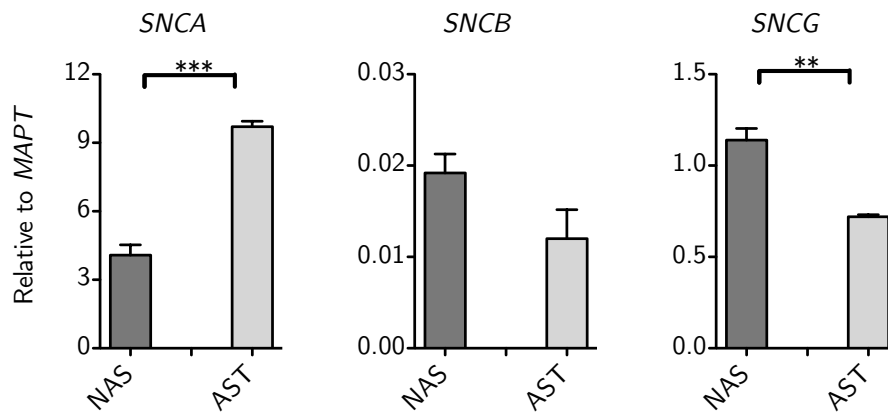
Figure 5.12: Quantitative RT-PCR data for *SNCA*, *SNCB* and *SNCG* shows that expression of *SNCA* is significantly higher, and *SNCG* significantly lower, in AST iPSC-derived neurons when efficiency of neuralisation is controlled for, by normalising to expression of the pan-neuronal marker *MAPT*. In contrast, differences in expression levels of *SNCB* were not observed. Error bars represent standard deviation of technical replicates, $n = 3$. ***, $P < 0.0005$; **, $P < 0.005$ (Student's *t*-test, unpaired, two-tailed).

SNCA has two paralogous genes, *SNCB* and *SNCG*, which respectively encode β- and γ-synuclein. All have been found in neuritic pathology in PD and dementia with Lewy bodies (DLB) (Galvin et al., 1999). Wildtype β-synuclein inhibits α-synuclein aggregation *in vitro* and limits pathology due to human α-synuclein expression in transgenic mice, but can cause neurodegeneration when mutated (Hashimoto et al., 2001; Fujita et al., 2010). In contrast, transgenic overexpression of wildtype γ-synuclein leads to neurodegeneration (Ninkina et al., 2009). Overall, β-synuclein appears to be protective whilst γ-synuclein may exert its own toxicity. *SNCG* expression was significantly lower in AST neurons, suggesting a possible compensatory mechanism. No significant difference was observed in the expression of *SNCB* (Figure 5.12).

To further probe the possibility of clonal variation, the level of expression of *SNCA* in multiple NAS and AST iPSC lines was investigated. The iPSC lines AST13, AST18, NAS2 and NAS9 gave robust yields of neurons on repeated trials of neuralisation. In order to con-
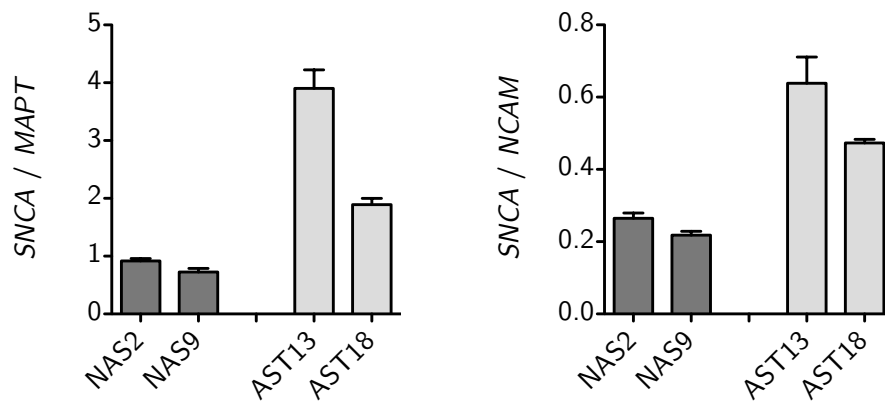
Figure 5.13: Quantitative RT–PCR analysis of *SNCA* expression, normalized to pan-neuronal markers (*NCAM*, *MAPT*) to directly control for efficiency of differentiation, shows a twofold or greater increase in *SNCA* expression in neurons derived from AST iPSCs. Error bars represent standard deviation of technical replicates, $n = 3$.

trol for heterogeneity of neuronal differentiation, *SNCA* expression was normalised to pan-neuronal markers (*MAPT* and *NCAM*). As for the dopaminergic markers (Figure 5.8), some variation was observed between lines, but a doubling (or more) of *SNCA* expression was consistently found in AST-derived neurons when compared to NAS-derived neurons (Figure 5.13).

Next, the level of α-synuclein protein expression was examined in a pair of iPSC lines that differentiated with similar efficiency, AST18 and NAS2. A two-fold increase in α-synuclein protein expression was observed in AST18 (Figure 5.14), which agreed with the difference in mRNA expression.

5.3.8 *α-Synuclein release is increased in patient neurons*

Finally, it was asked whether AST-iPSC-derived neurons might release more α-synuclein into cell culture media than NAS-derived neurons, since this protein is known to be secreted by cells in culture (Alvarez-Erviti et al., 2011). Conditioned media at 48 hr time points was analysed from several AST and NAS neuronal cultures. Signifi-
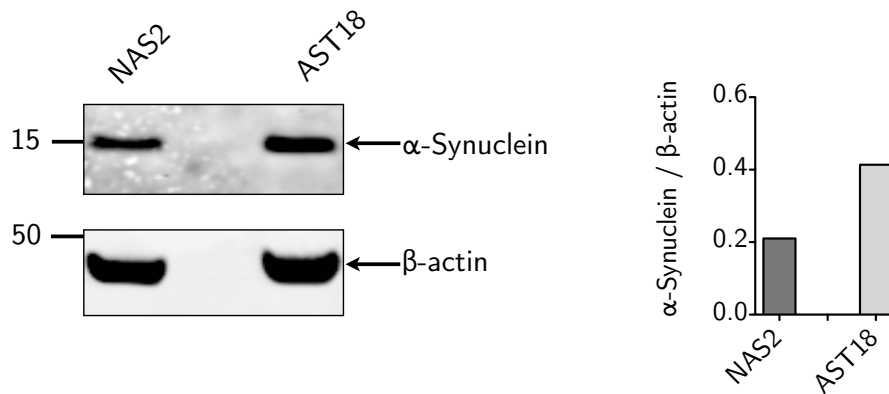
Figure 5.14: α-Synuclein protein is increased in patient-derived neurons demonstrated by western blot (representative blot shown).
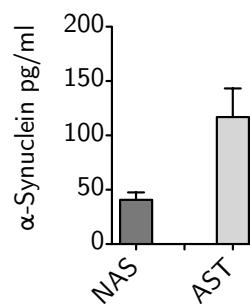
Figure 5.15: ELISA detects significantly more α-synuclein in 48 hr conditioned media from AST neuronal cultures than equivalently conditioned media from NAS neuronal cultures. Error bars represent standard deviation of biological replicates, $n = 2$.

cantly more α-synuclein was found to be released into the media from AST neurons by a sensitive ELISA method (Figure 5.15).

5.3.9 *Gene set enrichment analysis of potential disease pathways*

GSEA (described in Section 5.3.3) was used to assess whether the expression of sets of genes associated with specific cell pathways might be altered in patient-derived compared with control neurons. The Kyoto Encyclopedia of Genes and Genomes (KEGG) Pathway database (http://www.genome.jp/kegg/) was used as a source of hand-curated gene sets. The following pathways were chosen based on their established or possible link with PD pathogenesis:
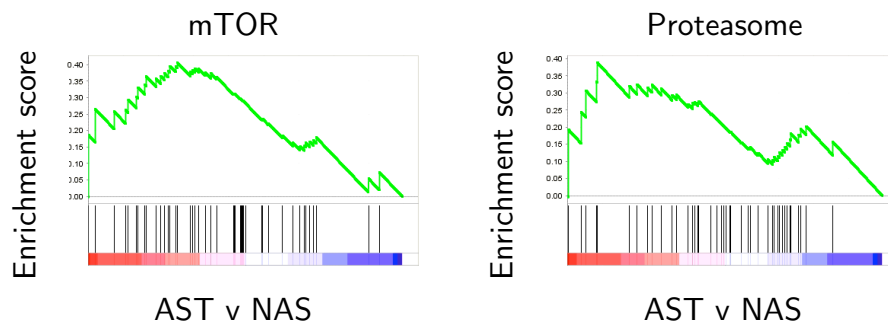
Figure 5.16: Gene set enrichment analysis provides preliminary evidence that mTOR and proteasome gene sets are upregulated in AST neurons.

- KEGG_PARKINSONS_DISEASE

- KEGG_PROTEASOME

- KEGG_REGULATION_OF_AUTOPHAGY

- KEGG_MTOR_SIGNALING_PATHWAY

- KEGG_MAPK_SIGNALING_PATHWAY

- KEGG_WNT_SIGNALING_PATHWAY

- KEGG_JAK_STAT_SIGNALING_PATHWAY

This analysis demonstrated a significant enrichment (nominal $P<0.05$) of the mTOR and proteasome gene sets within AST as compared to NAS neurons (Figure 5.16), whilst the other gene sets did not show enrichment. Given that multiple tests were carried out, these results are only provisional and need to be validated with an independent data set.

By extending this study with more samples, additional pathways may be highlighted which would help guide future experimental work.

5.4 DISCUSSION

iPSC lines from the patient and unaffected relative have been successfully differentiated into TH+ neurons with midbrain identity.

Persistence of gene dosage doubling has been confirmed in these neurons, and a more than two-fold higher expression of *SNCA* in the patient-derived neurons has been demonstrated in a subset of lines.

Furthermore, provisional results from an analysis of transcriptome data from iPSC-derived neuronal cultures suggest that genes associated with the mTOR and proteasome pathway are upregulated in cultures bearing *SNCA* triplication. Both of these pathways have been implicated in PD pathogenesis. Proteasomal dysfunction is seen in sporadic Parkinson's disease (McNaught et al., 2003) and mTOR dysfunction has been implicated as the pathological mediator of mutations in *LRRK2* (outlined in Section 2.1.1). Taken together, these findings suggest that this collection of cell lines has the potential to be a useful cell model of PD.

5.4.1 *Interpretation of iPSC disease models is constrained by variation*

In the model presented here, each neuronally differentiated patient-derived iPSC clone is expected to exhibit a doubling of *SNCA* expression. Therefore, this is a simple and stringent system for examining the robustness of the iPSC disease-modelling paradigm. The data presented here highlight two potential sources of variation: differences between iPSC clones, and differences in response to neuralisation, reiterating existing reports of the differentiation capacity of iPSC lines (Hu et al., 2010; Feng et al., 2010). Many genetic and epigenetic changes occur during reprogramming (Gore et al., 2011; Hussein et al., 2011; Lister et al., 2011), highlighting the importance of generating multiple iPSC lines from each parent fibroblast line, so that clonal variation can be taken into account when comparing disease and control lines.

5.4.2 *Avoiding variation due to genetic heterogeneity*

Differences in genetic background between patient and control may contribute to differences in phenotype, not specifically due to disease-causing mutations. Fibroblasts were obtained from a patient and a first-degree relative, to minimise this. However, the ideal system would be a cell line with a disease-causing mutation, which is then genetically corrected, creating cell lines that are isogenic apart from the disease-associated locus. This has been carried out to correct the genetic defect in Fanconi anaemia iPSCs (Raya et al., 2009). Newer methods involving zinc finger nucleases (ZFNs) and more recently transcription activator-like effector nucleases (TALENs) have made this process more efficient (Hockemeyer et al., 2009, 2011) and ZFNs have recently been used to correct A53T and A30P *SNCA* mutations in iPSCs bearing these mutations (Soldner et al., 2011). These techniques can also be used with human ESC lines, avoiding iPSC technology altogether. However, a possible advantage of patient-derived iPSCs is that the disease-causing mutation is present in the context of the disease phenotype. Generating the same mutations in a different genetic background may be an oversimplification, particularly for diseases with a polygenic basis, but likely also for monogenic diseases (as is the case here) where the penetrance is variable.

As an extension of this, an important additional control for this project would be to knockout additional copies of *SNCA* to restore diploidy in the patient-derived neurons, to verify that any phenotypic differences are due to *SNCA* overexpression and not due to overexpression of any other gene in the triplicated region. Gene targeting employing ZFNs or TALENs would be a valid approach. An alternative strategy would be to employ RNA interference to knockdown *SNCA* expression. This has been used successfully to deplete α-synuclein in cell cultures (Fountaine et al., 2008).

5.4.3 *Minimising variation due to cell type heterogeneity*

It is important to note that current ESC and iPSC differentiation pro-
tocols generate heterogenous populations of cells, albeit populations
enriched for cell types of interest. Narrowing the cellular type derived
from stem cells is a challenge to using these cells. Potential solutions
to this include employing fluorescence activated cell sorting (FACS)
strategies to enrich for cells of interest, with or without cell-type
specific lineage reporters. Currently, no cell surface markers of hu-
man dopaminergic neurons are available, though antibodies directed
against Corin have been used successfully in mouse (Ono et al., 2007).
An alternative would be to examine the differentiated population on a
single cell basis, either via blinded single cell PCR, which would be
extremely laborious, or using laser-capture microdissection.

Part V

CONCLUSION

CONCLUSIONS AND FUTURE DIRECTIONS

6.1 A BRIEF SUMMARY

This thesis has utilised iPSC technology to develop a novel human cell model of PD. Given that the iPSC field was new at the time of project development, a degree of risk was involved. Therefore, studies were also conducted on patient-derived skin fibroblasts as a safer parallel project. These yielded mixed results, the overall impression being that fibroblasts are not the optimal cell type in which to study a neuronal disease. Generation of a cell model with closer affinity to the cells that are specifically vulnerable in PD may be required to see the toxic effects of mutant LRRK2 – corroborating the iPSC approach to model disease.

Generation of iPSCs from adult human fibroblasts proved to be technically challenging. Several different approaches were tried in earnest before a method was adopted that could successfully reprogram adult human fibroblasts with sufficient efficiency to use with patient samples. Use of retrovirus bearing the four transcription factors *Oct4*, *Sox2*, *c-Myc*, and *Klf4*, as originally described by Takahashi et al. (2007b), proved to be a reliable and efficient reprogramming strategy.

Thus far, all iPSC disease models have employed retroviral-based reprogramming factors, which integrate into the genome of target cells. These integration sites will be different for separate iPSC clones. Although unlikely, given the size of the entire genome relative to that portion that is expressed or important for regulation of expression, these different integrations may have a bearing on cell behaviour. This can be circumvented by using an integration-free method of reprogramming (Okita et al., 2008; Stadtfeld et al., 2008; Zhou et al.,

2009; Gonzalez et al., 2009; Yu et al., 2009; Fusaki et al., 2009; Warren et al., 2010; Okita et al., 2011), or one in which the reprogramming factors can be seamlessly removed (Kaji et al., 2009; Woltjen et al., 2009). However, patient-derived cells are a finite resource, and these techniques currently lack the reprogramming efficiency needed to generate iPSC lines from a limited number of cells, although recent improvements in episomal reprogramming techniques are showing promise (Okita et al., 2011).

6.2 RECAPITULATING A DISEASE OF AGING

Returning to the original hypothesis of the project, is the iPSC paradigm appropriate for studying PD? The long latency of PD, being more common in old age, is challenging to mimic in a cell culture system (Saha and Jaenisch, 2009). Also, any contribution made by epigenetic factors to the disease process would be erased during the iPSC reprogramming process. This is why a fully penetrant, early onset and rapidly progressive familial form of PD was chosen to offset these two problems as far as possible. The data presented herein supports the thesis that a human neuronal model can replicate the genetic insult that results in disease in patients with *SNCA* triplication, but whether these cell lines recapitulate PD pathogenesis *in vitro* remains uncertain.

Soldner et al. 2009 described the first iPSC model of PD, using fibroblasts from patients with sporadic disease as a starting point, but a phenotype has not been documented as yet. More recently, Nguyen et al. (2011) have shown that neurons derived from iPSCs bearing mutations in *LRRK2* are more susceptible to oxidative stress. Sánchez-Danés et al. (2012) have described a large set of LRRK2 iPSC lines (derived from seven patients): neurons derived from these cells accumulate autophagic vacuoles and exhibit reduced neurite outgrowth. A very recently published report of iPSCs bearing triplication of *SNCA* (derived from fibroblasts from a different donor than reported here,

but from the same kindred) has shown that neurons derived from these cells appear to be more sensitive to oxidative stress (Byers et al., 2011). An iPSC model of *PINK1*-associated PD has also been reported (Seibler et al., 2011). Dopaminergic neurons derived from these cells exhibited impaired recruitent of lentivirally expressed parkin to mitochondria, reiterating previous reports of this phenomenon in knockdown systems and non-neuronal cell models (Narendra et al., 2010; Rakovic et al., 2010; Vives-Bauza et al., 2010). Although these reports do not necessarily provide novel insight into disease mechanisms, they certainly support the view that cells in culture can go some way to recapitulating disease processes seen in PD.

Indeed, it is important to emphasise that such models can be seen as a system in which the early pathogenic changes that lead to disease can be studied, rather than a model in which the fully fledged end stage pathology of PD can be observed. This is potentially advantageous for two reasons. First, observing these earliest responses might afford greatest hope for deriving a treatment that can stop the disease before it progresses. Second, pathological changes occurring at a late stage in the disease may in fact be protective rather than toxic (Cookson and van der Brug, 2008).

The model reported here opens the door to more complex cellular PD model systems, for example co-culture of neuronal and glial populations. It is likely that different cell types found in the brain contribute to the disease process in PD, paralleling the situation in amyotrophic lateral sclerosis (Wernig et al., 2008; Ilieva et al., 2009). Taking advantage of progress in stem cell technology, both mutant and wildtype glial and neuronal cells can be co-cultured to generate a more representative cellular model for PD (Di Giorgio et al., 2007). These cells might also prove useful in investigating cell-to-cell propagation of pathology, being pre-primed to develop disease (Brundin et al., 2008).

iPSCs carrying the *SNCA* triplication may also be of value in studying the related synucleinopathies *in vitro* – the pathology exhibited by

the Iowa kindred includes cases where glial deposition of α-synuclein, reminiscent of the glial cytoplasmic inclusions found in MSA, is described (Gwinn-Hardy et al., 2000). The differentiation of these iPSC lines towards an oligodendroglial fate may shed light on the cellular processes operating in this disorder (Wenning et al., 2008). In addition, differentiation towards cortical neurons (recently described by Shi et al. (2012)) might provide insight into α-synuclein pathogenesis in DLB, where pathology is largely cortical. Comparisons between cortical neurons and dopaminergic neurons would also be of interest in examining why different neuronal subtypes appear to differ in their susceptibility to the disease mechanisms operating in PD.

6.3 POTENTIAL FUTURE DIRECTIONS

6.3.1 *Synaptic transmission*

In this thesis, cells are described that exhibit neuronal morphology, and also express markers of midbrain dopaminergic identity. An important next step is to establish that these cells behave like neurons – having the capacity to fire action potentials, and release neurotransmitters, phasically and evoked. This further characterisation would be desirable when using iPSC-derived neuronal cells to model any disease, but is particularly warranted in the context of PD: presynaptic accumulation of α-synuclein is known to occur in neurodegeneration (Kramer and Schulz-Schaeffer, 2007) and overexpression of α-synuclein impairs neurotransmitter release (Nemani et al., 2010). Furthermore, α-synuclein facilitates the formation of complexes of SNARE (soluble NSF attachment protein receptor) proteins (Burré et al., 2010). SNARE proteins mediate vesicle fusion to allow exocytosis of transport vesicles, and play a pivotal role in permitting the precisely timed and targetted release of neurotransmitters at the synapse (Südhof and Rothman, 2009).

Taken together, these studies suggest that PD – in particular when due to α-synuclein overabundance – may begin at the synapse, and spread from there. Indeed, deletion of Munc18-1, which prevents synaptic transmission during development, leads to widespread neurodegeneration in mouse, whilst synaptic formation proceeds as normal, implying that transmission is a requirement of maintainenance of neuronal integrity, but not development (Verhage et al., 2000).

Therefore, an important avenue to explore is whether midbrain dopaminergic neurons bearing triplication of *SNCA* have impaired release of dopamine in response to firing action potentials with consequent influx of calcium, hence recapitulating the mouse model. The next step would be to study the mechanistic basis for such a disturbance, if it were present.

6.3.2 *Mitochondrial physiology*

The importance of mitochondria in maintaining the health of midbrain dopaminergic neurons was highlighted by the accidental exposure of a group of Californian drug users to the neurotoxin MPTP in the early 1980s (Langston et al., 1983). This caused an acute, irreversible Parkinsonian syndrome via the MPTP metabolite MPP+, which inhibits complex I of the mitochondrial electron transport chain, causing increased free radical production and increased intracellular calcium via decreased ATP. Reduced complex I activity has also been found in sporadic PD brain at postmortem (Schapira et al., 1989). A causal link has been provided by chronic systemic administration of the complex I inhibitor rotenone to rats, which subsequently develop a Parkinsonian syndrome with α-synuclein inclusions (Betarbet et al., 2000).

The link between mitochondrial dysfunction and PD has been reinforced by the analysis of PD caused by mutations in *parkin* Kitada et al. 1998, *PINK1* (Valente et al., 2004) and *DJ1* (Bonifati et al., 2003). *PINK1* encodes a serine-threonine kinase with an amino-terminal mi-

tochondrial import sequence. It seems to have a role in maintaining mitochondrial integrity in the face of cellular stressors (Pridgeon et al., 2007). PINK1 and parkin function in a common pathway to regulate mitochondrial dynamics: parkin overexpression rescues mitochondrial abnormalities seen in *Pink1*-knockout flies and *PINK1* silenced mammalian cells (Park et al., 2006; Clark et al., 2006; Exner et al., 2007), suggesting that it operates downstream of PINK1. At normal expression levels, PINK1 is required for the recruitment of parkin to damaged mitochondria for their clearance via mitophagy (Narendra et al., 2008). Furthermore, mice and fly brains are rendered sensitive to oxidative stress when DJ1 is knocked down by small interfering RNA (Kim et al., 2005) and DJ1-deficient cells display an aberrant mitochondrial phenotype that can be rescued with the expression of parkin or PINK1, or by applying ROS scavengers (Irrcher et al., 2010). Overall, the possibility of finding mitochondrial pathology in the patient-derived neurons described herein should be a fruitful area to examine.

6.4 CONCLUDING REMARKS

This thesis is a demonstration of the feasibility of generating iPSCs and midbrain dopaminergic neurons from a patient with a fully penetrant form of familial PD. It also highlights that, in its current form, the inherent variation in iPSC clones, neuronal differentiations and expression of disease-related genes will make the interpretation of these models challenging.

Part VI

APPENDIX

A

APPENDIX

A.1 PCR PRIMERS

GENE	PRIMER SEQUENCE 5´ - 3´	SYBR OR UPL NO.
SNCA ex1	AAAGGCCAAGGAGGGAGTT ATCCTAACCCATCACTCATGAAC	SYBR
SNCA ex4	CCTGTGGATCCTGACAATGA TGCAAGTTGTCCACGTAATGA	SYBR
HBB	TTGGACCCAGAGGTTCTTTG GAGCCAGGCCATCACTAAAG	SYBR
B2M	CTCACGTCATCCAGCAGAGA AGTGGGGTGAATTCAGTGT	SYBR
mOct4	GTTGGAGAAGGTGGAACCAA CTCCTTCTGCAGGGCTTTC	SYBR
mSox2	ACAGCTACGCGCACATGA GGTAGCCCAGCTGCTCCT	SYBR
mc-Myc	CCTAGTGCTGCATGAGGAGA TCTTCCTCATCTTCTTGCTCTTC	SYBR
mKlf4	CGGGAAGGGAGAAGACACT GAGTTCCTCACGCCAACG	SYBR
TBP	GCTGGCCCATAGTGATCTTT CTTCACACGCCAAGAAACAGT	SYBR
OCT4	TGCCGTGAAACTGGAGAAG GCTTGGCAAATTGTTCGAGT	#78

GENE	PRIMER SEQUENCE 5´ - 3´	SYBR OR UPL NO.
SOX2	TGCTGCCTCTTTAAGACTAGGAC CCTGGGGCTCAAACTTCTCT	#35
NANOG	TCTCCAACATCCTGAACCTCA TTGCTATTCTTCGGCCAGTT	#87
REX1	GGCCTTCACTCTAGTAGTGCTCA CTCCAGGCAGTAGTGATCTGAGT	#62
GAPDH	GCTAGGGACGGCCTGAAG GCCCAATACGACCAAATCC	#60
NURR1	ATTTCCTCGAAAACGCCTGT CATACTGCGCCTGAACACAA	#41
LMX1A	AGAGCTCGCCTACCAGGTC GAAGGAGGCCGAGGTGTC	#25
MAPT	ACCACAGCCACCTTCTCCT CAGCCATCCTGGTTCAAAGT	#55
NCAM	GCGTTGGAGAGTCCAAATTC GGGAGAACCAGGAGATGTCTTT	#51
SNCA	GAGGGAGTGGTGCATGGT TGCTGTCACACCCGTCAC	#68
SNCB	GCGGAGAAAACCAAGCAG ACACCTTCTCGGGTCTTGC	#70
SNCG	CGGTGGAAAAGACCAAGC CTGAGGTCACGCTCTGTACAAC	#38
DAT	CCAGCTACAACAAGTTCACCAA AGAAGCTCGTCAGGGAGTTG	#10
TH	GTAAGCAGAACGGGGAGGT TCTCAGGCTCCTCAGACAGG	#56

A.2 ANTIBODIES

- Phospho 4E-BP (Serine 65) (Cell Signaling #9451, rabbit polyclonal, 1:1000)

- Phospho 4E-BP (Threonine 37/46) (Cell Signaling #9459, rabbit polyclonal, 1:1000)

- Phospho 4E-BP (Threonine 70) (Cell Signaling #9455, rabbit polyclonal, 1:1000)

- β-actin (Sigma clone AC-74 #A2228, mouse IgG2a, 1:5000)

- total 4E-BP (Cell Signaling #9452, rabbit polyclonal, 1:1000)

- OCT4 (Santa Cruz #5279, mouse IgG2b, 1:200)

- TRA 1-81 (Biolegend #330701, mouse IgMκ, 1:600)

- SSEA4 (DSHB, mouse IgG3κ, neat)

- NANOG (Abcam #ab21624, rabbit IgG, 1:1000)

- TUJ-1 (R&D systems #MAB1195, mouse IgG2A)

- TH (R&D systems #MAB1423 clone TH-2, mouse IgG1)

- LMX1B (Rabbit polyclonal from Dai et al. (2008), 1:2000)

- α-synuclein (BD Transduction Laboratories #610787, mouse IgG1)

- AlexaFluor-488 and AlexaFluor-596-labelled secondary antibodies (Molecular Probes)

BIBLIOGRAPHY

Aarsland D, Zaccai J, Brayne C (2005) A systematic review of prevalence studies of dementia in Parkinson's disease. Mov Disord 20: 1255–63.

Abeliovich A, Schmitz Y, Farinas I, Choi-Lundberg D, Ho WH, et al. (2000) Mice lacking alpha-synuclein display functional deficits in the nigrostriatal dopamine system. Neuron 25: 239–52.

Aguzzi A, Sigurdson C, Heikenwaelder M (2008) Molecular mechanisms of prion pathogenesis. Annu Rev Pathol 3: 11–40.

Ahn TB, Kim SY, Kim JY, Park SS, Lee DS, et al. (2008) alpha-Synuclein gene duplication is present in sporadic Parkinson disease. Neurology 70: 43–49.

Alvarez-Erviti L, Seow Y, Schapira AH, Gardiner C, Sargent IL, et al. (2011) Lysosomal dysfunction increases exosome-mediated alpha-synuclein release and transmission. Neurobiol Dis 42: 360–7.

Ambros V (2004) The functions of animal microRNAs. Nature 431: 350–5.

Anderson JM, Hampton DW, Patani R, Pryce G, Crowther RA, et al. (2008) Abnormally phosphorylated tau is associated with neuronal and axonal loss in experimental autoimmune encephalomyelitis and multiple sclerosis. Brain 131: 1736–48.

Andreadis A (2005) Tau gene alternative splicing: expression patterns, regulation and modulation of function in normal brain and neurodegenerative diseases. Biochim Biophys Acta 1739: 91–103.

Anokye-Danso F, Trivedi CM, Juhr D, Gupta M, Cui Z, et al. (2011) Highly efficient miRNA-mediated reprogramming of mouse and human somatic cells to pluripotency. Cell Stem Cell 8: 376–88.

Ascherio A, Chen H, Weisskopf MG, O'Reilly E, McCullough ML, et al. (2006) Pesticide exposure and risk for Parkinson's disease. Ann Neurol 60: 197–203.

Ballatore C, Lee VM, Trojanowski JQ (2007) Tau-mediated neurodegeneration in Alzheimer's disease and related disorders. Nat Rev Neurosci 8: 663–72.

Bancher C, Leitner H, Jellinger K, Eder H, Setinek U, et al. (1996) On the relationship between measles virus and Alzheimer neurofibrillary tangles in subacute sclerosing panencephalitis. Neurobiol Aging 17: 527–33.

Beck AT, Beck RW (1972) Screening depressed patients in family practice. A rapid technic. Postgrad Med 52: 81–5.

Betarbet R, Sherer TB, MacKenzie G, Garcia-Osuna M, Panov AV, et al. (2000) Chronic systemic pesticide exposure reproduces features of Parkinson's disease. Nat Neurosci 3: 1301–6.

Birkmayer W, Hornykiewicz O (1961) [The L-3,4-dioxyphenylalanine (DOPA)-effect in Parkinson-akinesia]. Wien Klin Wochenschr 73: 787–8.

Biskup S, Moore DJ, Celsi F, Higashi S, West AB, et al. (2006) Localization of LRRK2 to membranous and vesicular structures in mammalian brain. Ann Neurol 60: 557–69.

Bjorklund A, Dunnett SB, Brundin P, Stoessl AJ, Freed CR, et al. (2003) Neural transplantation for the treatment of Parkinson's disease. Lancet Neurol 2: 437–45.

Bock C, Kiskinis E, Verstappen G, Gu H, Boulting G, et al. (2011) Reference Maps of human ES and iPS cell variation enable high-

throughput characterization of pluripotent cell lines. Cell 144: 439–52.

Bonifati V (2006) Parkinson's disease: the LRRK2-G2019S mutation: opening a novel era in Parkinson's disease genetics. Eur J Hum Genet 14: 1061–2.

Bonifati V, Rizzu P, van Baren MJ, Schaap O, Breedveld GJ, et al. (2003) Mutations in the DJ-1 gene associated with autosomal recessive early-onset parkinsonism. Science 299: 256–9.

Botta-Orfila T, Tolosa E, Gelpi E, Sànchez-Pla A, Martí MJ, et al. (2012) Microarray expression analysis in idiopathic and LRRK2-associated Parkinson's disease. Neurobiol Dis 45: 462–8.

Bottomley RH, Trainer AL, Griffin MJ (1969) Enzymatic and chromosomal characterization of HeLa variants. J Cell Biol 41: 806–15.

Boulting GL, Kiskinis E, Croft GF, Amoroso MW, Oakley DH, et al. (2011) A functionally characterized test set of human induced pluripotent stem cells. Nat Biotechnol 29: 279–86.

Braak H, Braak E (2000) Pathoanatomy of Parkinson's disease. J Neurol 247 Suppl 2: II3–10.

Braak H, Del Tredici K, Rub U, de Vos RA, Jansen Steur EN, et al. (2003) Staging of brain pathology related to sporadic Parkinson's disease. Neurobiol Aging 24: 197–211.

Bradley A, Evans M, Kaufman MH, Robertson E (1984) Formation of germ-line chimaeras from embryo-derived teratocarcinoma cell lines. Nature 309: 255–6.

Bringhurst R (2004) The elements of typographic style. 3rd ed., Point Roberts, WA: Hartley and Marks, Publishers.

Brundin P, Li JY, Holton JL, Lindvall O, Revesz T (2008) Research in motion: the enigma of Parkinson's disease pathology spread. Nat Rev Neurosci 9: 741–5.

Burré J, Sharma M, Tsetsenis T, Buchman V, Etherton MR, et al. (2010) Alpha-synuclein promotes SNARE-complex assembly in vivo and in vitro. Science 329: 1663–7.

Byers B, Cord B, Nguyen HN, Schüle B, Fenno L, et al. (2011) SNCA triplication Parkinson's patient's iPSC-derived DA neurons accumulate [alpha]-synuclein and are susceptible to oxidative stress. PLoS One 6: e26159.

Carlsson A, Lindqvist M, Magnusson T (1957) 3,4-Dihydroxyphenylalanine and 5-hydroxytryptophan as reserpine antagonists. Nature 180: 1200.

Cervantes Saavedra Md (1605) El ingenioso hidalgo don Qvixote de la Mancha. Madrid: Por Iuan de la Cuesta, vendese en casa de Francisco de Robles, librero.

Chade AR, Kasten M, Tanner CM (2006) Nongenetic causes of Parkinson's disease. J Neural Transm Suppl pp. 147–51.

Chambers SM, Fasano CA, Papapetrou EP, Tomishima M, Sadelain M, et al. (2009) Highly efficient neural conversion of human ES and iPS cells by dual inhibition of SMAD signaling. Nat Biotechnol 27: 275–80.

Chan EM, Ratanasirintrawoot S, Park IH, Manos PD, Loh YH, et al. (2009) Live cell imaging distinguishes bona fide human iPS cells from partially reprogrammed cells. Nat Biotechnol 27: 1033–7.

Chartier-Harlin MC, Kachergus J, Roumier C, Mouroux V, Douay X, et al. (2004) Alpha-synuclein locus duplication as a cause of familial Parkinson's disease. Lancet 364: 1167–9.

Chiba-Falek O, Lopez GJ, Nussbaum RL (2006) Levels of alpha-synuclein mRNA in sporadic Parkinson disease patients. Mov Disord 21: 1703–8.

Chiba-Falek O, Nussbaum RL (2001) Effect of allelic variation at the NACP-Rep1 repeat upstream of the alpha-synuclein gene (SNCA) on transcription in a cell culture luciferase reporter system. Hum Mol Genet 10: 3101–9.

Chinta SJ, Mallajosyula JK, Rane A, Andersen JK (2010) Mitochondrial alpha-synuclein accumulation impairs complex I function in dopaminergic neurons and results in increased mitophagy in vivo. Neurosci Lett 486: 235–9.

Chu Y, Kordower JH (2007) Age-associated increases of alpha-synuclein in monkeys and humans are associated with nigrostriatal dopamine depletion: Is this the target for Parkinson's disease? Neurobiol Dis 25: 134–49.

Clark IE, Dodson MW, Jiang C, Cao JH, Huh JR, et al. (2006) Drosophila pink1 is required for mitochondrial function and interacts genetically with parkin. Nature 441: 1162–6.

Conway KA, Harper JD, Lansbury PT (1998) Accelerated in vitro fibril formation by a mutant alpha-synuclein linked to early-onset Parkinson disease. Nat Med 4: 1318–20.

Conway KA, Lee SJ, Rochet JC, Ding TT, Williamson RE, et al. (2000) Acceleration of oligomerization, not fibrillization, is a shared property of both alpha-synuclein mutations linked to early-onset Parkinson's disease: implications for pathogenesis and therapy. Proc Natl Acad Sci U S A 97: 571–6.

Cookson MR (2010) The role of leucine-rich repeat kinase 2 (LRRK2) in Parkinson's disease. Nat Rev Neurosci 11: 791–7.

Cookson MR, van der Brug M (2008) Cell systems and the toxic mechanism(s) of alpha-synuclein. Exp Neurol 209: 5–11.

Cotzias GC, Papavasiliou PS, Gellene R (1969) Modification of Parkinsonism–chronic treatment with L-dopa. N Engl J Med 280: 337–45.

Covy JP, Yuan W, Waxman EA, Hurtig HI, Van Deerlin VM, et al. (2009) Clinical and pathological characteristics of patients with leucine-rich repeat kinase-2 mutations. Mov Disord 24: 32–9.

Cronin KD, Ge D, Manninger P, Linnertz C, Rossoshek A, et al. (2009) Expansion of the Parkinson disease-associated SNCA-Rep1 allele up-regulates human alpha-synuclein in transgenic mouse brain. Hum Mol Genet 18: 3274–85.

Daher JPL, Pletnikova O, Biskup S, Musso A, Gellhaar S, et al. (2012) Neurodegenerative phenotypes in an A53T [alpha]-synuclein transgenic mouse model are independent of LRRK2. Hum Mol Genet 21: 2420–31.

Dai JX, Hu ZL, Shi M, Guo C, Ding YQ (2008) Postnatal ontogeny of the transcription factor Lmx1b in the mouse central nervous system. J Comp Neurol 509: 341–55.

Daniëls V, Vancraenenbroeck R, Law BMH, Greggio E, Lobbestael E, et al. (2011) Insight into the mode of action of the LRRK2 Y1699C pathogenic mutant. J Neurochem 116: 304–15.

Danzer KM, Krebs SK, Wolff M, Birk G, Hengerer B (2009) Seeding induced by alpha-synuclein oligomers provides evidence for spreading of alpha-synuclein pathology. J Neurochem 111: 192–203.

Dawson TM, Ko HS, Dawson VL (2010) Genetic animal models of Parkinson's disease. Neuron 66: 646–61.

Deng J, Lewis PA, Greggio E, Sluch E, Beilina A, et al. (2008) Structure of the ROC domain from the Parkinson's disease-associated leucine-rich repeat kinase 2 reveals a dimeric GTPase. Proc Natl Acad Sci U S A 105: 1499–504.

Desplats P, Lee HJ, Bae EJ, Patrick C, Rockenstein E, et al. (2009) Inclusion formation and neuronal cell death through neuron-to-neuron transmission of alpha-synuclein. Proc Natl Acad Sci U S A 106: 13010–5.

Devine MJ, Kaganovich A, Ryten M, Mamais A, Trabzuni D, et al. (2011) Pathogenic LRRK2 Mutations Do Not Alter Gene Expression in Cell Model Systems or Human Brain Tissue. PLoS ONE 6: e22489.

Di Fonzo A, Dekker MC, Montagna P, Baruzzi A, Yonova EH, et al. (2009) FBXO7 mutations cause autosomal recessive, early-onset parkinsonian-pyramidal syndrome. Neurology 72: 240–5.

Di Giorgio FP, Carrasco MA, Siao MC, Maniatis T, Eggan K (2007) Non-cell autonomous effect of glia on motor neurons in an embryonic stem cell-based ALS model. Nat Neurosci 10: 608–14.

Dimos JT, Rodolfa KT, Niakan KK, Weisenthal LM, Mitsumoto H, et al. (2008) Induced Pluripotent Stem Cells Generated from Patients with ALS Can Be Differentiated into Motor Neurons. Science 321: 1218–21.

Dolan CV, Boomsma DI, Neale MC (1999) A simulation study of the effects of assignment of prior identity-by-descent probabilities to unselected sib pairs, in covariance-structure modeling of a quantitative-trait locus. Am J Hum Genet 64: 268–80.

Doty RL, Deems DA, Stellar S (1988) Olfactory dysfunction in parkinsonism: a general deficit unrelated to neurologic signs, disease stage, or disease duration. Neurology 38: 1237–44.

Duda JE, Giasson BI, Mabon ME, Miller DC, Golbe LI, et al. (2002) Concurrence of alpha-synuclein and tau brain pathology in the Contursi kindred. Acta Neuropathol 104: 7–11.

Ebert AD, Yu J, Rose J F F, Mattis VB, Lorson CL, et al. (2009) Induced pluripotent stem cells from a spinal muscular atrophy patient. Nature 457: 277–80.

Ehringer H, Hornykiewicz O (1960) [Distribution of noradrenaline and dopamine (3-hydroxytyramine) in the human brain and their behavior in diseases of the extrapyramidal system]. Klin Wochenschr 38: 1236–9.

El-Agnaf OM, Salem SA, Paleologou KE, Curran MD, Gibson MJ, et al. (2006) Detection of oligomeric forms of alpha-synuclein protein in human plasma as a potential biomarker for Parkinson's disease. FASEB J 20: 419–25.

Eriksen JL, Przedborski S, Petrucelli L (2005) Gene dosage and pathogenesis of Parkinson's disease. Trends Mol Med 11: 91–6.

Evans M (2008) Embryonic stem cells: the mouse source–vehicle for mammalian genetics and beyond (Nobel lecture). Chembiochem 9: 1690–6.

Evans MJ, Kaufman MH (1981) Establishment in culture of pluripotential cells from mouse embryos. Nature 292: 154–6.

Exner N, Treske B, Paquet D, Holmstrom K, Schiesling C, et al. (2007) Loss-of-function of human PINK1 results in mitochondrial pathology and can be rescued by parkin. J Neurosci 27: 12413–8.

Farrer M, Chan P, Chen R, Tan L, Lincoln S, et al. (2001a) Lewy bodies and parkinsonism in families with parkin mutations. Ann Neurol 50: 293–300.

Farrer M, Gwinn-Hardy K, Muenter M, DeVrieze FW, Crook R, et al. (1999) A chromosome 4p haplotype segregating with Parkinson's disease and postural tremor. Hum Mol Genet 8: 81–5.

Farrer M, Kachergus J, Forno L, Lincoln S, Wang DS, et al. (2004) Comparison of kindreds with parkinsonism and alpha-synuclein genomic multiplications. Ann Neurol 55: 174–9.

Farrer M, Maraganore DM, Lockhart P, Singleton A, Lesnick TG, et al. (2001b) alpha-Synuclein gene haplotypes are associated with Parkinson's disease. Hum Mol Genet 10: 1847–51.

Fasano CA, Chambers SM, Lee G, Tomishima MJ, Studer L (2010) Efficient derivation of functional floor plate tissue from human embryonic stem cells. Cell Stem Cell 6: 336–47.

Feany MB, Bender WW (2000) A Drosophila model of Parkinson's disease. Nature 404: 394–8.

Feng Q, Lu SJ, Klimanskaya I, Gomes I, Kim D, et al. (2010) Hemangioblastic derivatives from human induced pluripotent stem cells exhibit limited expansion and early senescence. Stem Cells 28: 704–12.

Findley L, Aujla M, Bain PG, Baker M, Beech C, et al. (2003) Direct economic impact of Parkinson's disease: a research survey in the United Kingdom. Mov Disord 18: 1139–45.

Folstein MF, Folstein SE, McHugh PR (1975) "Mini-mental state". A practical method for grading the cognitive state of patients for the clinician. J Psychiatr Res 12: 189–98.

Fountaine TM, Venda LL, Warrick N, Christian HC, Brundin P, et al. (2008) The effect of alpha-synuclein knockdown on MPP+ toxicity in models of human neurons. Eur J Neurosci 28: 2459–73.

Franke A, McGovern DPB, Barrett JC, Wang K, Radford-Smith GL, et al. (2010) Genome-wide meta-analysis increases to 71 the number of confirmed Crohn's disease susceptibility loci. Nat Genet 42: 1118–25.

Fuchs J, Nilsson C, Kachergus J, Munz M, Larsson EM, et al. (2007) Phenotypic variation in a large Swedish pedigree due to SNCA duplication and triplication. Neurology 68: 916–22.

Fuchs J, Tichopad A, Golub Y, Munz M, Schweitzer KJ, et al. (2008) Genetic variability in the SNCA gene influences alpha-synuclein levels in the blood and brain. FASEB J 22: 1327–34.

Fujita M, Sugama S, Sekiyama K, Sekigawa A, Tsukui T, et al. (2010) A beta-synuclein mutation linked to dementia produces neurodegeneration when expressed in mouse brain. Nat Comm 1: 110–9.

Funayama M, Hasegawa K, Ohta E, Kawashima N, Komiyama M, et al. (2005) An LRRK2 mutation as a cause for the parkinsonism in the original PARK8 family. Ann Neurol 57: 918–21.

Fusaki N, Ban H, Nishiyama A, Saeki K, Hasegawa M (2009) Efficient induction of transgene-free human pluripotent stem cells using a vector based on Sendai virus, an RNA virus that does not integrate into the host genome. Proc Jpn Acad Ser B Phys Biol Sci 85: 348–62.

Gai H, Leung ELH, Costantino PD, Aguila JR, Nguyen DM, et al. (2009) Generation and characterization of functional cardiomyocytes using induced pluripotent stem cells derived from human fibroblasts. Cell Biol Int 33: 1184–93.

Galen (1539) Claudii Galeni Pergameni Definitiones medicae. Lvgdvni: Apvd Franciscvm Ivstvm.

Galpern WR, Lang AE (2006) Interface between tauopathies and synucleinopathies: a tale of two proteins. Ann Neurol 59: 449–58.

Galvin JE, Uryu K, Lee VM, Trojanowski JQ (1999) Axon pathology in Parkinson's disease and Lewy body dementia hippocampus contains alpha-, beta-, and gamma-synuclein. Proc Natl Acad Sci U S A 96: 13450–5.

Gandhi PN, Wang X, Zhu X, Chen SG, Wilson-Delfosse AL (2008) The Roc domain of leucine-rich repeat kinase 2 is sufficient for interaction with microtubules. J Neurosci Res 86: 1711–20.

Garcia de Ancos J, Correas I, Avila J (1993) Differences in microtubule binding and self-association abilities of bovine brain tau isoforms. J Biol Chem 268: 7976–82.

Gehrke S, Imai Y, Sokol N, Lu B (2010) Pathogenic LRRK2 negatively regulates microRNA-mediated translational repression. Nature 466: 637–41.

Giasson BI, Forman MS, Higuchi M, Golbe LI, Graves CL, et al. (2003) Initiation and synergistic fibrillization of tau and alpha-synuclein. Science 300: 636–40.

Gibb WR, Lees AJ (1988) The relevance of the Lewy body to the pathogenesis of idiopathic Parkinson's disease. J Neurol Neurosurg Psychiatry 51: 745–52.

Gibbs JR, Singleton A (2006) Application of Genome-Wide Single Nucleotide Polymorphism Typing: Simple Association and Beyond. PLoS Genet 2: e150.

Gingras AC, Raught B, Gygi SP, Niedzwiecka A, Miron M, et al. (2001) Hierarchical phosphorylation of the translation inhibitor 4E-BP1. Genes Dev 15: 2852–64.

Giordana MT, D'Agostino C, Albani G, Mauro A, Di Fonzo A, et al. (2007) Neuropathology of Parkinson's disease associated with the LRRK2 Ile1371Val mutation. Mov Disord 22: 275–8.

Gonzalez F, Barragan Monasterio M, Tiscornia G, Montserrat Pulido N, Vassena R, et al. (2009) Generation of mouse-induced pluripotent stem cells by transient expression of a single nonviral polycistronic vector. Proc Natl Acad Sci U S A 106: 8918–22.

Gorbatyuk OS, Li S, Nash K, Gorbatyuk M, Lewin AS, et al. (2010) In vivo RNAi-mediated alpha-synuclein silencing induces nigrostriatal degeneration. Mol Ther 18: 1450–7.

Gore A, Li Z, Fung HL, Young JE, Agarwal S, et al. (2011) Somatic coding mutations in human induced pluripotent stem cells. Nature 470: 63–7.

Goris A, Williams-Gray CH, Clark GR, Foltynie T, Lewis SJ, et al. (2007) Tau and alpha-synuclein in susceptibility to, and dementia in, Parkinson's disease. Ann Neurol 62: 145–53.

Greggio E, Jain S, Kingsbury A, Bandopadhyay R, Lewis P, et al. (2006) Kinase activity is required for the toxic effects of mutant LRRK2/dardarin. Neurobiol Dis 23: 329–41.

Greggio E, Zambrano I, Kaganovich A, Beilina A, Taymans JM, et al. (2008) The Parkinson disease-associated leucine-rich repeat kinase 2 (LRRK2) is a dimer that undergoes intramolecular autophosphorylation. J Biol Chem 283: 16906–14.

Greten-Harrison B, Polydoro M, Morimoto-Tomita M, Diao L, Williams AM, et al. (2010) alphabetagamma-Synuclein triple knockout mice reveal age-dependent neuronal dysfunction. Proc Natl Acad Sci U S A 107: 19573–78.

Gurdon JB (1962) The developmental capacity of nuclei taken from intestinal epithelium cells of feeding tadpoles. J Embryol Exp Morphol 10: 622–40.

Gwinn K, Devine MJ, Jin LW, Johnson J, Bird T, et al. (2011) Clinical features, with video documentation, of the original familial Lewy body parkinsonism caused by alpha-synuclein triplication (Iowa kindred). Mov Disord 26: 2134–6.

Gwinn-Hardy K, Mehta ND, Farrer M, Maraganore D, Muenter M, et al. (2000) Distinctive neuropathology revealed by alpha-synuclein antibodies in hereditary parkinsonism and dementia linked to chromosome 4p. Acta Neuropathol 99: 663–72.

Hanna J, Saha K, Pando B, van Zon J, Lengner CJ, et al. (2009) Direct cell reprogramming is a stochastic process amenable to acceleration. Nature 462: 595–601.

Hansen C, Angot E, Bergstrom AL, Steiner JA, Pieri L, et al. (2011) alpha-Synuclein propagates from mouse brain to grafted dopaminergic neurons and seeds aggregation in cultured human cells. J Clin Invest 121: 715–25.

Hardy J (2005) Expression of normal sequence pathogenic proteins for neurodegenerative disease contributes to disease risk: 'permissive templating' as a general mechanism underlying neurodegeneration. Biochem Soc Trans 33: 578–81.

Hardy J (2006) Amyloid double trouble. Nat Genet 38: 11–12.

Hardy J, Lewis P, Revesz T, Lees A, Paisan-Ruiz C (2009) The genetics of Parkinson's syndromes: a critical review. Curr Opin Genet Dev 19: 254–65.

Hashimoto M, Rockenstein E, Mante M, Mallory M, Masliah E (2001) beta-Synuclein inhibits alpha-synuclein aggregation: a possible role as an anti-parkinsonian factor. Neuron 32: 213–23.

Hatano T, Kubo S, Imai S, Maeda M, Ishikawa K, et al. (2007) Leucine-rich repeat kinase 2 associates with lipid rafts. Hum Mol Genet 16: 678–90.

Hawkes CH, Del Tredici K, Braak H (2007) Parkinson's disease: a dual-hit hypothesis. Neuropathol Appl Neurobiol 33: 599–614.

Hay N, Sonenberg N (2004) Upstream and downstream of mTOR. Genes Dev 18: 1926–45.

Healy DG, Abou-Sleiman PM, Lees AJ, Casas JP, Quinn N, et al. (2004) Tau gene and Parkinson's disease: a case-control study and meta-analysis. J Neurol Neurosurg Psychiatry 75: 962–5.

Henchcliffe C, Beal MF (2008) Mitochondrial biology and oxidative stress in Parkinson disease pathogenesis. Nat Clin Pract Neurol 4: 600–9.

Herzig MC, Bidinosti M, Schweizer T, Hafner T, Stemmelen C, et al. (2012) High LRRK2 Levels Fail to Induce or Exacerbate Neuronal Alpha-Synucleinopathy in Mouse Brain. PLoS One 7: e36581.

Hockemeyer D, Soldner F, Beard C, Gao Q, Mitalipova M, et al. (2009) Efficient targeting of expressed and silent genes in human ESCs and iPSCs using zinc-finger nucleases. Nat Biotechnol 27: 851–7.

Hockemeyer D, Wang H, Kiani S, Lai CS, Gao Q, et al. (2011) Genetic engineering of human pluripotent cells using TALE nucleases. Nat Biotechnol 29: 731–4.

Hoehn MM, Yahr MD (1967) Parkinsonism: onset, progression and mortality. Neurology 17: 427–42.

Hoepken HH, Gispert S, Azizov M, Klinkenberg M, Ricciardi F, et al. (2008) Parkinson patient fibroblasts show increased alpha-synuclein expression. Exp Neurol 212: 307–13.

Hotta A, Ellis J (2008) Retroviral vector silencing during iPS cell induction: an epigenetic beacon that signals distinct pluripotent states. J Cell Biochem 105: 940–8.

Hsu CH, Chan D, Greggio E, Saha S, Guillily MD, et al. (2010a) MKK6 binds and regulates expression of Parkinson's disease-related protein LRRK2. J Neurochem 112: 1593–604.

Hsu CH, Chan D, Wolozin B (2010b) LRRK2 and the stress response: interaction with MKKs and JNK-interacting proteins. Neurodegener Dis 7: 68–75.

Hu BY, Weick JP, Yu J, Ma LX, Zhang XQ, et al. (2010) Neural differentiation of human induced pluripotent stem cells follows developmental principles but with variable potency. Proc Natl Acad Sci U S A 107: 4335–40.

Huangfu D, Osafune K, Maehr R, Guo W, Eijkelenboom A, et al. (2008) Induction of pluripotent stem cells from primary human fibroblasts with only Oct4 and Sox2. Nat Biotechnol 26: 1269–75.

Hughes AJ, Daniel SE, Lees AJ (2001) Improved accuracy of clinical diagnosis of Lewy body Parkinson's disease. Neurology 57: 1497–9.

Hulihan MM, Ishihara-Paul L, Kachergus J, Warren L, Amouri R, et al. (2008) LRRK2 Gly2019Ser penetrance in Arab-Berber patients from Tunisia: a case-control genetic study. Lancet Neurol 7: 591–4.

Hussein SM, Batada NN, Vuoristo S, Ching RW, Autio R, et al. (2011) Copy number variation and selection during reprogramming to pluripotency. Nature 470: 58–62.

Hutton M, Lendon CL, Rizzu P, Baker M, Froelich S, et al. (1998) Association of missense and 5′-splice-site mutations in tau with the inherited dementia FTDP-17. Nature 393: 702–5.

Ibanez P, Bonnet AM, Debarges B, Lohmann E, Tison F, et al. (2004) Causal relation between alpha-synuclein gene duplication and familial Parkinson's disease. Lancet 364: 1169–71.

Ibanez P, Lesage S, Janin S, Lohmann E, Durif F, et al. (2009) Alpha-synuclein gene rearrangements in dominantly inherited parkinsonism: frequency, phenotype, and mechanisms. Arch Neurol 66: 102–8.

Ikeuchi T, Kakita A, Shiga A, Kasuga K, Kaneko H, et al. (2008) Patients homozygous and heterozygous for SNCA duplication in a family with parkinsonism and dementia. Arch Neurol 65: 514–9.

Ilieva H, Polymenidou M, Cleveland DW (2009) Non-cell autonomous toxicity in neurodegenerative disorders: ALS and beyond. J Cell Biol 187: 761–72.

Imai Y, Gehrke S, Wang HQ, Takahashi R, Hasegawa K, et al. (2008) Phosphorylation of 4E-BP by LRRK2 affects the maintenance of dopaminergic neurons in Drosophila. EMBO J 27: 2432–43.

Iqbal K, Alonso Adel C, Chen S, Chohan MO, El-Akkad E, et al. (2005) Tau pathology in Alzheimer disease and other tauopathies. Biochim Biophys Acta 1739: 198–210.

Irrcher I, Aleyasin H, Seifert EL, Hewitt SJ, Chhabra S, et al. (2010) Loss of the Parkinson's disease-linked gene DJ-1 perturbs mitochondrial dynamics. Hum Mol Genet 19: 3734–46.

Jakel RJ, Schneider BL, Svendsen CN (2004) Using human neural stem cells to model neurological disease. Nat Rev Genet 5: 136–44.

Jaleel M, Nichols RJ, Deak M, Campbell DG, Gillardon F, et al. (2007) LRRK2 phosphorylates moesin at threonine-558: characterization of

how Parkinson's disease mutants affect kinase activity. Biochem J 405: 307–17.

Jankovic J (2008) Parkinson's disease: clinical features and diagnosis. J Neurol Neurosurg Psychiatry 79: 368–76.

Jensen PH, Hager H, Nielsen MS, Hojrup P, Gliemann J, et al. (1999) alpha-synuclein binds to Tau and stimulates the protein kinase A-catalyzed tau phosphorylation of serine residues 262 and 356. J Biol Chem 274: 25481–9.

Jones D (2011) The long march of antisense. Nat Rev Drug Discov 10: 401–2.

Kaji K, Norrby K, Paca A, Mileikovsky M, Mohseni P, et al. (2009) Virus-free induction of pluripotency and subsequent excision of reprogramming factors. Nature 458: 771–5.

Kamp F, Exner N, Lutz AK, Wender N, Hegermann J, et al. (2010) Inhibition of mitochondrial fusion by alpha-synuclein is rescued by PINK1, Parkin and DJ-1. EMBO J 29: 3571–89.

Kauffmann A, Huber W (2010) Microarray data quality control improves the detection of differentially expressed genes. Genomics 95: 138–42.

Kawasaki H, Mizuseki K, Nishikawa S, Kaneko S, Kuwana Y, et al. (2000) Induction of midbrain dopaminergic neurons from ES cells by stromal cell-derived inducing activity. Neuron 28: 31–40.

Kempster PA, O'Sullivan SS, Holton JL, Revesz T, Lees AJ (2010) Relationships between age and late progression of Parkinson's disease: a clinico-pathological study. Brain 133: 1755–62.

Khan NL, Jain S, Lynch JM, Pavese N, Abou-Sleiman P, et al. (2005) Mutations in the gene LRRK2 encoding dardarin (PARK8) cause familial Parkinson's disease: clinical, pathological, olfactory and functional imaging and genetic data. Brain 128: 2786–96.

Kim RH, Smith PD, Aleyasin H, Hayley S, Mount MP, et al. (2005) Hypersensitivity of DJ-1-deficient mice to 1-methyl-4-phenyl-1,2,3,6-tetrahydropyrindine (MPTP) and oxidative stress. Proc Natl Acad Sci U S A 102: 5215–20.

Kitada T, Asakawa S, Hattori N, Matsumine H, Yamamura Y, et al. (1998) Mutations in the parkin gene cause autosomal recessive juvenile parkinsonism. Nature 392: 605–8.

Kleinsmith LJ, Pierce GB Jr (1964) Multipotentiality of single embryonal carcinoma cells. Cancer Res 24: 1544–51.

Klivenyi P, Siwek D, Gardian G, Yang L, Starkov A, et al. (2006) Mice lacking alpha-synuclein are resistant to mitochondrial toxins. Neurobiol Dis 21: 541–8.

Knott AB, Perkins G, Schwarzenbacher R, Bossy-Wetzel E (2008) Mitochondrial fragmentation in neurodegeneration. Nat Rev Neurosci 9: 505–18.

Kordower JH, Chu Y, Hauser RA, Freeman TB, Olanow CW (2008a) Lewy body-like pathology in long-term embryonic nigral transplants in Parkinson's disease. Nat Med 14: 504–6.

Kordower JH, Chu Y, Hauser RA, Olanow CW, Freeman TB (2008b) Transplanted dopaminergic neurons develop PD pathologic changes: a second case report. Mov Disord 23: 2303–6.

Kramer ML, Schulz-Schaeffer WJ (2007) Presynaptic alpha-synuclein aggregates, not Lewy bodies, cause neurodegeneration in dementia with Lewy bodies. J Neurosci 27: 1405–10.

Krüger R, Kuhn W, Müller T, Woitalla D, Graeber M, et al. (1998) Ala30Pro mutation in the gene encoding alpha-synuclein in Parkinson's disease. Nat Genet 18: 106–8.

Kruger R, Vieira-Saecker AM, Kuhn W, Berg D, Muller T, et al. (1999) Increased susceptibility to sporadic Parkinson's disease by a certain

combined alpha-synuclein/apolipoprotein E genotype. Ann Neurol 45: 611–7.

Kumar A, Greggio E, Beilina A, Kaganovich A, Chan D, et al. (2010) The Parkinson's disease associated LRRK2 exhibits weaker in vitro phosphorylation of 4E-BP compared to autophosphorylation. PLoS ONE 5: e8730.

Kwok JB, Teber ET, Loy C, Hallupp M, Nicholson G, et al. (2004) Tau haplotypes regulate transcription and are associated with Parkinson's disease. Ann Neurol 55: 329–34.

Langston JW, Ballard P, Tetrud JW, Irwin I (1983) Chronic Parkinsonism in humans due to a product of meperidine-analog synthesis. Science 219: 979–80.

Langston JW, Irwin I, Langston EB, Forno LS (1984) Pargyline prevents MPTP-induced parkinsonism in primates. Science 225: 1480–2.

Larsen K, Hedegaard C, Bertelsen MF, Bendixen C (2009) Threonine 53 in alpha-synuclein is conserved in long-living non-primate animals. Biochem Biophys Res Commun 387: 602–5.

Lashuel HA, Hartley D, Petre BM, Walz T, Lansbury PT (2002) Neurodegenerative disease: amyloid pores from pathogenic mutations. Nature 418: 291.

Lee G, Papapetrou EP, Kim H, Chambers SM, Tomishima MJ, et al. (2009) Modelling pathogenesis and treatment of familial dysautonomia using patient-specific iPSCs. Nature 461: 402–6.

Lee HJ, Patel S, Lee SJ (2005) Intravesicular localization and exocytosis of alpha-synuclein and its aggregates. J Neurosci 25: 6016–24.

Leroy E, Boyer R, Auburger G, Leube B, Ulm G, et al. (1998) The ubiquitin pathway in Parkinson's disease. Nature 395: 451–2.

Lewis J, Melrose H, Bumcrot D, Hope A, Zehr C, et al. (2008) In vivo silencing of alpha-synuclein using naked siRNA. Mol Neurodegener 3: 19.

Lewis PA, Greggio E, Beilina A, Jain S, Baker A, et al. (2007) The R1441C mutation of LRRK2 disrupts GTP hydrolysis. Biochem Biophys Res Commun 357: 668–71.

Lewy F (1912) Paralysis agitans. 1. Pathologische anatomie, pp. 920–933. Berlin: Springer.

Li JY, Englund E, Holton JL, Soulet D, Hagell P, et al. (2008) Lewy bodies in grafted neurons in subjects with Parkinson's disease suggest host-to-graft disease propagation. Nat Med 14: 501–3.

Li X, Tan YC, Poulose S, Olanow CW, Huang XY, et al. (2007) Leucine-rich repeat kinase 2 (LRRK2)/PARK8 possesses GTPase activity that is altered in familial Parkinson's disease R1441C/G mutants. J Neurochem 103: 238–47.

Liao J, Wu Z, Wang Y, Cheng L, Cui C, et al. (2008) Enhanced efficiency of generating induced pluripotent stem (iPS) cells from human somatic cells by a combination of six transcription factors. Cell Res 18: 600–3.

Lim Y, Kehm VM, Lee EB, Soper JH, Li C, et al. (2011) alpha-Syn Suppression Reverses Synaptic and Memory Defects in a Mouse Model of Dementia with Lewy Bodies. J Neurosci 31: 10076–87.

Lin X, Parisiadou L, Gu XL, Wang L, Shim H, et al. (2009) Leucine-rich repeat kinase 2 regulates the progression of neuropathology induced by Parkinson's-disease-related mutant alpha-synuclein. Neuron 64: 807–27.

Linnertz C, Saucier L, Ge D, Cronin KD, Burke JR, et al. (2009) Genetic regulation of alpha-synuclein mRNA expression in various human brain tissues. PLoS ONE 4: e7480.

Liou AK, Leak RK, Li L, Zigmond MJ (2008) Wild-type LRRK2 but not its mutant attenuates stress-induced cell death via ERK pathway. Neurobiol Dis 32: 116–24.

Lister R, Pelizzola M, Kida YS, Hawkins RD, Nery JR, et al. (2011) Hotspots of aberrant epigenomic reprogramming in human induced pluripotent stem cells. Nature 470: 68–73.

Lo Bianco C, Ridet JL, Schneider BL, Deglon N, Aebischer P (2002) alpha -Synucleinopathy and selective dopaminergic neuron loss in a rat lentiviral-based model of Parkinson's disease. Proc Natl Acad Sci U S A 99: 10813–8.

Loeb V, Yakunin E, Saada A, Sharon R (2010) The transgenic overexpression of alpha-synuclein and not its related pathology associates with complex I inhibition. J Biol Chem 285: 7334–43.

Looyenga BD, Furge KA, Dykema KJ, Koeman J, Swiatek PJ, et al. (2011) Chromosomal amplification of leucine-rich repeat kinase-2 (LRRK2) is required for oncogenic MET signaling in papillary renal and thyroid carcinomas. Proc Natl Acad Sci U S A 108: 1439–44.

Lowry WE, Richter L, Yachechko R, Pyle AD, Tchieu J, et al. (2008) Generation of human induced pluripotent stem cells from dermal fibroblasts. Proc Natl Acad Sci U S A 105: 2883–8.

Lwin A, Orvisky E, Goker-Alpan O, LaMarca ME, Sidransky E (2004) Glucocerebrosidase mutations in subjects with parkinsonism. Mol Genet Metab 81: 70–3.

MacLeod D, Dowman J, Hammond R, Leete T, Inoue K, et al. (2006) The familial Parkinsonism gene LRRK2 regulates neurite process morphology. Neuron 52: 587–93.

Maehr R, Chen S, Snitow M, Ludwig T, Yagasaki L, et al. (2009) Generation of pluripotent stem cells from patients with type 1 diabetes. Proc Natl Acad Sci U S A 106: 15768–73.

Maraganore DM, de Andrade M, Elbaz A, Farrer MJ, Ioannidis JP, et al. (2006) Collaborative analysis of alpha-synuclein gene promoter variability and Parkinson disease. JAMA 296: 661–70.

Marin I (2006) The Parkinson disease gene LRRK2: evolutionary and structural insights. Mol Biol Evol 23: 2423–33.

Maroteaux L, Campanelli JT, Scheller RH (1988) Synuclein: a neuron-specific protein localized to the nucleus and presynaptic nerve terminal. J Neurosci 8: 2804–15.

Martin ER, Scott WK, Nance MA, Watts RL, Hubble JP, et al. (2001) Association of single-nucleotide polymorphisms of the tau gene with late-onset Parkinson disease. JAMA 286: 2245–50.

Martin LJ, Pan Y, Price AC, Sterling W, Copeland NG, et al. (2006) Parkinson's disease alpha-synuclein transgenic mice develop neuronal mitochondrial degeneration and cell death. J Neurosci 26: 41–50.

Masliah E, Rockenstein E, Adame A, Alford M, Crews L, et al. (2005) Effects of alpha-synuclein immunization in a mouse model of Parkinson's disease. Neuron 46: 857–68.

Mayshar Y, Ben-David U, Lavon N, Biancotti JC, Yakir B, et al. (2010) Identification and classification of chromosomal aberrations in human induced pluripotent stem cells. Cell Stem Cell 7: 521–31.

Mazzulli JR, Xu YH, Sun Y, Knight AL, McLean PJ, et al. (2011) Gaucher disease glucocerebrosidase and alpha-synuclein form a bidirectional pathogenic loop in synucleinopathies. Cell 146: 37–52.

McCall S, Vilensky JA, Gilman S, Taubenberger JK (2008) The relationship between encephalitis lethargica and influenza: a critical analysis. J Neurovirol 14: 177–85.

McCormack AL, Mak SK, Henderson JM, Bumcrot D, Farrer MJ, et al. (2010) Alpha-synuclein suppression by targeted small interfering RNA in the primate substantia nigra. PLoS ONE 5: e12122.

McKeith IG, Burn DJ, Ballard CG, Collerton D, Jaros E, et al. (2003) Dementia with Lewy bodies. Semin Clin Neuropsychiatry 8: 46–57.

McNaught KSP, Belizaire R, Isacson O, Jenner P, Olanow CW (2003) Altered proteasomal function in sporadic Parkinson's disease. Exp Neurol 179: 38–46.

Miller DW, Hague SM, Clarimon J, Baptista M, Gwinn-Hardy K, et al. (2004) Alpha-synuclein in blood and brain from familial Parkinson disease with SNCA locus triplication. Neurology 62: 1835–38.

Muenter MD, Forno LS, Hornykiewicz O, Kish SJ, Maraganore DM, et al. (1998) Hereditary form of parkinsonism–dementia. Ann Neurol 43: 768–81.

Muller FJ, Schuldt BM, Williams R, Mason D, Altun G, et al. (2011) A bioinformatic assay for pluripotency in human cells. Nat Methods 8: 315–7.

Mutez E, Larvor L, Leprêtre F, Mouroux V, Hamalek D, et al. (2011) Transcriptional profile of Parkinson blood mononuclear cells with LRRK2 mutation. Neurobiol Aging 32: 1839–48.

Nakamura K, Nemani VM, Azarbal F, Skibinski G, Levy JM, et al. (2011) Direct membrane association drives mitochondrial fission by the Parkinson disease-associated protein alpha-synuclein. J Biol Chem 286: 20710–26.

Narendra D, Tanaka A, Suen DF, Youle RJ (2008) Parkin is recruited selectively to impaired mitochondria and promotes their autophagy. J Cell Biol 183: 795–803.

Narendra DP, Jin SM, Tanaka A, Suen DF, Gautier CA, et al. (2010) PINK1 is selectively stabilized on impaired mitochondria to activate Parkin. PLoS Biol 8: e1000298.

Nemani VM, Lu W, Berge V, Nakamura K, Onoa B, et al. (2010) Increased expression of alpha-synuclein reduces neurotransmitter

release by inhibiting synaptic vesicle reclustering after endocytosis. Neuron 65: 66–79.

Neumann M, Sampathu DM, Kwong LK, Truax AC, Micsenyi MC, et al. (2006) Ubiquitinated TDP-43 in frontotemporal lobar degeneration and amyotrophic lateral sclerosis. Science 314: 130–3.

Nguyen HN, Byers B, Cord B, Shcheglovitov A, Byrne J, et al. (2011) LRRK2 Mutant iPSC-Derived DA Neurons Demonstrate Increased Susceptibility to Oxidative Stress. Cell Stem Cell 8: 267–80.

Nikonova EV, Xiong Y, Tanis KQ, Dawson VL, Vogel RL, et al. (2012) Transcriptional responses to loss or gain of function of the leucine-rich repeat kinase 2 (LRRK2) gene uncover biological processes modulated by LRRK2 activity. Hum Mol Genet 21: 163–74.

Ninkina N, Peters O, Millership S, Salem H, van der Putten H, et al. (2009) Gamma-synucleinopathy: neurodegeneration associated with overexpression of the mouse protein. Hum Mol Genet 18: 1779–94.

Nishioka K, Hayashi S, Farrer MJ, Singleton AB, Yoshino H, et al. (2006) Clinical heterogeneity of alpha-synuclein gene duplication in Parkinson's disease. Ann Neurol 59: 298–309.

Nishioka K, Ross OA, Ishii K, Kachergus JM, Ishiwata K, et al. (2009) Expanding the clinical phenotype of SNCA duplication carriers. Mov Disord 24: 1811–9.

Noguchi-Shinohara M, Tokuda T, Yoshita M, Kasai T, Ono K, et al. (2009) CSF alpha-synuclein levels in dementia with Lewy bodies and Alzheimer's disease. Brain Res 1251: 1–6.

Norris EH, Uryu K, Leight S, Giasson BI, Trojanowski JQ, et al. (2007) Pesticide exposure exacerbates alpha-synucleinopathy in an A53T transgenic mouse model. Am J Pathol 170: 658–66.

Ohnuki M, Takahashi K, Yamanaka S (2009) Generation and characterization of human induced pluripotent stem cells. Curr Protoc Stem Cell Biol Chapter 4: Unit 4A.2.

Okita K, Matsumura Y, Sato Y, Okada A, Morizane A, et al. (2011) A more efficient method to generate integration-free human iPS cells. Nat Methods 8: 409–12.

Okita K, Nakagawa M, Hyenjong H, Ichisaka T, Yamanaka S (2008) Generation of mouse induced pluripotent stem cells without viral vectors. Science 322: 949–53.

Ono Y, Nakatani T, Sakamoto Y, Mizuhara E, Minaki Y, et al. (2007) Differences in neurogenic potential in floor plate cells along an anteroposterior location: midbrain dopaminergic neurons originate from mesencephalic floor plate cells. Development 134: 3213–25.

Osafune K, Caron L, Borowiak M, Martinez RJ, Fitz-Gerald CS, et al. (2008) Marked differences in differentiation propensity among human embryonic stem cell lines. Nat Biotechnol 26: 313–5.

Outeiro TF, Lindquist S (2003) Yeast cells provide insight into alpha-synuclein biology and pathobiology. Science 302: 1772–5.

Ozelius LJ, Foroud T, May S, Senthil G, Sandroni P, et al. (2007) G2019S mutation in the leucine-rich repeat kinase 2 gene is not associated with multiple system atrophy. Mov Disord 22: 546–9.

Paisan-Ruiz C, Jain S, Evans EW, Gilks WP, Simon J, et al. (2004) Cloning of the gene containing mutations that cause PARK8-linked Parkinson's disease. Neuron 44: 595–600.

Paisán-Ruíz C, Nath P, Washecka N, Gibbs JR, Singleton AB (2008) Comprehensive analysis of LRRK2 in publicly available Parkinson's disease cases and neurologically normal controls. Hum Mutat 29: 485–90.

Papaioannou VE, McBurney MW, Gardner RL, Evans MJ (1975) Fate of teratocarcinoma cells injected into early mouse embryos. Nature 258: 70–73.

Park IH, Lerou PH, Zhao R, Huo H, Daley GQ (2008a) Generation of human-induced pluripotent stem cells. Nat Protoc 3: 1180–6.

Park IH, Zhao R, West JA, Yabuuchi A, Huo H, et al. (2008b) Reprogramming of human somatic cells to pluripotency with defined factors. Nature 451: 141–6.

Park J, Lee SB, Lee S, Kim Y, Song S, et al. (2006) Mitochondrial dysfunction in Drosophila PINK1 mutants is complemented by parkin. Nature 441: 1157–61.

Parkinson J (1817) An essay on the shaking palsy. London: Sherwood, Neely and Jones.

Pastor P, Ezquerra M, Munoz E, Marti MJ, Blesa R, et al. (2000) Significant association between the tau gene A0/A0 genotype and Parkinson's disease. Ann Neurol 47: 242–5.

Perrier AL, Tabar V, Barberi T, Rubio ME, Bruses J, et al. (2004) Derivation of midbrain dopamine neurons from human embryonic stem cells. Proc Natl Acad Sci U S A 101: 12543–8.

Plowey ED, Cherra SJ 3rd, Liu YJ, Chu CT (2008) Role of autophagy in G2019S-LRRK2-associated neurite shortening in differentiated SH-SY5Y cells. J Neurochem 105: 1048–56.

Polymeropoulos MH, Lavedan C, Leroy E, Ide SE, Dehejia A, et al. (1997) Mutation in the alpha-synuclein gene identified in families with Parkinson's disease. Science 276: 2045–7.

Pramstaller PP, Schlossmacher MG, Jacques TS, Scaravilli F, Eskelson C, et al. (2005) Lewy body Parkinson's disease in a large pedigree with 77 Parkin mutation carriers. Ann Neurol 58: 411–22.

Pridgeon JW, Olzmann JA, Chin LS, Li L (2007) PINK1 protects against oxidative stress by phosphorylating mitochondrial chaperone TRAP1. PLoS Biol 5: e172.

Qing H, Wong W, McGeer EG, McGeer PL (2009) Lrrk2 phosphorylates alpha synuclein at serine 129: Parkinson disease implications. Biochem Biophys Res Commun 387: 149–52.

Rajput A, Dickson DW, Robinson CA, Ross OA, Dachsel JC, et al. (2006) Parkinsonism, Lrrk2 G2019S, and tau neuropathology. Neurology 67: 1506–8.

Rakovic A, Grünewald A, Seibler P, Ramirez A, Kock N, et al. (2010) Effect of endogenous mutant and wild-type PINK1 on Parkin in fibroblasts from Parkinson disease patients. Hum Mol Genet 19: 3124–37.

Ramirez A, Heimbach A, Grundemann J, Stiller B, Hampshire D, et al. (2006) Hereditary parkinsonism with dementia is caused by mutations in ATP13A2, encoding a lysosomal type 5 P-type ATPase. Nat Genet 38: 1184–91.

Raya A, Rodriguez-Piza I, Guenechea G, Vassena R, Navarro S, et al. (2009) Disease-corrected haematopoietic progenitors from Fanconi anaemia induced pluripotent stem cells. Nature 460: 53–9.

Ross OA, Braithwaite AT, Skipper LM, Kachergus J, Hulihan MM, et al. (2008a) Genomic investigation of alpha-synuclein multiplication and parkinsonism. Ann Neurol 63: 743–50.

Ross OA, Soto-Ortolaza AI, Heckman MG, Aasly JO, Abahuni N, et al. (2011) Association of LRRK2 exonic variants with susceptibility to Parkinson's disease: a case-control study. Lancet Neurol 10: 898–908.

Ross OA, Whittle AJ, Cobb SA, Hulihan MM, Lincoln SJ, et al. (2006) Lrrk2 R1441 substitution and progressive supranuclear palsy. Neuropathol Appl Neurobiol 32: 23–5.

Ross OA, Wu YR, Lee MC, Funayama M, Chen ML, et al. (2008b) Analysis of Lrrk2 R1628P as a risk factor for Parkinson's disease. Ann Neurol 64: 88–92.

Rudenko IN, Kaganovich A, Hauser DN, Beylina A, Chia R, et al. (2012) The G2385R Variant of Leucine-Rich Repeat Kinase 2 Associated with Parkinson's Disease is a Partial Loss of Function Mutation. Biochem J .

Ruff RM, Light RH, Parker SB, Levin HS (1996) Benton Controlled Oral Word Association Test: reliability and updated norms. Arch Clin Neuropsychol 11: 329–38.

Saha K, Jaenisch R (2009) Technical challenges in using human induced pluripotent stem cells to model disease. Cell Stem Cell 5: 584–95.

Sánchez-Danés A, Richaud-Patin Y, Carballo-Carbajal I, Jiménez-Delgado S, Caig C, et al. (2012) Disease-specific phenotypes in dopamine neurons from human iPS-based models of genetic and sporadic Parkinson's disease. EMBO Mol Med 4: 380–95.

Sandberg MK, Al-Doujaily H, Sharps B, Clarke AR, Collinge J (2011) Prion propagation and toxicity in vivo occur in two distinct mechanistic phases. Nature 470: 540–42.

Santacruz K, Lewis J, Spires T, Paulson J, Kotilinek L, et al. (2005) Tau suppression in a neurodegenerative mouse model improves memory function. Science 309: 476–81.

Sapru MK, Yates JW, Hogan S, Jiang L, Halter J, et al. (2006) Silencing of human alpha-synuclein in vitro and in rat brain using lentiviral-mediated RNAi. Exp Neurol 198: 382–90.

Sarkar S, Davies JE, Huang Z, Tunnacliffe A, Rubinsztein DC (2007) Trehalose, a novel mTOR-independent autophagy enhancer, accelerates the clearance of mutant huntingtin and alpha-synuclein. J Biol Chem 282: 5641–52.

Satake W, Nakabayashi Y, Mizuta I, Hirota Y, Ito C, et al. (2009) Genome-wide association study identifies common variants at four loci as genetic risk factors for Parkinson's disease. Nat Genet 41: 1303–7.

Schapira AH, Cooper JM, Dexter D, Jenner P, Clark JB, et al. (1989) Mitochondrial complex I deficiency in Parkinson's disease. Lancet 333: 1269.

Schmidt ML, Zhukareva V, Newell KL, Lee VM, Trojanowski JQ (2001) Tau isoform profile and phosphorylation state in dementia pugilistica recapitulate Alzheimer's disease. Acta Neuropathol 101: 518–24.

Schmittgen TD, Livak KJ (2008) Analyzing real-time PCR data by the comparative C(T) method. Nat Protoc 3: 1101–8.

Scholz SW, Houlden H, Schulte C, Sharma M, Li A, et al. (2009) SNCA variants are associated with increased risk for multiple system atrophy. Ann Neurol 65: 610–4.

Schroeder A, Mueller O, Stocker S, Salowsky R, Leiber M, et al. (2006) The RIN: an RNA integrity number for assigning integrity values to RNA measurements. BMC Mol Biol 7: 3.

Schulz JB, Falkenburger BH (2004) Neuronal pathology in Parkinson's disease. Cell Tissue Res 318: 135–47.

Scott WK, Nance MA, Watts RL, Hubble JP, Koller WC, et al. (2001) Complete genomic screen in Parkinson disease: evidence for multiple genes. JAMA 286: 2239–44.

Seibler P, Graziotto J, Jeong H, Simunovic F, Klein C, et al. (2011) Mitochondrial Parkin recruitment is impaired in neurons derived from mutant PINK1 induced pluripotent stem cells. J Neurosci 31: 5970–6.

Sekine T, Kagaya H, Funayama M, Li Y, Yoshino H, et al. (2010) Clinical course of the first Asian family with Parkinsonism related to SNCA triplication. Mov Disord 25: 2871–75.

Shi Y, Kirwan P, Smith J, Robinson HPC, Livesey FJ (2012) Human cerebral cortex development from pluripotent stem cells to functional excitatory synapses. Nat Neurosci 15: 477–86, S1.

Shimura H, Hattori N, Kubo S, Mizuno Y, Asakawa S, et al. (2000) Familial Parkinson disease gene product, parkin, is a ubiquitin-protein ligase. Nat Genet 25: 302–5.

Shimura H, Schlossmacher MG, Hattori N, Frosch MP, Trockenbacher A, et al. (2001) Ubiquitination of a new form of alpha-synuclein by parkin from human brain: implications for Parkinson's disease. Science 293: 263–9.

Shin CW, Kim HJ, Park SS, Kim SY, Kim JY, et al. (2010) Two Parkinson's disease patients with alpha-synuclein gene duplication and rapid cognitive decline. Mov Disord 25: 957–9.

Simon-Sanchez J, Schulte C, Bras JM, Sharma M, Gibbs JR, et al. (2009) Genome-wide association study reveals genetic risk underlying Parkinson's disease. Nat Genet 41: 1308–12.

Singleton AB, Farrer M, Johnson J, Singleton A, Hague S, et al. (2003) alpha-Synuclein locus triplication causes Parkinson's disease. Science 302: 841.

Sironi F, Trotta L, Antonini A, Zini M, Ciccone R, et al. (2010) alpha-Synuclein multiplication analysis in Italian familial Parkinson disease. Parkinsonism Relat Disord 16: 228–31.

Sly WS, Grubb J (1979) Isolation of fibroblasts from patients. Methods Enzymol 58: 444–50.

Smith WW, Pei Z, Jiang H, Dawson VL, Dawson TM, et al. (2006) Kinase activity of mutant LRRK2 mediates neuronal toxicity. Nat Neurosci 9: 1231–3.

Smith WW, Pei Z, Jiang H, Moore DJ, Liang Y, et al. (2005) Leucine-rich repeat kinase 2 (LRRK2) interacts with parkin, and mutant LRRK2 induces neuronal degeneration. Proc Natl Acad Sci U S A 102: 18676–81.

Soldner F, Hockemeyer D, Beard C, Gao Q, Bell GW, et al. (2009) Parkinson's disease patient-derived induced pluripotent stem cells free of viral reprogramming factors. Cell 136: 964–77.

Soldner F, Laganière J, Cheng AW, Hockemeyer D, Gao Q, et al. (2011) Generation of isogenic pluripotent stem cells differing exclusively at two early onset Parkinson point mutations. Cell 146: 318–31.

Spellman GG (1962) Report of familial cases of parkinsonism. Evidence of a dominant trait in a patient's family. JAMA 179: 372–4.

Spillantini MG, Goedert M (2000) The alpha-synucleinopathies: Parkinson's disease, dementia with Lewy bodies, and multiple system atrophy. Ann N Y Acad Sci 920: 16–27.

Spillantini MG, Schmidt ML, Lee VM, Trojanowski JQ, Jakes R, et al. (1997) Alpha-synuclein in Lewy bodies. Nature 388: 839–40.

Stadtfeld M, Nagaya M, Utikal J, Weir G, Hochedlinger K (2008) Induced pluripotent stem cells generated without viral integration. Science 322: 945–9.

Steele JC, McGeer PL (2008) The ALS/PDC syndrome of Guam and the cycad hypothesis. Neurology 70: 1984–90.

Stern G (1989) Did parkinsonism occur before 1817? J Neurol Neurosurg Psychiatry Suppl: 11–2.

Subramanian A, Tamayo P, Mootha VK, Mukherjee S, Ebert BL, et al. (2005) Gene set enrichment analysis: a knowledge-based approach for interpreting genome-wide expression profiles. Proc Natl Acad Sci U S A 102: 15545–50.

Südhof TC, Rothman JE (2009) Membrane fusion: grappling with SNARE and SM proteins. Science 323: 474–7.

Syntichaki P, Troulinaki K, Tavernarakis N (2007) eIF4E function in somatic cells modulates ageing in Caenorhabditis elegans. Nature 445: 922–6.

Tada M, Takahama Y, Abe K, Nakatsuji N, Tada T (2001) Nuclear reprogramming of somatic cells by in vitro hybridization with ES cells. Curr Biol 11: 1553–8.

Takahashi K, Okita K, Nakagawa M, Yamanaka S (2007a) Induction of pluripotent stem cells from fibroblast cultures. Nat Protoc 2: 3081–9.

Takahashi K, Tanabe K, Ohnuki M, Narita M, Ichisaka T, et al. (2007b) Induction of pluripotent stem cells from adult human fibroblasts by defined factors. Cell 131: 861–72.

Takahashi K, Yamanaka S (2006) Induction of pluripotent stem cells from mouse embryonic and adult fibroblast cultures by defined factors. Cell 126: 663–76.

Tan EK (2007) The role of common genetic risk variants in Parkinson disease. Clin Genet 72: 387–93.

Tan EK, Matsuura T, Nagamitsu S, Khajavi M, Jankovic J, et al. (2000) Polymorphism of NACP-Rep1 in Parkinson's disease: an etiologic link with essential tremor? Neurology 54: 1195–8.

Tanaka K, Suzuki T, Hattori N, Mizuno Y (2004) Ubiquitin, proteasome and parkin. Biochim Biophys Acta 1695: 235–47.

Tateishi K, He J, Taranova O, Liang G, D'Alessio AC, et al. (2008) Generation of insulin-secreting islet-like clusters from human skin fibroblasts. J Biol Chem 283: 31601–7.

Thomson JA, Itskovitz-Eldor J, Shapiro SS, Waknitz MA, Swiergiel JJ, et al. (1998) Embryonic stem cell lines derived from human blastocysts. Science 282: 1145–7.

Toft M, Sando SB, Melquist S, Ross OA, White LR, et al. (2005) LRRK2 mutations are not common in Alzheimer's disease. Mech Ageing Dev 126: 1201–5.

Tretiakoff C (1919) Contribution a l'etude de l'anatomie pathologique du locus niger de Soemmering avec quelques deductions relatives a la athogenie des troubles du tonus musculaire et de la maladie de Parkinson. Paris: Jouve and Co.

Uchiyama T, Ikeuchi T, Ouchi Y, Sakamoto M, Kasuga K, et al. (2008) Prominent psychiatric symptoms and glucose hypometabolism in a family with a SNCA duplication. Neurology 71: 1289–91.

Uversky VN (2007) Neuropathology, biochemistry, and biophysics of alpha-synuclein aggregation. J Neurochem 103: 17–37.

Valente EM, Abou-Sleiman PM, Caputo V, Muqit MM, Harvey K, et al. (2004) Hereditary early-onset Parkinson's disease caused by mutations in PINK1. Science 304: 1158–60.

Velayati A, Yu WH, Sidransky E (2010) The role of glucocerebrosidase mutations in Parkinson disease and Lewy body disorders. Curr Neurol Neurosci Rep 10: 190–8.

Verhage M, Maia AS, Plomp JJ, Brussaard AB, Heeroma JH, et al. (2000) Synaptic assembly of the brain in the absence of neurotransmitter secretion. Science 287: 864–9.

Vilariño-Güell C, Wider C, Ross OA, Dachsel JC, Kachergus JM, et al. (2011) VPS35 mutations in Parkinson disease. Am J Hum Genet 89: 162–7.

Vives-Bauza C, Zhou C, Huang Y, Cui M, de Vries RL, et al. (2010) PINK1-dependent recruitment of Parkin to mitochondria in mitophagy. Proc Natl Acad Sci U S A 107: 378–83.

Warren L, Manos PD, Ahfeldt T, Loh YH, Li H, et al. (2010) Highly efficient reprogramming to pluripotency and directed differentiation of human cells with synthetic modified mRNA. Cell Stem Cell 7: 618–30.

Waters CH, Miller CA (1994) Autosomal dominant Lewy body parkinsonism in a four-generation family. Ann Neurol 35: 59–64.

Wenning GK, Stefanova N, Jellinger KA, Poewe W, Schlossmacher MG (2008) Multiple system atrophy: a primary oligodendrogliopathy. Ann Neurol 64: 239–46.

Wernig M, Zhao JP, Pruszak J, Hedlund E, Fu D, et al. (2008) Neurons derived from reprogrammed fibroblasts functionally integrate into the fetal brain and improve symptoms of rats with Parkinson's disease. Proc Natl Acad Sci U S A 105: 5856–61.

West AB, Moore DJ, Biskup S, Bugayenko A, Smith WW, et al. (2005) Parkinson's disease-associated mutations in leucine-rich repeat kinase 2 augment kinase activity. Proc Natl Acad Sci U S A 102: 16842–7.

West AB, Moore DJ, Choi C, Andrabi SA, Li X, et al. (2007) Parkinson's disease-associated mutations in LRRK2 link enhanced GTP-binding and kinase activities to neuronal toxicity. Hum Mol Genet 16: 223–32.

Westerlund M, Hoffer B, Olson L (2010) Parkinson's disease: Exit toxins, enter genetics. Prog Neurobiol 90: 146–56.

White LR, Toft M, Kvam SN, Farrer MJ, Aasly JO (2007) MAPK-pathway activity, Lrrk2 G2019S, and Parkinson's disease. J Neurosci Res 85: 1288–94.

Wider C, Dickson DW, Wszolek ZK (2010) Leucine-rich repeat kinase 2 gene-associated disease: redefining genotype-phenotype correlation. Neurodegener Dis 7: 175–9.

Wilmut I, Schnieke AE, McWhir J, Kind AJ, Campbell KH (1997) Viable offspring derived from fetal and adult mammalian cells. Nature 385: 810–3.

Winslow AR, Chen CW, Corrochano S, Acevedo-Arozena A, Gordon DE, et al. (2010) alpha-Synuclein impairs macroautophagy: implications for Parkinson's disease. J Cell Biol 190: 1023–37.

Wittmann CW, Wszolek MF, Shulman JM, Salvaterra PM, Lewis J, et al. (2001) Tauopathy in Drosophila: neurodegeneration without neurofibrillary tangles. Science 293: 711–4.

Woltjen K, Michael IP, Mohseni P, Desai R, Mileikovsky M, et al. (2009) piggyBac transposition reprograms fibroblasts to induced pluripotent stem cells. Nature 458: 766–70.

Wood SJ, Wypych J, Steavenson S, Louis JC, Citron M, et al. (1999) alpha-synuclein fibrillogenesis is nucleation-dependent. Implications for the pathogenesis of Parkinson's disease. J Biol Chem 274: 19509–12.

Xu J, Kao SY, Lee FJ, Song W, Jin LW, et al. (2002) Dopamine-dependent neurotoxicity of alpha-synuclein: a mechanism for selective neurodegeneration in Parkinson disease. Nat Med 8: 600–6.

Yamanaka S (2009) Ekiden to iPS Cells. Nat Med 15: 1145–8.

Yanamandra K, Gruden MA, Casaite V, Meskys R, Forsgren L, et al. (2011) alpha-synuclein reactive antibodies as diagnostic biomarkers in blood sera of Parkinson's disease patients. PLoS ONE 6: e18513.

Ye L, Chang JC, Lin C, Sun X, Yu J, et al. (2009) Induced pluripotent stem cells offer new approach to therapy in thalassemia and sickle cell anemia and option in prenatal diagnosis in genetic diseases. Proc Natl Acad Sci U S A 106: 9826–30.

Yu J, Hu K, Smuga-Otto K, Tian S, Stewart R, et al. (2009) Human induced pluripotent stem cells free of vector and transgene sequences. Science 324: 797–801.

Yu J, Vodyanik MA, Smuga-Otto K, Antosiewicz-Bourget J, Frane JL, et al. (2007) Induced Pluripotent Stem Cell Lines Derived from Human Somatic Cells. Science 318: 1917–20.

Yu PB, Hong CC, Sachidanandan C, Babitt JL, Deng DY, et al. (2008) Dorsomorphin inhibits BMP signals required for embryogenesis and iron metabolism. Nat Chem Biol 4: 33–41.

Zarranz JJ, Alegre J, Gómez-Esteban JC, Lezcano E, Ros R, et al. (2004) The new mutation, E46K, of alpha-synuclein causes Parkinson and Lewy body dementia. Ann Neurol 55: 164–73.

Zhang FR, Huang W, Chen SM, Sun LD, Liu H, et al. (2009) Genomewide association study of leprosy. N Engl J Med 361: 2609–18.

Zhang M, Guller S, Huang Y (2007) Method to enhance transfection efficiency of cell lines and placental fibroblasts. Placenta 28: 779–82.

Zhong SC, Luo X, Chen XS, Cai QY, Liu J, et al. (2010) Expression and subcellular location of alpha-synuclein during mouse-embryonic development. Cell Mol Neurobiol 30: 469–82.

Zhou H, Wu S, Joo JY, Zhu S, Han DW, et al. (2009) Generation of induced pluripotent stem cells using recombinant proteins. Cell Stem Cell 4: 381–4.

Zhou W, Freed CR (2009) Adenoviral gene delivery can reprogram human fibroblasts to induced pluripotent stem cells. Stem Cells 27: 2667–74.

Zhu X, Rottkamp CA, Boux H, Takeda A, Perry G, et al. (2000) Activation of p38 kinase links tau phosphorylation, oxidative stress, and cell cycle-related events in Alzheimer disease. J Neuropathol Exp Neurol 59: 880–8.

Zimprich A, Benet-Pagès A, Struhal W, Graf E, Eck SH, et al. (2011) A mutation in VPS35, encoding a subunit of the retromer complex, causes late-onset Parkinson disease. Am J Hum Genet 89: 168–75.

Zimprich A, Biskup S, Leitner P, Lichtner P, Farrer M, et al. (2004) Mutations in LRRK2 cause autosomal-dominant parkinsonism with pleomorphic pathology. Neuron 44: 601–7.